UNIVERSITY OF SOUTHAMPTON

Faculty Of Science

Theoretical Studies Of Quantum Hall Systems

by Keith A. Benedict

A Thesis Submitted for the Degree of Doctor of Philosophy

September 1986

UNIVERSITY OF SOUTHAMPTON

FACULTY OF SCIENCE

DEPARTMENT OF PHYSICS

Abstract

Doctor of Philosophy

Theoretical Studies of Quantum Hall Systems

by Keith A. Benedict

The aim of this thesis is to explore the physics of systems in which the quantum Hall effect is observed by theoretical study of a particular model: the two-dimensional electron gas in a strong magnetic field and a random potential. The general approach has been to seek exactly solvable limits of the model and to then use these as a basis for controlled approximations. The first chapter is a review of some of the background to the quantum Hall effect and the study of disordered electronic systems. The second chapter examines the model in a régime in which there is a minimum length scale for fluctuations in the random potential which is much longer than the length scale for fluctuations in the wavefunction of the electrons. A systematic perturbation theory is set up using the ratio of these two length scales as a small parameter which is found to be useful in the calculation of the density of states but not for the evaluation of transport quantities. The third chapter examines an exactly solvable limit of the model in which the Fermi energy is supposed to lie in the n^{th} Landau level in the limit $n\to\infty$. The vanishing of quantum interference between scattered wavepackets in this limit permits the calculation of the density of states, diffusion constant and conductivity tensor for a wide range of types of random potential. The elimination of quantum interference effects causes all eigenstates to be extended, but an attempt to use $1/n$ as a small parameter in which to perform an expansion which might lead to localising corrections in the transport quantities is reviewed. The Final chapter uses a field thoeretic technique to examine the density of states far from the centre of the disorder broadened n^{th} Landau level in the large-n limit. It is found that the Lifshitz tails of high Landau levels are exponentially supressed

Acknowledgements

First and foremost I would like to take this opportunity to thank Dr. John Chalker for his inspiration and support over the past three years. In addition I would also like to thank the following people for their interest and useful discussions: Stephen Lovesey, Brian Rainford, Ken Barnes, Tim Sluckin, Paolo Carra, Geoff Daniell, Mike Gunn, Tony Hey, Douglas Ross, Chris Sachrajda and George Thomson. Finally I gratefully aknowledge the financial support of the SERC.

The calculations presented in chapters two, three and four have appeared, or are about to appear, in abbreviated form, in the following publications.

Chapter 2: Benedict and Chalker (1985) J. Phys. C: Solid State Physics 18, 3981.

Chapter 3 (except for 3.7): Benedict and Chalker (1986) J. Phys. C: Solid State Physics 19, 3587.

Chapter 4: Benedict (1986) Nuclear Physics B: Field Theory and Statistical Systems, to appear shortly.

In addition the 1/n Corrections briefly reviewed in section 3.7 are to be the subject of a forthcoming preprint: Carra, Chalker and Benedict (1986). The whole of the calculation described in chapter 3 is the subject of the preprint Chalker, Carra and Benedict (1986)

Contents

Chapter Three

Disordered Electrons in High Landau Levels

Chapter Four

The Fate of The Lifshitz Tails of High Landau Levels

General Introduction

The discovery of the integer quantum Hall effect by von Klitzing (von Klitzing, Dorda and Pepper 1980) was an entirely unexpected result of research into the novel properties of low dimensional structures: systems in which the current carrying electrons are constrained to move in two (or one) dimensions (Ando, Fowler and Stern 1982) such as the inversion layers of MIS (Metal-Insulator-Semiconductor) devices and multilayer heterostructures. The experimental results showed unequivocably that some new macroscopic quantum phenomena was at work which pinned the Hall conductivity over a range of electron densities at an integer multiple of the fundamental constant e^2/h with an unparalelled accuracy of a few parts in 10^6 (subsequently 10^8). It was immediately realised that Anderson localisation was important to the understanding of this effect. The very existence of a Hall current in the two-dimensional electron gas implied that the scaling theory of Abrahams, Anderson, Licciardello and Ramakrishnan (1979), which predicts that all electronic states in two-dimensions should be localised and therefore carry no current, is not directly applicable to systems in the presence of a strong magnetic field. Some features of the effect had been predicted by Ando (Ando, Matsumoto and Uemura 1975) but the precision of the quantisation was only explained a year later by Laughlin (1981). Although a qualitative understanding of the quantum Hall effect exists there remain some detailed questions to be answered.

The aim of the work described in this thesis is to examine a simplified model of systems in which the quantum Hall effect occurs: the disordered non-interacting two-dimensional electron gas in a strong magnetic field. The approach used has been to seek exactly solvable limits of the model and to then use appropriate small parameters to control a perturbative expansion for physical quantities about the solvable limit.

Glossary of Notation

All real-space 2-vectors are denoted by bold letters, **V**, their components are denoted thus: V_μ $\mu=1,2$ or $\mu=x,y$.

There are two scalar products for 2-D vectors:

$$\mathbf{a}\cdot\mathbf{b} = a_\mu b_\mu\text{: the conventional inner product}$$

$$\mathbf{a}\wedge\mathbf{b} = \varepsilon_{\mu\nu}a_\mu b_\nu\text{: the scalar cross product.}$$

Vector differential operators are analagously defined

$$\text{Grad } F(\mathbf{r}) = \nabla F \quad \text{which has components } \partial_\mu F$$

$$\text{Div } \mathbf{V}(\mathbf{r}) = \nabla\cdot\mathbf{V}(\mathbf{r}) = \partial_\mu V_\mu(\mathbf{r})$$

$$\text{Curl } \mathbf{V}(\mathbf{r}) = \nabla\wedge\mathbf{V}(\mathbf{r}) = \varepsilon_{\mu\nu}\partial_\mu V_\nu(\mathbf{r})$$

Ordinary 3-dimensional vectors are denoted by underlined letters: $\underline{V}=(V_x,V_y,V_z)$.

Standard Functions as Defined in Abramowitz and Stegun 1965

$L^\alpha_n(x)$ is an associated Laguerre polynomial

$H_n(x)$ is the n^{th} order Hermite polynomial

$\chi_n(x)$ is the n^{th} normalised, harmonic oscillator wavefunction.

Length Scales

L, L_x, L_y: System size

L_d: Correlation length for a random potential

L_{in}: Inelastic Scattering Length

ξ_L: Localisation length

l_c; Cyclotron length

Energy Scales

$\hbar\omega_c$: Cyclotron energy

v: Energy scale of a random potential

kT: Thermal Energy

E_f: Fermi Energy

Chapter1

An Introduction to Quantum Hall Systems

This chapter will review some of the background to the quantum Hall effect and describe some of the unanswered questions regarding this phenomenon to be addressed in subsequent chapters. The first section describes the behaviour of a non-interacting two-dimensional electron gas in a strong magnetic field. Section two relates some of the important features of electronic systems caused by the presence of disorder. Section three reviews attempts to measure the density of states in quantum Hall systems. The integer quantum Hall effect and its explanation in terms of Anderson localisation are described in section four. Section five introduces the mathematical techniques employed in the description of disorder in an electronic system and introduces the Green function formalism to be used throughout this thesis. Sections six and seven define two mathematical quantities of importance in the study of transport phenomena in electronic systems: the diffusion constant and the conductivity tensor, and describes their relation to the physical behaviour of quantum Hall systems. The final section is an introduction to two of the important features of quantum Hall systems which are due to the interactions between the electrons: Wigner crystallisation and the fractional quantum Hall effect.

1.1 The Two-Dimensional Electron Gas in a Strong Magnetic Field

The model system we have chosen to consider consists of a plane of area $\Omega(=L_x \times L_y)$ in which electrons of effective mass m (which subsumes the effect of the crystal lattice present in the real quantum Hall systems) and charge q move under the influence of a uniform static magnetic field $\underline{B}$ applied perpendicular to the plane and a static random potential $V(\mathbf{r})$. The interactions between the electrons are neglected except of course for the requirement that the many-body wavefunction be totally antisymmetric.

Firstly we shall consider the model in the absence of the random potential. Each particle moves independently so we shall commence with an examination of the motion of a single particle in an otherwise empty system (Landau and Lifshitz (1975) and (1977)). The Hamiltonian for the particle is

$$H^0 = \frac{1}{2m}\left(\mathbf{p} - q\mathbf{A}(r) \right)^2 \qquad (1.1)$$

where $\mathbf{p}$ is the momentum of the particle and $\mathbf{A}(\mathbf{r})$ is the vector potential of the magnetic field ($\nabla\wedge\mathbf{A}(\mathbf{r})=\mathbf{B}$). Classically the particle will move in a circular orbit of radius $R=|\mathbf{p}|/qB$ ($|\mathbf{p}|$ is a conserved quantity) with angular frequency $\omega_c=qB/m$ (the cyclotron frequency).

If an electric field, $\mathbf{E}$, is applied in the plane then the particle will move on a trochoid with a net drift velocity $V_\mu=\varepsilon_{\mu\nu}E_\nu/B$ in the direction perpendicular to the electric field (in terms of three-vectors $\underline{V}_{drift}=\underline{E}\times\underline{B}/|\underline{B}|^2$). Hence a gas of such particles of density ρ will have a current density of $q\rho V_{drift}$ and therefore a Hall conductivity $\sigma_{II}=q\rho/B$.

The equivalent quantum mechanical problem can be solved exactly from the Hamiltonian (1.1). The energy eigenvalues of the quantum particle are $E_n=(n+\frac{1}{2})\hbar\omega_c$ where n is a non-negative integer. Each of these Landau levels is highly degenerate with $eB/2\pi\hbar$ states per level per unit area. The quantum motion has a characteristic length scale, the cyclotron length defined as $l_c=(\hbar/eB)^{1/2}$, which is the radius of the smallest Bohr-Sommerfeld quantised orbit.

As usual the degenerate set of states within one Landau level is described in terms of a basis comprising simultaneous eigenstates of H^0 and some other commuting operator. For a given commuting operator the calculation is greatly simplified by an appropriate choice of gauge. The two most commonly used gauges are the Landau gauge and the symmetric gauge.

(i) The Landau gauge: $A_x(x,y)=0$, $A_y(x,y)=Bx$.

H^0 is clearly independent of y in this gauge and therefore $[H^0,p_y]=0$. We therefore use the basis set $\{|n,k\rangle\}$ where

$$H^0|n,k\rangle = (n+\tfrac{1}{2})\hbar\omega_c|n,k\rangle \qquad (1.2a)$$

$$p_y|n,k\rangle = \hbar k|n,k\rangle \qquad (1.2b)$$

$$\langle x,y|n,k\rangle = \Psi_{n,k}(x,y) = Ce^{iky}\,\chi_n\left[\frac{x}{l_c} + l_c k\right] \qquad (1.2c)$$

where χ_n is the n^{th} harmonic oscillator wavefunction. The normalisation constant, C, and the range of values taken by the quantum number, k, depend on the boundary conditions of the system. If the system is taken to be of infinite extent then k can take any real value. If the states are normalised by the condition

$$\langle n,k|n',k'\rangle = \delta[l_c^2(k-k')]\;\delta_{n,n'} \qquad (1.3)$$

then $C=(2\pi l_c^2)^{-1/2}$. If the system is taken to be a rectangle of dimension $L_x \times L_y$ then $k=2\pi m/L_y$ for integer m and $C=(L_y l_c^2)^{-1/2}$. The range of k is further restricted by the fact that $l_c^2 k$ is the centre of the probability density variation of the state in the x direction and must, therefore, be inside the system. Thus, if $0 \leqslant x \leqslant L_x$ then $0 \leqslant k \leqslant L_x l_c^{-2} \Rightarrow 0 \leqslant m \leqslant \Omega/2\pi l_c^2$.

(ii) The symmetric Gauge: $A_\mu(r) = B\varepsilon_{\mu\nu}r_\nu/2$.

In this gauge the Hamiltonian commutes with the angular momentum $L(=r\wedge p)$ and we therefore define the basis states $\{|n,m\rangle\}$ where

$$H^0|n,m\rangle = (n+\tfrac{1}{2})\hbar\omega_c|n,m\rangle \qquad (1.4a)$$

$$L|n,m\rangle = m\hbar|n,m\rangle \qquad (1.4b)$$

$$\langle r|n,m\rangle = \xi_m(r/l_c) = e^{im\theta}\;R_{n,m}(r/l_c) \qquad (1.4c)$$

where

$$R_{n,m}(r) = C_{n,m}\;e^{-r^2/4}\;r^{|m|}\;L_{\nu_m}^{|m|}(r^2/2)\;, \qquad (1.4d)$$

$$\nu_m = n+\tfrac{1}{2}(m-|m|) \quad \text{and} \quad C_{n,m} = \left[\frac{\nu_m!}{2^{|m|}\,(\nu_m+|m|)!}\right]^{1/2}.$$

The angular momentum, m, can take any integer value in the range $-n \leqslant m < \infty$ (we always assume that the system is infinite with this choice of gauge).

If we now consider a gas of charged fermions with density, ρ, but neglect interactions between them, then the particles will occupy the lowest available energy states. The many-body ground state will obviously not be unique unless ρ is an integer multiple of $(2\pi l_c^2)^{-1}$ (ie a whole number of Landau levels are filled) because of the

macroscopic degeneracy of the single particle states. If we now apply an electric field, E, in the x direction then p_y will still be a good quantum number for each particle in the Landau gauge and we can still solve exactly. The degeneracy of the Landau levels is now lifted and the energy eigenvalues become $E_n(k)=(n+\frac{1}{2})\hbar\omega_c+|E|k-|E|^2/4$ (weak field means that $|E|\ll\hbar\omega_c l_c^2/L_x$ ie the smearing of the Landau levels does not cause them to overlap). The current density of the quantum gas can be calculated exactly and is the same as for the classical gas. Thus if ν is the number of filled Landau levels (including fractional fillings) then the Hall conductivity can be written in the form $\sigma_H=\nu e^2/h$. As in the classical case the current is entirely in the direction perpendicular to the electric field and is therefore dissipationless.

This behaviour is familiar in the context of the Hall effect. Consider the inversion layer of a semiconductor device subject to a perpendicular magnetic field as depicted in Figure 1. If electrons are injected into the system, from a battery say, with velocity $\underline{V}$, the Lorentz force on each electron is $\underline{F}=-e\underline{V}\times\underline{B}$ and the electrons are deflected toward one side of the system (dotted path in the figure). The build up of electrons on one side, and the subsequent depletion of electrons from the other, sets up an electric field, $\underline{E}_H$ across the system. In the stationary state the total force on the electrons is zero, ie $-e\underline{E}_H-e\underline{V}\times\underline{B}=0 \Rightarrow \underline{V}=\underline{E}_H\times\underline{B}/|\underline{B}|^2$, hence the steady state current (full line in the figure) is perpendicular to the Hall field.

If the particles are electrons then we must consider their spin degree of freedom. The component of spin in the direction of the magnetic field is conserved, and the Landau levels are split by the energy shift $g\mu B/2$, hence there are separate Landau levels for spin up and spin down electrons. We shall always assume that the spin splitting is sufficiently large that the spin up and spin down Landau levels are widely separated and do not overlap.

There are a number of ways in which an electronic system may be disordered including substitutional and topological disorder in the underlying crystal lattice. Here, however, we shall only consider disorder in the form of a static randomly varying potential field, V(r), drawn from some prescribed probability distribution P[V(r)]. The single-particle Hamiltonian for the model is therefore

$$H = \frac{1}{2m}\left[\, \mathbf{p}-e\mathbf{A}(\mathbf{r}) \,\right]^2 + V(\mathbf{r}) = H^0 + V(\mathbf{r}) \quad .$$

In much of the following we shall work in units in which $l_c=1$ and $\hbar\omega_c=1$ in order to simplify the expressions. The formulae may easily be recast in normal units by dimensional analysis.

1.2 The Effects of Disorder on Electronic Systems

In this section we shall review two aspects of disorder in electronic systems, including the model system defined in section 1, namely disorder broadening and Anderson localisation which are both important for the understanding of the quantum Hall effect.

Many features of the behaviour of electrons in an ordered system, for example a perfect lattice, can be determined with ease from consideration of the symmetry of the system alone (Bloch's theorem for example uses the exact symmetry of the lattice to severely constrain the possible form of the electronic wavefunctions). The behaviour of disordered electronic systems is much more complex and harder to determine because of the complete absence of such symmetries. In this section certain qualitative features of disordered systems will be discussed. There are a number of good reviews of the general subject of disordered electron systems including those by Thouless (1974), Elliott, Krumhansl and Leath (1974) and Lee and Ramakrishnan (1985).

We consider disorder to be in the form of a static (quenched) randomly varying potential field. The system is characterised by a number of parameters, related to the statistical properties of the distribution from which the random function is drawn. The principal parameters are the typical energy and length scales for the fluctuations in the random potential: v and L_d. The energy scale, v, can be thought of as the scale for fluctuations in the potential at a point. For homogeneously disordered systems, which we consider exclusively here, v is independent of position. The length scale, L_d, is the correlation length for fluctuations in the random potential.

The addition of a random potential to the Hamiltonian of an electronic system will obviously alter its spectrum; in particular, since almost all configurations of the random potential have no symmetry, all degeneracies (except for those due to time reversal

symmetry if there is no magnetic field) will be lifted. For the disordered two-dimensional electron gas in a strong magnetic field this means that the sharp Landau levels will be smeared out into bands. We now have a precise definition of a strong magnetic field: it is a sufficiently strong field that the width of a disorder broadened Landau level is much less than the spacing between levels, $\hbar\omega_c$. The definition of the edge of the band is, however, somewhat vague because, as Lifshitz (1964) has shown, for many choices of random potential there will be a small (exponentially small in fact) density of states arbitrarily far from the level of the pure system; these (localised) states are supported by regions containing exceptional configurations of the random potential.

The density of states in the lowest Landau level has been calculated exactly by Wegner (1983) for a Gaussian white-noise potential and by Brézin, Gross and Itzykson (1984) for a variety of types of disorder. Approximate calculations of the density of states of the two-dimensional electron gas in a strong magnetic field have been performed by Ando et al (Ando and Uemura (1974), Ando (1974a,b and c) and Ando Matsumoto and Uemura (1975)) using a generalised Born Approximation and by Gerhardts (1975) using a path integral method. The calculation of the structure of the Landau bands is one of the major concerns of the following chapters.

A more surprising effect of the disorder is the phenomena of Anderson localisation (Anderson (1959)). Anderson found that some of the electronic eigenstates of a disordered system are not extended throughout the system in the way that Bloch states, for example, are. Some of the stationary states are localised in a particular region of the system with exponentially small probability density outside that region. An example of this is the states in the Lifshitz tails which have their support on regions of exceptionally high (or low) potential only. The scale for the size of the region in which a localised state has its support concentrated is the localisation length ξ_L. This leads to the currently accepted picture of an energy band in a disordered electronic system as illustrated in Figure 2b. The variation in the density of states is shown by the unbroken line. The states near the centre of the band are extended over the whole

system, while those in the shaded region, away from the centre are localised. The energies E_c and E_c', where the transition between the two kinds of state occur, are known as the mobility edges.

The expected behaviour of two physical quantities is also shown on this diagram. The localisation length (dashed line) is finite inside the region of localised states but diverges at the mobility edge. The energy dependent diffusion constant, D(E), (dotted line) will be discussed in section 1.6: essentially it describes the diffusion of probability for a wavepacket made up of eigenstates with energies in a narrow range around E. This quantity is finite if E is in the region of extended states, but vanishes as the mobility edge is approached: an electron in a localised state remains within a region of size ξ_1 nearly all the time whereas a wavepacket composed of extended states will diffuse away from its starting point and will cover an arbitrarily large area after sufficient time. The diffusion constant is, however, not a measurable quantity. The most direct physical distinction between localised and extended states is their response to an infinitesimal electric field. Extended states will carry a DC current under such conditions even at zero temperature but localised states cannot carry such a current as they require either a finite electric field to be applied before they can conduct or a non-zero temperature to allow phonon assisted hopping between states. In experimental systems phonon assisted hopping will be small at low temperatures and its temperature dependence is well known (Mott (1968)). Hence knowledge of the zero temperature D.C. conductivity as a function of the Fermi energy or electron density will be of considerable importance in studying the nature of the states.

Finite size effects act in a similar way to those in the theory of critical phenomena in that the position of the mobility edge is blurred. The transition from localised to extended states is no longer at uniquely defined energies because a localised state with a localisation length larger than the system size is indistinguishable from an extended state.

Much is known about localisation in the absence of a magnetic field from exactly solvable models in one dimension, from tight-binding models and from weak scattering expansions in higher dimensions. The analogy between the transition from localised to

extended states at a critical energy E_c and a thermodynamic phase transition has been exploited (see, for example Wegner (1979a) and McKane and Stone (1981)). The most important result is that of Abrahams, Anderson, Licciardello and Ramakrishnan (1979) who used a scaling argument, based on the idea that the localisation length is the only relevant length scale, to show that all states in two or less dimensions are localised.

Localisation in a magnetic field is much less well understood. The experimental fact that two-dimensional electron gases show the Hall effect at low temperatures implies the existence of some extended states. The scaling argument of Abrahams, Anderson, Licciardello and Ramakrishnan breaks down because the cyclotron length is a relevant parameter. The high degree of degeneracy in the ordered system means that there is no weak scattering limit (this will be discussed in greater detail in section 1.5) and there have, heretofore, been no exactly solved models of the disordered two-dimensional electron gas in a strong magnetic field.

One very elegant way of thinking about localisation in a field is that of Luryi and Kazarinov (1982) and Trugman (1983). They consider a very strong magnetic field and a slowly varying random potential (ie with a very long correlation length $L_d \gg l_c$). In this situation the electrons are constrained to move on the equipotential contours; the wavefunction has the form of a plane wave along an equipotential, and a harmonic oscillator wavefunction perpendicular to it (the width of the oscillator wavefunction going to zero as $B \to \infty$). Clearly there are two types of equipotentials: those that close on themselves and those that stretch across the system. Employing the Bohr-Sommerfeld quantisation prescription, the only closed equipotentials which are acceptable are those for which the phase change around the contour is an integer multiple of 2π. This implies that the area enclosed by an allowed contour must be threaded by a whole number of flux quanta. States occupying closed contours are localised, while those on open contours correspond to extended states. This picture fails at energies close to the mobility edge because of the possibility of tunneling between nearby contours, so that it demonstrates localisation but leaves open questions of the existence of extended states and the position of mobility edges.

One of the most crucial questions to be answered is where the mobility edges are within the disorder broadened Landau level. The calculations of Levine, Libby and Pruisken ((1983), (1984)) show that the effective field theory (a zero component non-linear sigma model) for the transition between localised and extended states differs from that in the absence of a magnetic field by the inclusion of a topological term which does not show up in perturbation theory, but controls an extra fixed point of the renormalisation group. Their main result is that only states at the very centre of the Landau band are extended. This result is also indicated by the numerical calculations of Schweitzer, Kramer and Mackinnon (1984) and Aoki and Ando (1985).

1.3 Experimental Studies of the Density of States

In this section we will review some of the experiments performed on quantum Hall systems which attempt to determine the form of the electronic density of states. In each experiment a particular thermodynamic property, $\mathcal{F}$, of the system is measured which depends on the density of states $\rho(E)$. The functional relation $\mathcal{F}=\mathcal{F}[\rho(E)]$ is usually very complicated and cannot be directly inverted unless some strong a-prioiri assumptions are made about the form of the density of states (Azbel (1986)). Consequently the proce dure adopted in the analysis of experiments is to use various trial forms for the density of states, ρ_i, in the relation and to then vary the parameters of ρ_i to find the best fit to the measured $\mathcal{F}$. In all cases only relatively simple forms for ρ have been tried. The form most consistent with all of these experiments is

$$\rho(E) = C + A(2\pi v^2)^{-1/2} \sum_n \exp - \left\{ \frac{(E-(n+\tfrac{1}{2})\hbar\omega_c)^2}{2\,v^2} \right\}$$

where A, C and v are adjustable parameters. Hence this picture corresponds to a sequence of gaussian Landau bands superimposed on a constant background density.

The first experiment was that of Gornik et al (1985) who measured the magnetic field dependence of the specific heat of a multilayer device. They assumed that the lattice contribution to the specific heat would be independent of the magnetic field and could

therefore be subtracted off leaving only the contribution from the two-dimensional electron gases at the heterojunctions. The specific heat of the electron gas is given by

$$C(B) = \int E\ \rho(E;B)\ \frac{df(E;T)}{dT}\ dE$$

where f(E;T) is the Fermi function for temperature T.

Eisenstein et al measured the magnetic field dependence of the magnetisation of the electrons in single layer and multilayer GaAs/AlGaAs devices. The oscillatory variation which they found is the well known de Haas-van Alphen effect. As the magnetic field is varied the electrons redistribute themselves within the spin split Landau levels causing the variation in the total magnetisation. The specific form of the variation depends on the density of states of the electrons and these experiments were consistent with a series of Gaussian Landau levels with width proportional to $B^{1/2}$ indicating short ranged correlations in the randomness (Ando and Uemura 1974).

Smith et al (1985) measured the magnetic field dependence of the capacitance of a heterojunction. The potential difference, U, across the junction controls the Fermi energy of the two-dimensional electron gas formed there while the total charge Q depends on $N(E_f)$: the mean number of occupied states. Thus the differential capacitance of the two-dimensional layer is

$$C_L(B) = \frac{dQ}{dV} \sim \frac{dN(E_f)}{dE_f} = \rho(E_f;B).$$

Smith et al further assume that the bulk capacitance of the device is a constant, C_B, so that the measured capacitance C_m is given by

$$\frac{1}{C_m(B)} = \frac{1}{C_B} + \frac{1}{C_L(B)}\ .$$

The results were only fitted to a Gaussian form for the density of states but this was found to give good agreement.

Stahl et al (1985) and Gavrilov and Kukushkin (1986) measured the thermally activated magnetoconductivity in heterostructures and MIS (Metal-Insulator-Semiconductor) structures respectively. The process they were observing involves the thermal promotion of an electron from a localised state to a vacant extended state. Analysis of the temperature dependence of the magnetoconductivity yields the distance of the Fermi energy from the mobility edge. They assumed, on

experimental grounds, that all the extended states were at the Landau energy $(n+\frac{1}{2})\hbar\omega_c$. Various trial forms for $\rho(E)$ were fitted to the results. The best fit was again given by a sequence of Gaussian bands superposed on a constant background.

1.4 The Integer Quantum Hall Effect

In section one we have seen that the Hall conductivity of an ideal two-dimensional electron gas in a strong magnetic field is linear in the electron density. Experiments on the two-dimensional electron gas formed in the inversion layer of a field effect transistor at low temperatures (von Klitzing, Dorda and Pepper (1980)) show that in these systems the variation of Hall conductivity is much more complex; in addition the longitudinal (ie in the direction of the electric field) conductivity is not identically zero but shows oscillatory behaviour as the electron density is varied. This behaviour is the quantum Hall effect.

The geometry of the experimental system is that of a field effect transistor with extra contacts to the inversion layer for the measurement of the longitudinal and Hall conductivities. The effective potential felt by the crystal electrons has the form of a deep well at the metal oxide-semiconductor interface. At low temperatures only the lowest sub-band of this quantum well is occupied and the electron gas is two-dimensional. Extra, Ohmic, contacts to the two-dimensional electron gas were diffused into the substrate to allow the measurement of the voltage drop along and across the conducting channel formed between the source and the drain. Variation of the gate potential allows direct control of the Fermi energy and therefore the electron density.

Figure 2a is a schematic illustration of the variation of the longitudinal and Hall conductivities with Fermi energy in the quantum Hall effect (full lines). The points marked on the Fermi energy axis correspond to exactly filled Landau levels. The longitudinal conductivity is in arbitrary units but the Hall conductivity axis is graduated in units of $e^2/2\pi\hbar$. The dotted line gives the Hall conductivity predicted by a naive model (the two-dimensional electron gas in a strong magnetic field in the absence of any disorder); the longitudinal conductivity is predicted by this model to be zero

everywhere. The measured Hall conductivity is constant over wide ranges of Fermi energy to an accuracy of a few parts in 10^8, but increases monotonically in the intervening regions. The value at which the Hall conductivity is quantised is the value predicted by the naive model for the full Landau level. The longitudinal conductivity falls to zero in the regions in which σ_H is quantised (apart from thermally activated processes which are negligible because of the low temperatures) but becomes quite large in the intervening regions indicating the importance of impurity scattering.

The observation of the quantum Hall effect raises three questions:

(i) Why does the Hall conductivity show plateaux and the longitudinal conductivity show oscillations?

(ii) Why is the Hall conductivity so accuratly quantised at the value predicted by the ideal model for a filled Landau level?

(iii) Can we predict where the plateaux edges will be?

The answers to the first two questions have been found; attempting to answer the third is one of the pricipal motivations for the work in this thesis

The existence of the plateaux in σ_H and the oscillations in σ_L can be explained in terms of the Anderson localisation of some of the states in the disorder broadened Landau level as follows. Figure 2 shows the variation of the conductivities with the Fermi energy and the variation in the character of the states with energy on the same horizontal scale to illustrate this explanation.

(i) The Hall conductivity

All the occupied extended states (ie all those below the Fermi energy at zero temperature) will carry a Hall current. Thus if E_f is in the region of extended states then the addition of an extra electron to the system, slightly increasing E_f, will result in the occupation of an extended state and therefore there will be an increase in the Hall current. If, however, E_f is in the localised region then any extra electron will occupy a localised state and the Hall current will not change.

(ii) The Longitudinal Conductivity

Longitudinal conduction occurs by the impurity scattering of electrons, in states at the Fermi energy, along the system. This process only gives rise to a bulk current if the states at the Fermi energy are extended. If the Fermi energy is in the localised régime then no longitudinal current will flow.

The accuracy of the quantisation and the fact that the quantised value is that of a filled Landau level in the ideal model was explained by Laughlin (1981) using gauge "invariance" arguments and by Avron and Seiler (1984) and Niu, Thouless and Wu (1985) by a topological argument. The basic result of these is that whenever the Fermi energy lies in a mobility gap(ie a region with no extended states) the Hall conductivity is an integer (possibly zero) multiple of $e^2/2\pi\hbar$.

A consequence of the fact that σ_H is so quantised is that the extended states of the system must carry more Hall current than the states in the naive model in order that the total current in a filled Landau level be the same regardless of the presence of disorder. A demonstration of this effect is given in Chalker (1983).

The Anderson localisation explanation of the quantum Hall effect indicates that the edges of the plateaux should correspond to the Fermi energy being at the mobility edge of the Landau level, hence question (iii) reduces to finding E_c, where the nature of the states changes from localised to extended.

Useful reviews of the quantum Hall effect are Cage and Girvin (1983) and Halperin (1983). The modulation of the Hall and longitudinal conductivities had been predicted by Ando et al. (Ando, Matsumoto and Uemura (1975)) but not the exactness of the quantisation.

1.5 Theoretical Techniques For Disordered Systems

In this section we shall introduce the mathematical formalism used in the study of disordered electronic systems using Green functions including the perturbative scheme of Edwards (1958)

The solution of any problem for an arbitrary, random potential is clearly impossible; even the solution for a given configuration of the random potential is only possible by numerical methods. Clearly

the best one can conceivably do analytically is to find the probability distributions for various physical quantities given the probability distribution for the random potential. This is far too difficult in all but the simplest of models and in general one has to calculate the mean value of physical quantities and possibly their first few moments. This is not too restrictive as most physical quantities pertaining to macroscopic systems are believed to be self-averaging: the measured value of the quantity will always be near to its mean value over the distribution. The justification for this can be expressed in the following way. Consider a sample to be composed of a large number of macroscopic systems joined together; each such system has a particular configuration of the random potential. The measured value of the physical quantity will be an average over the whole sample of the value of the quantity in each system. In the limit of an infinite sample composed of an infinite number of subsystems this becomes equivalent to averaging a single subsystem over all configurations of the random potential, weighted by their probability of appearing. In the following we assume that all relevant physical quantities are self-averaging (the argument given above neglects the possibility of correlations between the values of a quantity in different sub-system and is by no means watertight) and we shall therefore be concerned with calculating their average values.

A particular configuration of the random potential, $V(\mathbf{r})$, will arise with probability $P[V(\mathbf{r})]$; the average value of a quantity, $Q[V(\mathbf{r})]$, will then be

$$\bar{Q} = \int \mathcal{D}V(\mathbf{r})\ P[V]\ Q[V] \qquad (5.1)$$

In all of the following we will always take $P[V]$ to depend only on $V(\mathbf{r})$ and not separately on $\mathbf{r}$; in other words we assume that the disorder is homogeneous.

The most convenient way of describing the behaviour of a single quantum mechanical particle in a complicated potential is to use the Green function formalism (see Economou (1979) or Ziman (1979)) which we will briefly review here. The single particle Green function is defined as

$$\gamma(\mathbf{r},\mathbf{r}';t;[V(\mathbf{r})]) = \theta(t)\langle \mathbf{r}|e^{-iH[V]t/\hbar}|\mathbf{r}'\rangle; \text{ where } \theta(t)=\begin{cases}1 & t>0\\ 0 & t<0\end{cases} \qquad (5.2a)$$

Physically this is the probability amplitude for a particle initially (ie at t=0) at $\mathbf{r}$ to be at $\mathbf{r}'$ at a later time t. This Green function generates solutions of the inhomogeneous time-dependent Schrödinger equation. It is often more convenient to work with the Green function of the time-independent Schrödinger equation defined as

$$\Delta(\mathbf{r},\mathbf{r}';z;[V(\mathbf{r})]) = \langle \mathbf{r}|(z-H)^{-1}|\mathbf{r}'\rangle \qquad (5.2b)$$

where z is a complex energy parameter. These two functions are related by a Fourier transform as follows

$$\gamma(t) = \frac{1}{2\pi\hbar i}\int_{-\infty+i0}^{+\infty+i0} e^{-izt/\hbar}\,\Delta(z)\,dz \qquad (5.3a)$$

$$\Delta(z) = i\int_{-\infty}^{+\infty} e^{izt/\hbar}\,\gamma(t)\,dt \qquad (5.3b)$$

$\Delta(z)$ is an analytic function everywhere in the complex plane except on the real axis where poles and cuts arise for values of z corresponding to discrete and continuous eigenvalues of H respectively. The integration contour in equation 5.3a is chosen so that, when it is completed by the appropriate semicircle at infinity, the poles are enclosed by the contour for t>0 but not when t<0.

If we know the eigenstates of H, $\{|\alpha\rangle\}$, we can write

$$\Delta(\mathbf{r},\mathbf{r}';z) = \sum_{\alpha}\frac{\psi_\alpha(\mathbf{r})\overset{*}{\psi}_\alpha(\mathbf{r}')}{(z-E_\alpha)} \qquad \text{where } \psi_\alpha(\mathbf{r})=\langle \mathbf{r}|\alpha\rangle \qquad (5.4)$$

(note that the sum is replaced by an integral if the eigenvalues form a continuum). The local density of states per unit area can be written in terms of the imaginary part of Δ as follows

$$\rho(\mathbf{r};E) = -\frac{1}{\pi}\lim_{\varepsilon\to 0^+}\mathrm{Im}\left[\,\Delta(\mathbf{r},\mathbf{r};E+i\varepsilon)\,\right] \qquad (5.5)$$

If the system is translationally invariant then this will be independent of $\mathbf{r}$. In any case we can define the average density of states per unit area

$$\rho(E) = \frac{1}{\Omega}\int d^2\mathbf{r}\;\rho(\mathbf{r},E) \qquad (5.6)$$

If $V(\mathbf{r})$ is some random potential and $H=H^0+V$ then we can define the disorder averaged Green functions as $G(\mathbf{r},\mathbf{r}';z) = \overline{\Delta(\mathbf{r},\mathbf{r}';z;[V(\mathbf{r})])}$ and $\Gamma(\mathbf{r},\mathbf{r}';t) = \overline{\gamma(\mathbf{r},\mathbf{r}';t;[V(\mathbf{r})])}$. The disorder averaged density of states per unit area is then

$$\overline{\rho(E)} = -\frac{1}{\pi}\lim_{\varepsilon\to 0} \mathrm{Im}\left[\, G(\mathbf{r},\mathbf{r};z)\,\right] \tag{5.7}$$

which is automaticallly translationally invariant for homogeneous disorder.

For the two-dimensional electron gas in a strong magnetic field in the absence of disorder we can use the simultaneous eigenfunctions of H^0 and p_y (equation 1.2) to write (see Appendix 1.7)

$$\begin{aligned} G^0(\mathbf{r},\mathbf{r}';z) &= \Delta(\mathbf{r},\mathbf{r}';z;[V(\mathbf{r})=0]) \\ &= \sum_n \left[\, z-(n+\tfrac{1}{2})\hbar\omega_c \,\right]^{-1} C_n(\mathbf{r},\mathbf{r}') \end{aligned} \tag{5.8a}$$

and

$$\begin{aligned} \Gamma^0(\mathbf{r},\mathbf{r}';t) &= \gamma(\mathbf{r},\mathbf{r}';t;[V(\mathbf{r})=0]) \\ &= \theta(t)\sum_n e^{-i(n+\frac{1}{2})\omega_c t} C_n(\mathbf{r},\mathbf{r}') \end{aligned} \tag{5.8b}$$

where $$C_n(\mathbf{r},\mathbf{r}') = \frac{1}{2\pi l_c^2}\, e^{i\upsilon(\mathbf{r},\mathbf{r}')} \exp\left\{-\frac{|\mathbf{r}-\mathbf{r}'|^2}{4l_c^2}\right\} L_n\left[\frac{|\mathbf{r}-\mathbf{r}'|^2}{2l_c^2}\right]$$

and $\upsilon(\mathbf{r},\mathbf{r}')=(x+x')(y-y')/2l_c^2$ (see Appendix 1.6). The only gauge dependent part of this expression is υ. It is useful to note that C_n obeys the following relations

$$C_n(\mathbf{r},\mathbf{r}) = \frac{1}{2\pi l_c^2} \tag{5.9a}$$

and

$$\int d^2\mathbf{r}'\; C_n(\mathbf{r},\mathbf{r}')C_m(\mathbf{r}',\mathbf{r}'') = \delta_{n,m}\, C_n(\mathbf{r},\mathbf{r}'') \tag{5.9b}$$

From the translational and rotational invariance assumed of the ensemble of random potentials it can be shown (Sher and Holstein (1966) and Keiter (1967)) that, if Landau level mixing is neglected, the propagator for the disordered two-dimensional electron gas in a strong magnetic field can be written in the form

$$G(\mathbf{r},\mathbf{r}';z) = \sum_n g_n(z)\, C_n(\mathbf{r},\mathbf{r}') . \tag{5.10}$$

In the absence of disorder this gives the free propagator (5.8) with $g_n^0(z) = \{z-(n+\frac{1}{2})\hbar\omega_c\}^{-1}$.

We also define the averaged two-particle Green functions

$$K(r_1,r_1';z_1;r_2,r_2';z_2) = \overline{\Delta(r_1,r_1';z_1)\Delta(r_2,r_2';z_2)} \qquad (5.11)$$

and $$\tilde{Q}(r-r',z) = \overline{|\Delta(r,r';z)|^2} = K(r,r';z;r',r;z^*) \qquad (5.12)$$

which will be important for the determination of transport properties. Since Q is a function of $r-r'$ only it is often convenient to employ a Fourier representation

$$Q(q,z) = \int d^2r\, \tilde{Q}(r,z)e^{iq\cdot r} \qquad (5.12a)$$

Finally we define the diffusion propagator

$$\Pi(r,r';t) = \overline{|\gamma(r,r';t)|^2} \qquad (5.13)$$

The interpretation placed on the imaginary part of the complex energy appearing in the definition of various Green functions is the following. It is taken as a rate for inelastic processes such as interactions between electrons and phonons. This interpretation allows us to incorporate, in a very simplistic way, some effects of the finite, but very low, temperature at which quantum Hall systems operate. The value of L, the system size is also related to thermal properties in that the effective size of the system described by the zero temperature model is of the order of the inelastic scattering length, L_{in}, unless the temperature is so low that this is greater than true sample size. A direct relation between ω and the inelastic scattering length L_{in} can be obtained by considering the electronic motion to be diffusive. The mean square distance moved by the particle between inelastic processes is $\langle x^2\rangle \sim D/\omega$, this must be the square of the inelastic scattering length so that $\omega \sim D/L_{in}^2$.

The foundation of all of the following work is the perturbative expansion of the disorder-averaged Green functions due to Edwards (1958). Consider the Hamiltonian $H=H^0+V(r)$. The Green function of the pure system, corresponding to H^0 alone, is

$$G^0(r,r';z) = \langle r|(z-H^0)^{-1}|r'\rangle \qquad (5.14)$$

The operator $(z-H[V])^{-1}$ can be written in the form $\{(z-H^0)-V\}^{-1}$. If V is is some sense small then we can use the following series expansion,

$$(A-B)^{-1} = A^{-1}\left\{1 + BA^{-1} + BA^{-1}BA^{-1} + \ldots\ldots\right\}, \qquad (5.15)$$

to give the series

$$\Delta(r,r';z) = G^0(r,r';z) + \int G^0(r,r'';z)\, V(r'')\, G^0(r'',r';z)\, d^2r''$$

$$+ \iint G^0(r,r_1;z)V(r_1)G^0(r_1,r_2;z)V(r_2)G^0(r_2,r';z)\, d^2r_1 d^2r_2 + \ldots\ldots (5.16)$$

This series can be represented diagrammatically as shown in Figure 3. The double line represents the full propagator $G(r,r';z)$, a single solid line represents the free propagator $G^0(r,r';z)$ and a dotted lines from a propagator to a cross represents an interaction with the random potential $V(r)$. We can now perform the average over the disorder term by term in this series to give

$$G(r,r';z) = G^0(r,r';z) + \int G^0(r,r'';z)\, G^0(r'',r';z)\, \Xi_1(r'')\, d^2r''$$

$$+ \iint G^0(r,r_1;z)G^0(r_1,r_2;z)G^0(r_2,r';z)\, \Xi_2(r_1,r_2)\, d^2r_1 d^2r_2 + \ldots (5.17)$$

where

$$\Xi_n(r_1,r_2,\ldots.r_n) = \overline{V(r_1)V(r_2)\ldots\ldots V(r_n)} \quad . \qquad (5.18)$$

This series can be represented by the sequence of diagrams shown in Figure 4a in which ν dotted lines with their free ends linked represent the average of ν interactions Ξ_ν. In the same way an expansion for the two-particle function, K can be set up to give

$$K(r_1,r_1';z_1;r_2,r_2';z_2) = G^0(r_1,r_1';z_1)G^0(r_2,r_2';z_2) +$$

$$\int d^2x\, \Xi_1(x) \left[G^0(r_1,x;z_1)G^0(x,r_1';z_1)G^0(r_2,r_2';z_2) + 1 \leftrightarrow 2 \right] +$$

$$\int d^2x d^2y\, \Xi_2(x,y) \left[G^0(r_1,x;z_1)G^0(x,y;z_1)G^0(y,r_1';z_1)G^0(r_2,r_2';z_2) + 1 \leftrightarrow 2 \right.$$

$$\left. + G^0(r_1,x;z_1)G^0(x,r_1';z_1)G^0(r_2,y;z_2)G^0(y,r_2';z_2) \right] + \ldots . \qquad (5.19)$$

which is depicted diagrammatically in Figure 4b.

In applications of this method the probability distribution is chosen to give particularly simple forms for the Ξ_ns. If the probability distribution is a Gaussian centred on zero then Ξ_n vanishes for odd n and the only independent function is Ξ_2. Higher correlators satisfy Wick's theorem, ie

$$\Xi_{2n}(r_1,r_2,..r_{2n}) = \frac{1}{2^n\, n!} \sum_{\zeta \in S_{2n}} \prod_{i=1}^{n} \Xi_2(r_{\zeta_{2i-1}}, r_{\zeta_{2i}}) \qquad (5.20)$$

where S_n is the symmetric group of n objects and ζ is a particular permutation of the numbers $\{1,\ldots 2n\}$. In terms of the diagrammatic expansion this choice of potential gives the diagrams in Figure 5 in which the dotted line represents Ξ_2.

Another type of random potential can be constructed by considering scattering centres each of which has a potential field of a fixed form but with a variable strength. The potential has the form

$$V(r) = \sum_{i=1}^{\rho\Omega} v_i F(r-R_i) \qquad (5.21)$$

where $\rho\Omega$ is the total number of scattering centres placed in the system of size Ω; R_i is the location of the i^{th} centre; v_i is the strength of the i^{th} centre and $F(r)$ is a fixed function. v_i can be a random variable (we shall only consider distributions for which the strengths of different centres are uncorrelated) with probability distribution function $P(v)$. The R_is are also random variables with a uniform distribution, hence the probability that a given centre is in a region of size A is A/Ω. We shall only consider the case where the scattering centres have zero range, ie $F(r)=\delta^2(r)$.

This type of random potential can also treated perturbatively. The series 5.1 can be rewritten in this case as

$$G(r,r';z) = G^0(r,r';z) + \Omega^{-1}\sum_{i=1}^{\rho\Omega} \overline{v_i} \int G^0(r,R_i;z)\, G^0(R_i,r';z)\, d^2R_i$$

$$+ \Omega^{-2}\sum_{i\neq j}^{\rho\Omega} \overline{v_i v_j} \iint G^0(r,R_i;z)G^0(R_i,R_j;z)G^0(R_j,r';z)\, d^2R_i d^2R_j + \ldots\ldots$$

$$+ \Omega^{-1} \sum_{i}^{\rho\Omega} \overline{[\, v_i \,]^2} \int G^0(r,R_i;z)G^0(R_i,R_i;z)G^0(R_i,r';z)\, d^2R_i \qquad (5.22)$$

This can be represented by the diagrams in Figure 6 where each labelled cross represents a scattering centre. After averaging over the positions of the scatterers the Feynman rule for the diagrams is the following: the term associated with a cross that has 2p propagator lines (ie a site that is visited by the electron p times) carries a factor $\rho\overline{(v_i)^p}$.

It will be convenient sometimes to consider Green functions in the basis of Landau states $\{|n,k\rangle\}$ rather than position states ie

$$\Delta_{n,n'}(k,k';z) = \langle n,k|(z-H[V(r)])^{-1}|n',k'\rangle$$

$$= \int d^2r\, d^2r'\, \langle n,k|r\rangle\, \Delta(r,r';z)\, \langle r'|n',k'\rangle . \qquad (5.23)$$

In the presence of a strong magnetic field the kinetic energy is quenched and $\hbar\omega_c$ is the energy scale against which the disorder must be compared (in the absence of the field it would be the Fermi energy). Since, in the experimental systems, the cyclotron energy is significantly greater than the disorder strength it is sensible to consider always the limit $\hbar\omega_c \to \infty$. Corrections to the result can always be calculated from simple quantum mechanical perturbation theory. However in making this approximation we are left with only one energy scale describing the system, v, and so there is no true small parameter and no weak scattering régime. This absence of a weak scattering régime is really a consequence of the highly singular nature of the unperturbed pure system with its macroscopically degenerate Landau levels.

In the absence of a magnetic field the weak scattering limit corresponds to the weak localisation régime in which the localisation length is large at all energies for sufficiently small disorder. One of the aims of the work described in this thesis has been to look for a weak localisation régime in a magnetic field despite the absence of a weak scattering limit.

1.6 Diffusion in Quantum Systems

One of the important mathematical quantities which we shall try to calculate in chapter 3 is the energy dependent diffusion constant which we define here by considering a wavepacket, constructed from a set of energy eigenstates within a narrow range of energies, and its subsequent time development.

The most intuitively obvious difference between localised and extended states is the long-time behaviour of wavepackets constructed from them. A localised eigenstate by itself can be considered as a wavepacket and its probability density is obviously time invariant. Consider a wavepacket, $\Psi_0(r)$, constructed from states in a narrow range of energies centred on E_0 which has its probability density

concentrated on a small region around the origin at t=0. If E_0 is in the region of localised states then as time passes the shape of the wavepacket may be modified but it will remain within a region of size $\xi_1(E_0)$ around the origin. If E_0 is in the régime of extended states then as time passes the wavepacket will spread out until, after a sufficiently long time, it covers an arbitrarily large area.

It is expected that, for long times, the disorder-averaged probability density, $P(\mathbf{r},t)=|\Psi_0(\mathbf{r},t)|^2$, of a wavepacket composed of extended states will behave diffusively, satisfying the equation

$$\frac{\partial}{\partial t} P(\mathbf{r},t) = D(E_0)\, \nabla^2 P(\mathbf{r},t) \qquad t\to\infty \tag{6.1}$$

where $D(E_0)$ is an effective diffusion constant. It is convenient to consider the wavevector dependent probability

$$P(\mathbf{q},t) = \int d^2\mathbf{r}\, e^{i\mathbf{q}\cdot\mathbf{r}}\, P(\mathbf{r},t) \tag{6.2}$$

which is expected to satisfy the equation

$$\frac{\partial}{\partial t} P(\mathbf{q},t) = -q^2 D(E_0) P(\mathbf{q},t) \quad \Rightarrow \quad P(\mathbf{q},t) = P(\mathbf{q},0)\, e^{-q^2 Dt}. \tag{6.3}$$

A convenient way of constructing the wavepacket is given in Appendix 1.2 which leads naturally to a description of $P(\mathbf{q},t)$, in terms of the Spectral function $S(\mathbf{q},E_1,E_2)$ (see Wegner (1979b)) which is a measure of the correlation between eigenstates of energy E_1 and E_2 at wavevector $\mathbf{q}$. It can be shown (Appendix 1.3) that if $P(\mathbf{q},t)$ is to have the expected time dependence for late times (equation 6.1) then the hydrodynamic (small q^2) behaviour of S must be

$$S(\mathbf{q},E_1,E_2) \sim \frac{C}{(E_1-E_2) + iDq^2} \qquad q^2\to 0. \tag{6.4}$$

The spectral function can be written in terms of two-particle Green functions and for small q^2 can be written in the form (Appendix 1.4)

$$S(\mathbf{q};E+i\varepsilon,E-i\varepsilon) \sim \frac{1}{2\pi^2}\, Q(\mathbf{q},E+i\varepsilon) \qquad q^2\to 0. \tag{6.5}$$

where $Q(\mathbf{q},E+i\varepsilon)$ is the advanced-retarded two-particle Green function defined in equation 5.11a. It therefore follows, using the sum rule derived in Appendix 1.5, that

$$Q(\mathbf{q},E+i\varepsilon) \sim \frac{\pi\rho(E)}{\varepsilon + \frac{1}{2} Dq^2} \qquad q^2,\varepsilon\to 0. \tag{6.6}$$

Thus we can extract the diffusion constant $D(E_0)$ from the hydrodynamic behaviour of the two-particle Green function. If E_0 is in the régime of localised states the probability density will not diffuse away and D(E) will be zero; one expects that $D(E)\to 0$ as $E\to E_c$ from the extended side.

The neccessity for using the average two-particle Green function in the calculation of the transport properties can be understood as follows. While $\Delta(\mathbf{r},\mathbf{r}';z)$ distinguishes between localised and extended states for a particular configuration of the random potential, when it is averaged over different configurations of the random potential it has a different, random, phase for each configuration unless $\mathbf{r}=\mathbf{r}'$, in which case the phase factor υ vanishes; hence the averaged Green function is short ranged and is not sensitive to localisation. $|\Delta(\mathbf{r},\mathbf{r}';z)|^2$ is positive definite and therefore its average, $Q(\mathbf{r}-\mathbf{r}',z)$, can be long ranged and sensitive to the nature of eigenstates.

1.7 Conductivity and Linear Response Theory

The quantities which are effectively measured in the quantum Hall effect are the longitudinal and Hall conductivities. The precise mathematical definition of these quantities and a brief outline of how they can be expressed in terms of Green functions for small electric fields using linear response theory is given here.

The current density operator for a quantum many-body system is

$$\hat{\mathbf{j}}^T(\mathbf{r},t) = \sum_i \left\{ \hat{\mathbf{v}}_i(t)\delta^2(\mathbf{r}-\hat{\mathbf{r}}_i) + \delta^2(\mathbf{r}-\hat{\mathbf{r}}_i)\hat{\mathbf{v}}_i(t) \right\} \qquad (7.1)$$

where $\mathbf{r}_i$ is the coordinate for the i^{th} particle and $\mathbf{v}_i(t)=-i[\mathbf{r}_i,H_T]$ is the corresponding velocity operator (H_T is the total Hamiltonian including the effect of an applied electric field). The microscopic current density is the average (thermal and quantum mechanical) of this operator. This microscopic current density has two components: one is the bulk current density, which is relevant to charge transport, the other is the magnetisation current $\nabla\wedge\mathbf{M}$. The macroscopic current density, which is the physically measurable quantity, is the average of the microscopic current over a small region of the sample; the average of the magnetisation current over this region is zero. After disorder averaging the macroscopic current

will be position independent so we define the bulk current density operator J to be the average over the entire sample of the microscopic current density.

$$\hat{J}^T(t) = \frac{1}{\Omega}\int d^2r\ \hat{j}^T(r,t) \tag{7.2}$$

The conductivity is defined to be the coeffi cient of linear (Ohmic) response to a uniform electric field $Ee^{i\omega t}$ which is varying periodically with time.

$$I_\mu(t) = \langle\hat{J}^T_\mu(t)\rangle = Tr\{\hat{\rho}(t)\hat{J}^T_\mu\} = \sigma_{\mu\nu}(\omega)E_\nu e^{i\omega t} \tag{7.3}$$

where $\rho(t)$ is the non-equilibrium density matrix describing the system and its interaction with the external field and a heat bath. We shall be primarily interested in the static or D.C. conductivity (ω=0) at zero temperature (thermal average replaced by the expectation value in the many-body ground state).

We can describe the application of a weak electric field to the disordered two-dimensional electron gas in a strong magnetic field by including an extra time dependent vector potential

$$\mathbf{A}'(t) = \frac{i}{\omega}\mathbf{E}\,e^{i\omega t} \quad \Rightarrow \mathbf{E}e^{i\omega t} = -\partial_t\mathbf{A}'(t) \tag{7.4}$$

in the Hamiltonian. To lowest order in **E** the Hamiltonian becomes

$$H_T = H - \frac{e}{m}\mathbf{A}'(t)\cdot\sum_i \hat{\mathbf{v}}_i = H - \frac{\Omega}{m}\mathbf{A}'(t)\cdot\hat{\mathbf{J}} \tag{7.5}$$

where H is the Hamiltonian for the disordered two-dimensional electron gas in a strong magnetic field. J is the current operator in the absence of the electric field related to $J^T(t)$ by $J^T(t)=J-ie^2\nu\mathbf{A}'(t)/m$ where ν is the mean density of the electrons. By the standard methods of linear response theory (Kubo (1957), see Lovesey (1980) for a review) the non-equlibrium density matrix can be written as

$$\hat{\rho}(t) = \hat{\rho}_0 + \frac{\Omega}{m\,\omega}\int_{-\infty}^{t} dt'\ e^{i\omega t'}[\hat{\rho}_0,\hat{J}(t'-t)]\cdot\mathbf{E} \tag{7.6}$$

where ρ_0 is the equilibrium density matrix in the absence of the field: $\rho_0=Z^{-1}\exp\{-\beta H\}$, $\beta=1/kT$ and the current is now a Heisenberg operator. The average of the bulk current is then

$$I_\mu(t) = \frac{\Omega}{m\omega}\int_{-\infty}^{t} e^{i\omega t'} E_\nu \, \mathrm{Tr}\left\{ \hat{\rho}_0 [\hat{J}_\nu(t'-t), \hat{J}_\mu(0)] \right\} dt' + \frac{ie^2 \rho E_\mu e^{-i\omega t}}{m\omega} \tag{7.7}$$

The zero temperature conductivity tensor then has the form

$$\sigma_{\mu\nu}(\omega) = -\frac{\Omega}{m\omega}\int_{0}^{\infty} e^{-i\omega t} \langle 0|[\hat{J}_\mu(t), \hat{J}_\nu(0)]|0\rangle \, dt + \frac{ie^2 \rho e^{-i\omega t}}{m\omega} \delta_{\mu\nu} \tag{7.8}$$

where $|0\rangle$ is the many-body ground state.

This can be rewritten in terms of many-body Green functions which, in the absence of interactions between electrons, reduce to the Green functions introduced in section 5. The results for the d.c. conductivity ($\omega \to 0$) (Smrcka and Streda (1977) and Streda (1982)) are as follows.

$$\sigma_{xx} = \frac{\pi\hbar e^2}{(2\pi i)^2 \Omega} \sum_{\alpha\beta\gamma\delta} \langle\alpha|v_x|\beta\rangle \langle\gamma|v_x|\delta\rangle \, \overline{\tilde{\Delta}_{\beta\gamma}(E_f) \, \tilde{\Delta}_{\delta\alpha}(E_f)} \; ; \tag{7.9}$$

$$\sigma_{xy} = \sigma_{xy}^{I} + \sigma_{xy}^{II} \; ;$$

where

$$\sigma_{xy}^{I} = \frac{-e^2\hbar}{4\pi\Omega} \sum_{\alpha\beta\gamma\delta} \langle\alpha|v_x|\beta\rangle \langle\gamma|v_y|\delta\rangle \left[\overline{\Delta^{+}_{\beta\gamma}(E_f) \, \tilde{\Delta}_{\delta\alpha}(E_f)} - \overline{\tilde{\Delta}_{\beta\gamma}(E_f) \, \Delta^{-}_{\delta\alpha}(E_f)} \right] \tag{7.10}$$

and

$$\sigma_{xy}^{II} = e \left.\frac{dN(E)}{dB}\right|_{E=E_f} ; \tag{7.11}$$

while $\Delta^{\pm}{}_{\alpha\beta}(E) = \Delta_{\alpha\beta}(E \pm i\varepsilon)$ is the single particle Green function in the Landau basis, $|\alpha\rangle = |n_\alpha, k_\alpha\rangle$,

$$\tilde{\Delta}(E) = \Delta^{+}(E) - \Delta^{-}(E) \, ,$$

E_f is the Fermi energy and $N(E)$ is the total number of states with energy less than E.

This Green function formulation leads to the diagrammatic expansion for the conductivity as a power series in the disorder strength. Clearly the fundamental quantity of interest is

$$\langle\alpha|v_\mu|\beta\rangle \langle\gamma|v_\nu|\delta\rangle \, \overline{\Delta^{+}_{\beta\gamma}(E_f) \, \Delta^{-}_{\delta\alpha}(E_f)} \tag{7.12}$$

The matrix elements of the velocity operator are given in Appendix 1.1. The first few terms of the diagrammatic expansion are shown in Figure 7, the solid lines are the bare propagator $G^0_{\alpha\beta}(z)$, the dotted lines are correlators of the random potential and the circles are the velocity matrix element insertions.

1.8 The Effect of Interactions

In this section we will discuss the effects of the Coulomb interaction between electrons. We have neglected interactions up until now because they are not believed to be crucial to the understanding of the integer quantum Hall effect which has been qualitatively explained using a disordered ideal gas model. These interactions, however, present the possibility of Wigner crystallisation, which we discuss first, and are believed to be crucial to the understanding of the fractional quantum Hall effect which will be described in the latter part of the section.

Wigner (1934) considered the following situation: a gas of N electrons is contained in a volume Ω which is made to be very large, such that the number density of electrons is small. The potential energy of the system is given by

$E_p \sim \frac{e^2}{4\pi\varepsilon_0 R}$ where R is the mean separation and therefore $R \sim n^{-1/3}$ thus $E_p \sim n^{1/3}$. The kinetic energy for a degenerate electron gas is $E_k = \frac{3}{5} E_f \sim n^{2/3}$. Thus, if n is sufficiently small, $E_p \gg E_k$ and the system will minimise its potential energy with the electrons sitting on the sites of a regular lattice. The density cannot get too small or the gas will become non-degenerate and its kinetic energy will be independent of n ($E_k \propto kT$). The nec essary range of electron densities was unavailable at that time but has more recently become available in semiconductors. Experimental detection of Wigner crystals has been claimed, but the interpretation of the results is controversial. The same effect is however possible in a two-dimensional electron gas. Calculations by Lozovik and Yudson (1975), Fukuyama (1976) and Tsukada (1977) indicate that a Wigner solid phase should occur for a certain range of values of n and T and that the electrons should form a triangular lattice. This lattice will of course not have true long

range order because of the disordering effects of acoustic phonons in two-dimensions (Peierls (1934)), but is expected to have algebraic order and to melt via a Kosterlitz-Thouless type transition mediated by dislocations (Kosterlitz and Thouless (1973), Nelson and Halperin (1979) and Young (1979)). The existence of a Wigner solid in a two-dimensional electron gas formed at the interface between air and a liquid Helium film was discovered by Grimes and Adams (1979) using a variant on a method proposed by Shikin (1970, 1971, 1979) in which the resonant absorption of an R.F. electric field by the phonons of the Wigner lattice was measured at well defined frequencies for which the phonon wavelength coincided with the wavelength of surface acoustic waves (ripplons) of that frequency. Fukuyama (1979) found that the application of a perpendicular magnetic field stabilized the Wigner lattice.

A more exotic effect of the interactions is the fractional quantum Hall effect. Tsui, Stormer and Gossard (1982) and subsequently others have observed that, at very low temeratures and in very high purity samples, there are plateau features in the Hall conductivity corresponding to quantisation of σ_H at certain fractional filling factors $\nu=p/q$ where q is odd and p and q are small co-prime integers. In addition in the regions where the Hall conductivity is quantised the longitudinal conductivity falls to zero as in the integer effect. The necessity for high purity samples implies that this fractional quantum Hall effect is not a consequence of disorder but a collective effect due to the Coulomb interactions. The typical Coulomb and spin splitting energies in the experimental systems are much less than the cyclotron energy so that it is still reasonable to negelect Landau level mixing and to treat all electrons as being spin polarised.

The explanation of the fractional quantum Hall effect is based on the idea that the quantum many-body ground state has especially low energies for particular filling fractions and that it is separated from the first excited state by an energy gap. It is believed that this ground state cannot be a Wigner crystal as this would be pinned by any impurities leading to non-Ohmic conductivity which is not observed. Laughlin (1983) has proposed a variational wavefunction for filling fractions of the form 1/q (q is odd):

$$\Psi(\{z_i\}) = \prod_{i<j} (z_i - z_j)^q \exp\left\{-\frac{1}{4}\sum_i |z_i|^2\right\} ; \quad z_i = x_i + iy_i \qquad (8.1)$$

which has a very low energy (lower than a Wigner crystal) and describes an incompressible quantum liquid which has a uniform density and so will not be pinned by impurities. It is believed that the fractionally charged excitations about this ground state will be Anderson localised and therefore addition of electrons to the quantum liquid will not alter the conductivity. An extension of this theory due to Haldane (1983) constructs a hierarchy of such quantum liquids, each level formed by a condensate of the quasiparticles of the previous level in order to explain the effect at other odd denominator fractional fillings. Excitations about the Laughlin state have been studied by Girvin, MacDonald and Platzman (1985,1986) using a method which is based on Feynmans (1953,1954,1972) roton theory of liquid Helium.

Other approaches to the problem of the fractional quantum Hall effect include the quantum solid approach of Kivelson, Kallin, Arovas and Schrieffer (1986) and the work of Tao and Thouless (1983) who performed a self-consistent many body calculation assuming that the ground state had the form of a lattice in space of occupation numbers of the single particle states $|n,k\rangle$, and using a random phase approximation which predicted special states at both even and odd denominator fillings. Thouless (1985) showed, however, that the assumed form of the ground state was, because of its implied long-ranged spatial correlations, inconsistent with Laughlins wavefunction and has abandoned this approach. Trugman and Kivelson (1985) have found a number of exact results for electrons with short ranged interactions, particularly that the Laughlin wavefunction becomes an exact ground state as the range of interactions goes to zero at the appropriate densities. Recent experimental work by Nicholas et al. (1985) has shown indications of features at even denominator fractions in the n=1 (spin-split) Landau levels, but it is not clear that these features are due to the same physical phenomena as those referred to as the fractional quantum Hall effect.

Appendix 1.1: Matrix Elements of the Velocity Operator

The matrix elements of the velocity operator, $\mathbf{v}=(\mathbf{p}-e\mathbf{A}(\mathbf{r}))/m$, in the Landau basis are important in the calculation of current densities. The elements of the two orthogonal components are given here.

The x-component has matrix elements,

$$\langle n,k|v_x|n',q\rangle = \langle n,k|p_x|n',q\rangle/m$$

$$= il_c\omega_c\delta(p-q)\left\{ (n'/2)^{\frac{1}{2}}\delta_{n,n'-1} - (n/2)^{\frac{1}{2}}\delta_{n,n'+1} \right\}. \qquad (A1.1)$$

The y-component has matrix elements,

$$\langle n,k|v_y|n',q\rangle = \langle n,k|(p_y - x)|n',q\rangle/m$$

$$= -l_c\omega_c\delta(k-q)\left\{(n'/2)^{\frac{1}{2}}\delta_{n,n'-1} + (n/2)^{\frac{1}{2}}\delta_{n,n'+1} \right\}. \qquad (A1.2)$$

Appendix 1.2: Constructing the Wavepacket

We wish to construct a wavepacket centred on $\mathbf{r}=\mathbf{0}$ from states near E_0 in energy and examine its time development. We shall take a linear combination of stationary states of the form

$$\Psi_0(r) = \int dE\ f(E,E_0)\ \psi_E(r) \qquad (A2.1)$$

where $\psi_E(r)$ is an eigenstate of the Hamiltonian H[V]. A suitable choice for f is

$$f(E,E_0) = \frac{\Gamma/\pi}{(E-E_0)^2 + \Gamma^2}\ \psi_E^*(0). \qquad (A2.2)$$

The presence of $\psi_E^*(0)$ concentrates the wavepacket near the origin while the Lorentzian factor restricts the range of energies. If Γ is small then only a few eigenstates contribute and Ψ_0 will be spread over a large area. If Γ is large more states will be included but Ψ_0 will be concentrated on a smaller region.

From the time dependent Schrodinger equation the probability density for the wavepacket, $P(r,t)=|\Psi(r,t)|^2$, is given by

$$P(r,t) = \int dE dE' \frac{\Gamma/\pi}{(E-E_0)^2 + \Gamma^2} \frac{\Gamma/\pi}{(E'-E_0)^2 + \Gamma^2} e^{-i(E-E')t} \times$$

$$\times \overline{\psi_E^*(r)\psi_E(0)\psi_{E'}^*(0)\psi_{E'}(r)} \qquad (A2.3)$$

and thus

$$P(q,t) = \frac{\Gamma^2}{\pi^2} \int dE dE' \frac{e^{-i(E-E')t} S(q,E+E_0,E'+E_0)}{[E^2+\Gamma^2]\ [E'^2+\Gamma^2]} \qquad (A2.4)$$

where the spectral function, S, is defined as

$$S(q;E,E') = \int d^2r\ e^{iq\cdot r}\ S(r;E,E') \qquad (A2.5)$$

and

$$S(r;E,E') = \overline{\int dE_1 dE_2 \delta(E-E_1)\delta(E'-E_2)\psi^*_{E_1}(r)\psi_{E_1}(0)\psi^*_{E_2}(0)\psi_{E_2}(r)}. \qquad (A2.6)$$

Appendix 1.3: The Asymptotic Form of The Spectral Function

We have seen that the disorder averaged probability density for the wave packet Ψ_0 can be written as an integral transform of the spectral function $S(q,E,E')$. We now define $\omega=E-E'$ and $\varepsilon=\frac{1}{2}(E+E')$; $P(q,t)$ now has the form

$$P(q,t) = \frac{16\ \Gamma^2}{\pi^2} \int d\varepsilon\ d\omega \frac{e^{-i\omega t}\ S(q;E_0+\varepsilon+\frac{\omega}{2}\ ,E_0+\varepsilon-\frac{\omega}{2})}{(\omega+\eta)(\omega-\eta)(\omega+\eta^*)(\omega-\eta^*)} = \frac{\Gamma^2}{\pi^2} \int d\varepsilon\ F(\varepsilon)$$

where $\eta=2(\varepsilon+i\Gamma)$ and $F(\varepsilon)$ is defined below. We shall simplify the notation by writing $S(q;E_0+\varepsilon+\omega/2\ ,E_0+\varepsilon-\omega/2) = s(\omega)$. Then $F(\varepsilon)$ has the form

$$F(\varepsilon) = \int \frac{s(\omega)e^{-i\omega t}}{(\omega+\eta)(\omega-\eta)(\omega+\eta^*)(\omega-\eta^*)}\ d\omega\ .$$

This Fourier integral can be performed by closing the contour of integration in the lower half-plane. There are contributions to the integral from the poles at $\omega=\eta^*$ and $\omega=-\eta$ and from any poles of $s(\omega)$. The residues of the poles at at η^* and $-\eta$ are of the form

$$\frac{s(\pm 2\varepsilon-2i\Gamma)e^{\pm 2i\varepsilon t-2\Gamma t}}{-8(\varepsilon^2+\Gamma^2)(\varepsilon\mp i\Gamma)}$$

which vanishes for $t\gg 1/(2\Gamma)$. We expect the probability to have the time dependence of equation 6.3. If this is the case then $s(\omega)$ must have a simple pole at $\omega=-iDq^2$, which will give the residue

$$\lim_{\omega\to -iDq^2} \frac{(\omega+iDq^2)\ s(\omega)e^{-q^2Dt}}{Z(q^2,\varepsilon,\Gamma)}$$

where $Z(q^2,\varepsilon,\Gamma) = D^4q^8 - 8D^2q^4(\varepsilon^2-\Gamma^2) + 16(\varepsilon^2+\Gamma^2)^2$

which is the dominant term at large times in the hydrodynamic régime ($q^2\to 0$). Thus the spectral function $s(\omega)$ has the asymptotic form

$$s(\omega) \sim \frac{C}{\omega+iDq^2} \qquad q^2\to 0 \ . \tag{A3.5}$$

The remaining ε integration cannot contribute to the time dependence and the probability density, therefore, has the form

$$P(q,t) \sim \frac{2i\Gamma^2}{\pi}\int d\varepsilon \ \frac{C}{Z(q^2,\varepsilon,\Gamma)}\ e^{-q^2Dt} = P(q,0)\ e^{-q^2Dt} \tag{A3.6}$$

as required.

Appendix 1.4: The Spectral Function and the Two-Particle Green Functions

The Spectral function is defined in Appendix 1.2. Consider the Lorentzian representation of the Dirac delta function

$$\delta(x) = \underset{\omega\to 0^+}{\text{Lim}} \frac{\omega/\pi}{x^2+\omega^2} = \frac{1}{2\pi i}\underset{\omega\to 0^+}{\text{Lim}}\left[\frac{1}{x-i\omega} - \frac{1}{x+i\omega}\right] \tag{A4.1}$$

hence

$$\int dE\ \delta(E_1-E)\psi_E^*(r)\psi_E(0) = \frac{1}{2\pi i}\left[\Delta(r,0;E_1-i\omega) - \Delta(r,0;E_1+i\omega)\right] \tag{A4.2}$$

and therefore $S(r,E_1,E_2)$ is given by the expression

$$-\frac{1}{4\pi^2}\ \underset{\omega\to 0^+}{\text{Lim}}\ \overline{\left[\Delta^-(r,0;E_1) - \Delta^+(r,0;E_1)\right]\left[\Delta^-(0,r;E_2) - \Delta^+(0,r;E_2)\right]}$$

where the retarded and advanced Green functions are defined as

$$\Delta^{\pm}(r,r';E) = \Delta(r,r';E\pm i\omega). \tag{A4.3}$$

On taking the average the ++ and -- terms are short ranged and so the long distance behaviour of $S(r)$ will come from the cross terms.

$$S(r;E_1,E_2) \sim (4\pi^2)^{-1}\ \underset{\omega\to 0}{\text{Lim}}\left[\overline{\Delta^+(r,0;E_1)\ \Delta^-(0,r;E_2)} + \overline{\Delta^-(r,0;E_1)\ \Delta^+(0,r;E_2)}\right] \qquad |r|\to\infty. \tag{A4.4}$$

We now choose $E_1=E+\omega+i0$ and $E_2=E-\omega-i0$ for small ε and let $\varepsilon=-i\omega$ to give

$$\begin{aligned} &S(r;E+i\varepsilon,E-i\varepsilon) \sim (2\pi^2)^{-1}\ \tilde{Q}(r,E+i\varepsilon) \quad |r|\to\infty \text{ and} \\ &S(q;E+i\varepsilon,E-i\varepsilon) \sim (2\pi^2)^{-1} Q(q,E+i\varepsilon) \quad q^2\to 0. \end{aligned} \tag{A4.5}$$

Appendix 1.5: A Sum Rule

We will now derive a useful sum rule due to Velicky (1969) connecting the one and two-particle Green functions. It is useful because it relates the hydrodynamic behaviour of the two-particle function $Q(q,E+i\varepsilon)$ to the density of states. In the field theoretic formulation of localisation problems this appears as a Ward identity (McKane and Stone 1981). Consider

$$I = 2i\omega \int d^2r' \; |\Delta(r,r';\varepsilon+i\omega)|^2$$

$$= 2i\omega \int d^2r' \int dE\, dE' \; \frac{\overset{*}{\psi}_E(r)\psi_E(r')\overset{*}{\psi}_{E'}(r')\psi_{E'}(r)}{(\varepsilon+i\omega-E)(\varepsilon-i\omega-E')} \qquad \text{(A5.1)}$$

Now

$$\int d^2r' \; \overset{*}{\psi}_E(r')\psi_{E'}(r') = \delta(E-E') \qquad \text{(A5.2)}$$

so

$$I = 2i\omega \int dE \; \frac{\overset{*}{\psi}_E(r)\psi_E(r)}{|\varepsilon+i\omega-E|^2} = \int dE \; \overset{*}{\psi}_E(r)\psi_E(r) \left[\frac{1}{\varepsilon-i\omega-E} - \frac{1}{\varepsilon+i\omega-E} \right]$$

$$= \Delta(r,r;\varepsilon-i\omega)-\Delta(r,r;\varepsilon+i\omega) \; . \qquad \text{(A5.3)}$$

Averaging over disorder gives

$$2i\omega \int d^2r' \; \tilde{Q}(r-r',\varepsilon+i\omega) = G(r,r;\varepsilon-i\omega) - G(r,r;\varepsilon+i\omega) \qquad \text{(A5.4)}$$

and therefore

$$\lim_{\omega\to 0} \; \omega \int d^2r' \; \tilde{Q}(r;\varepsilon+i\omega) = \pi\rho(\varepsilon)$$

or, Fourier transforming

$$\lim_{\omega\to 0^+\omega} \; Q(q=0;\varepsilon+i\omega) = \pi\rho(\varepsilon) \; .$$

Appendix 1.6: Fourier Transforms for Retarded Propagators

For use in subsequent chapters we shall evaluate the integral

$$I_n = \int_{-\infty+i0}^{+\infty+i0} dz \; \frac{e^{-izt}}{[\, z-C \,]^n} \; .$$

If $t<0$ then we can close the contour in the upper half plane. The closed contour contains no singularities of the intgrand and therefore the integral vanishes. If $t>0$ then we must close the contour in the lower half plane encircling the n^{th} order pole at $z=C$. Thus

$$I_n = -2\pi i\theta(t)\,\frac{1}{(n-1)!}\,\frac{d^{n-1}}{dz^{n-1}}\,e^{-izt}\Big|_{z=C}$$

that is

$$I_1 = -2\pi i\theta(t)e^{-iCt}$$

$$I_2 = -2\pi t\theta(t)e^{-iCt}$$

$$I_3 = -2\pi i\left[-\frac{t^2}{2}\right]\theta(t)\,e^{-iCt}$$

Appendix 1.7: Calculation of $C_n(r,r')$

We have seen (equation 5.4) that we can write the Green function in terms of the known stationary states of the system using the basis functions introduced in section 1.1 (equation 1.2)

$$G^0(r,r';z) = \sum_{n,k} (z-E_n)^{-1} \langle r|n,k\rangle\langle n,k|r'\rangle$$

using the explicit expressions for the wavefunctions and, assuming an infinite system, changing the sum over k into an integral and taking $1_c=1$

$$G^0(r,r';z) = \sum_{n} (z-E_n)^{-1}\, C_n(r,r')$$

where

$$C_n(r',r) = \frac{1}{2\pi}\int dk\; e^{ik(y-y')}\;\chi_n(x+k)\chi_n(x'+k)$$

shifting the integration variable gives

$$C_n(r',r) = e^{-ix(y-y')}\;I_n(x-x',y-y')$$

where

$$I_n(x,y) = \int dk\; e^{iky}\;\chi_n(k)\chi_n(k+x). \qquad (A7.1)$$

We now employ the generating function for the Hermite polynomials to give

$$I_n(x,y) = \frac{1}{2^n n!}\, e^{-(x^2+y^2)/4}\, e^{-ixy/2}\, \frac{\partial^{2n}}{\partial t^n\, \partial s^n} \left| e^{-y(t-s)+ix(t+s)+2ts} \right|_{t=s=0} .$$

This can be evaluated to yield

$$I_n(x,y) = e^{-ixy/2}\, e^{-(x^2+y^2)/4} \sum_{r=0}^{\infty} \frac{n!}{r!(n-r)!}\, \frac{(-1)^{n-r}}{(n-r)!} \left[\frac{x^2+y^2}{2} \right]^{n-r} .$$

(A7.2)

The infinite sum is a representation of the n^{th} order Laguerre polynomial so, substituting into the above expression for $C_n(r',r)$, this gives

$$C_n(r',r) = \frac{1}{2\pi}\, e^{i(x+x')(y-y')}\, e^{-\frac{1}{4}|r-r'|^2}\, L_n\left[\tfrac{1}{2}|r-r'|^2 \right]$$

which gives equation 5.7 on reinserting the dimensional constant l_c.

Figure1
Schematic illustration of the classical Hall effect

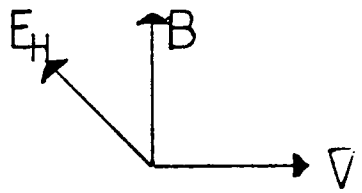

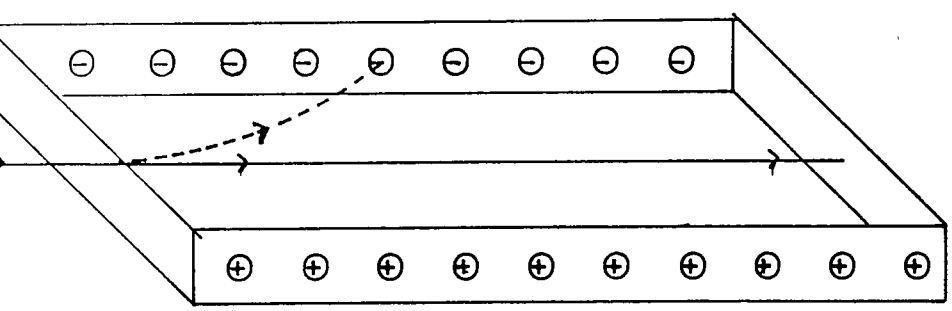

Figure 2
(a) Schematic graph of the variation of longitudinal and Hall conductivities with Fermi energy in the quantum Hall effect.
(b) The structure of a disorder broadened energy band.

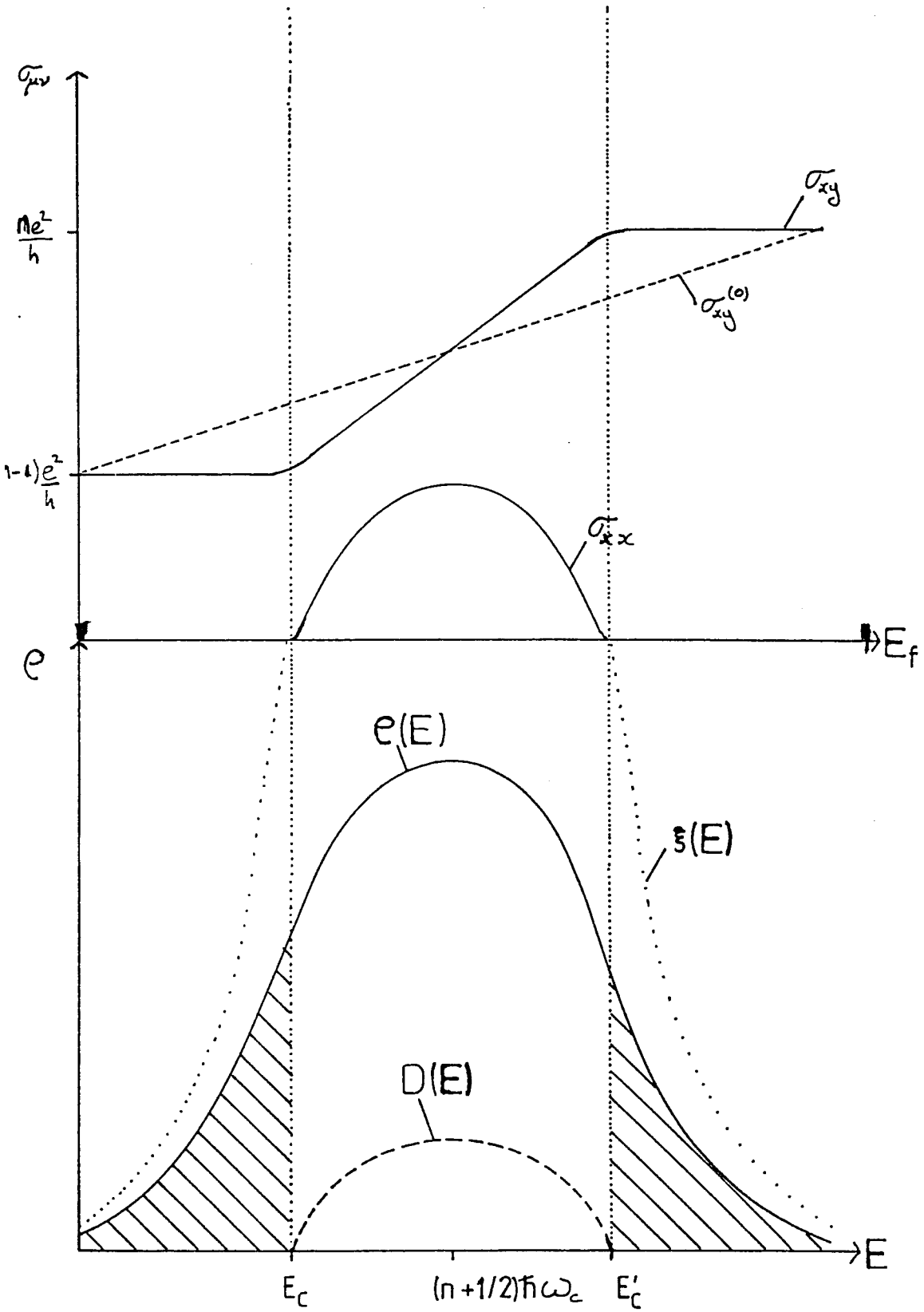

Figure 3
Diagrammatic form of the scattering expansion of equation (5.16)

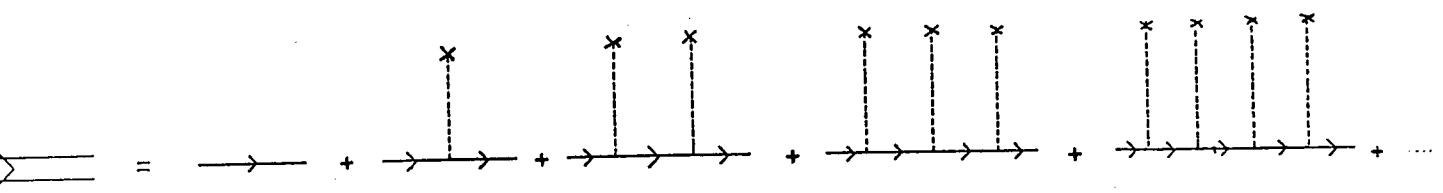

Figure 4
(a) Diagrammatic expansion of the disorder-averaged one-particle Green function (equation (5.17))

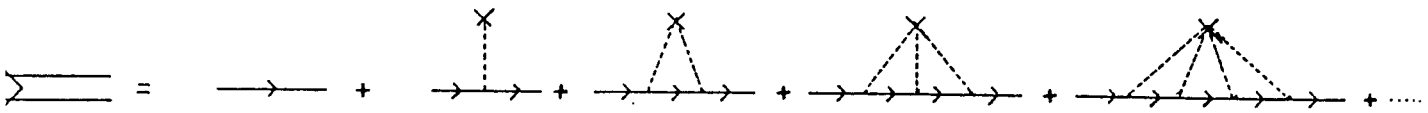

(b) Diagrammatic expansion of the disorder-averaged two-particle Green function (equation 5.19)

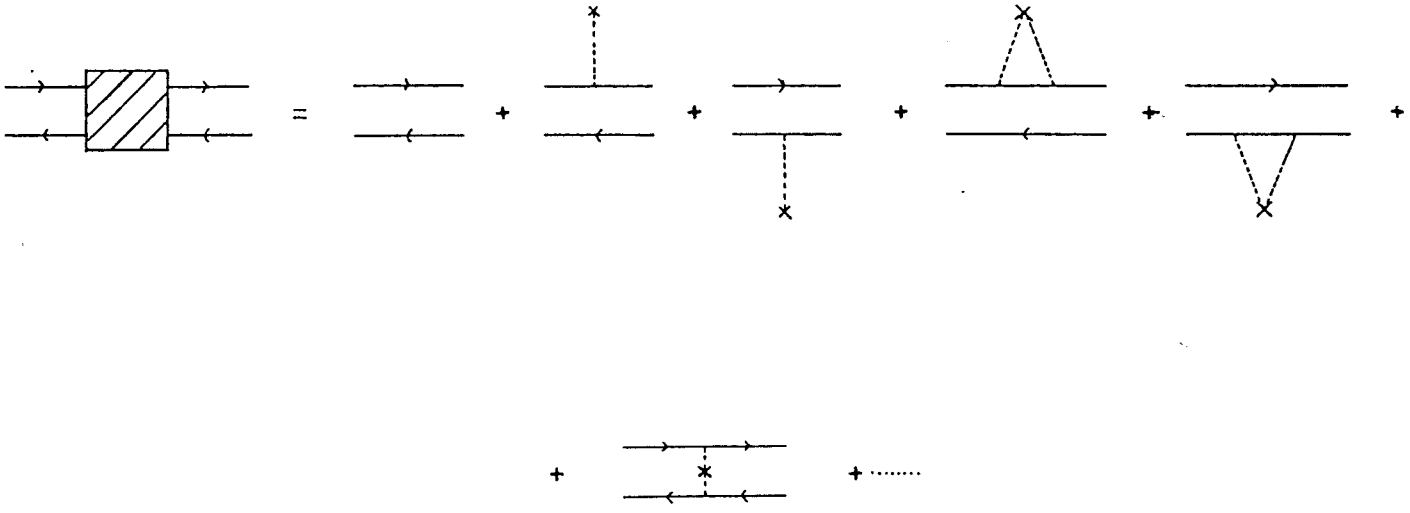

Figure 5
The diagrammatic expansion for the disorder-averaged one-particle Green function in the presence of a Gaussian random potential.

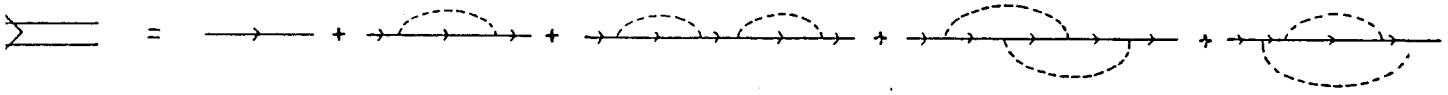

Figure 6
The diagrammatic expansion for the disorder-averaged one-particle Green function in the presence of a random distribution of scattering centres.

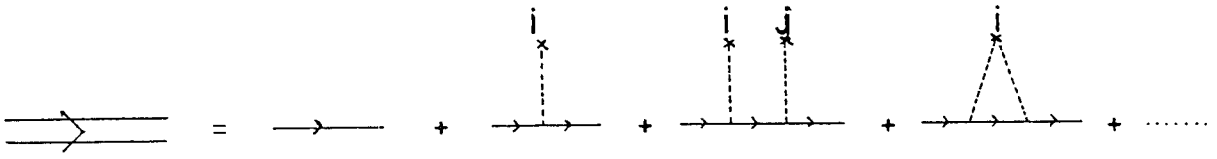

Figure 7
The diagrammatic expansion for the expression (7.12) used in the calculation of the conductivities.

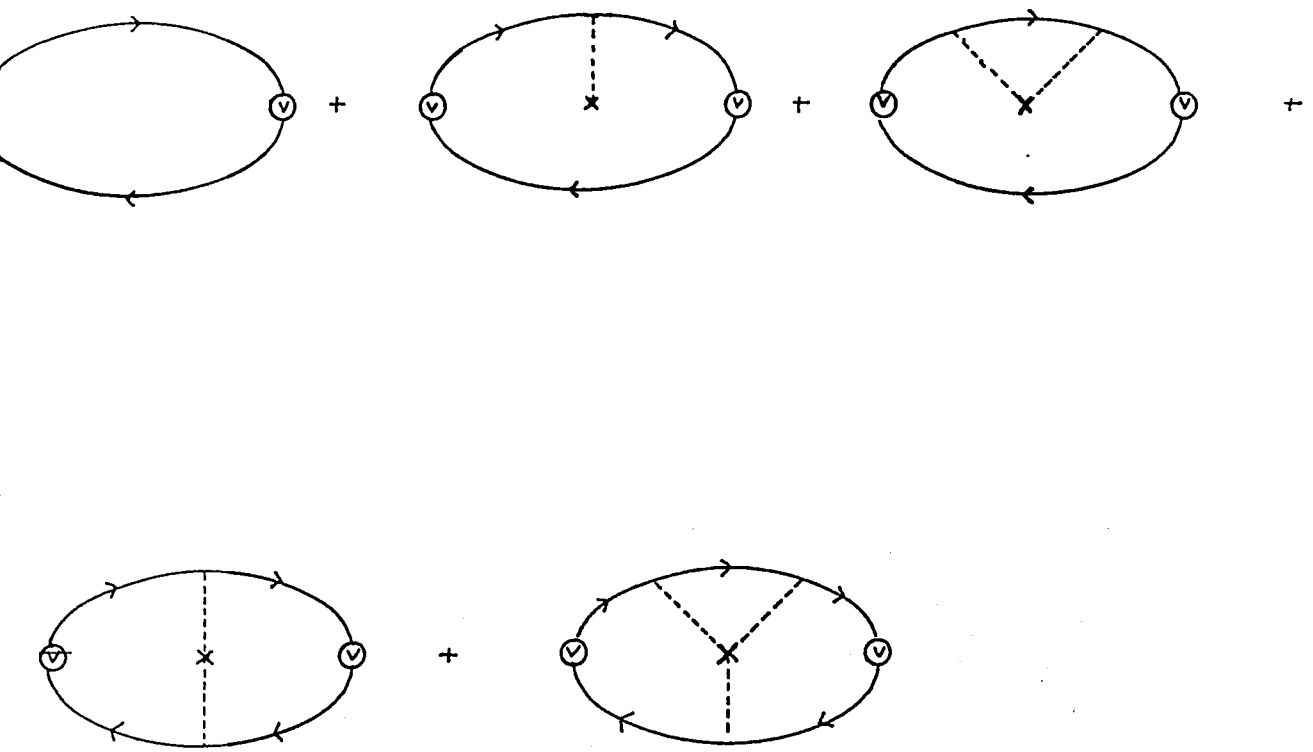

Chapter 2

The Smooth Random Potential

This chapter describes a method of finding the density of states of a two-dimensional electron gas in a strong magnetic field and a slowly (spatially) varying random potential. The method is applied to the problem of calculating transport properties but is found to correspond to a short time expansion for the behaviour of a wavepacket and so only describes ballistic motion.

The work described in this chapter was performed in close collaboration with Dr. J.T. Chalker and has been published as Benedict and Chalker (1985).

2.1 Introduction

As discussed in section 1.1, the two-dimensional electron gas in a strong magnetic field is characterised by four scales; a natural starting point for theoretical considerations is to examine extreme values of the two dimensionless ratios, $v/\hbar\omega_c$ and L_d/l_c, that can be formed from these quantities. The aim of this chapter is to treat the limit in which the correlation length of the random potential is much greater than the cyclotron length ($l_c/L_d \to 0$). We develop a systematic expansion for the disorder-averaged Green functions in powers of the quantity, $\Lambda=(l_c/L_d)^2$, from which physical properties are calculated. In particular we obtain zeroth and first order terms in an expansion for the density of states. The averaged two-particle Green function, which contains information on transport properties, can also be calculated in this manner but we find that the time scales relevant to diffusion and localisation are inaccessible. In all the following we shall employ units in which $l_c=1$ and $\hbar\omega_c=1$.

The random potential studied here is taken to be such that its Fourier components are, subject to the constraint $V^*(\mathbf{q})=V(-\mathbf{q})$ (neccessary in order that $V(r)$ be real), independent Gaussian random

variables. Hence the values of V(r) are correlated at different points, but the only non-zero cumulant is the second which has the form

$$\Xi_2(\mathbf{r},\mathbf{r}') = \overline{V(\mathbf{r})V(\mathbf{r}')} = v^2 e^{-\Lambda|\mathbf{r}-\mathbf{r}'|^2}, \qquad (1.1)$$

Our assumption is that the potential is a slowly varying function of position, on the scale of the cyclotron length, so that Λ is a small parameter.

The remainder of this chapter is organised as follows. In section two it is shown how partial resummation of the standard perturbation theory outlined in section 1.5 results in an expansion in powers of Λ. Results for the density of states are described in section three and for the two-particle time Green function in section four. Section five contains a brief summary.

2.2 Perturbation Theory

We wish to construct an alternative perturbation scheme to that outlined in chapter one, in which the averaged Green functions are expanded as a Taylor series in Λ, so that

$$G(\mathbf{r},\mathbf{r}';z) = G(\mathbf{r},\mathbf{r}';z)\Big|_{\Lambda=0} + \Lambda \left.\frac{dG(\mathbf{r},\mathbf{r}';z)}{d\Lambda}\right|_{\Lambda=0} + O(\Lambda^2) .$$

The first term in this series is simply a summation of the Edwards series in the limit $\Lambda \to 0$. This is the sum of all diagrams with the rule for the interaction part changed to only carry a factor of v^2. The summation can be performed (Appendix 2.1) giving

$$G(\mathbf{r},\mathbf{r}';z)\Big|_{\Lambda=0} = \int_{-\infty}^{\infty} G^0(\mathbf{r},\mathbf{r}';z-U)P(U)dU , \qquad (2.1)$$

where

$$P(U) = (2\pi v^2)^{-\frac{1}{2}} \exp\left\{ -\frac{U^2}{2v^2} \right\} , \qquad (2.2)$$

in the sense that, if we expand the resolvent in the propagator on the right hand side as a Taylor series in U, and then integrate term by term we generate the Edwards series for the left hand side. Although the series are not convergent we assume that that, because

we have effectively resummed to all orders in v, (2.1) is valid for any strength of disorder. The rhs is represented by the diagram in figure 1, where the "blob" denotes convolution with P(U).

That the result is obvious can be seen by considering the physical meaning of the $\Lambda \to 0$ limit. In this limit the values of the potential are correlated equally strongly at all distances, so the potential is a constant over the whole plane. The Green function for the Hamiltonian $H'=H_0+V_0$, where V_0 is a constant, is $G'(\mathbf{r},\mathbf{r}';z)=G^0(\mathbf{r},\mathbf{r}';z-V_0)$ so when we average over the configurations of the disorder, we merely have to average over all possible values of the constant potential V_0, which leads directly to equation (2.1).

To obtain the $O(\Lambda)$ correction to the Green function we must differentiate the Edwards series and evaluate the derivative at $\Lambda=0$. Each $2n^{th}$ order (in v) diagram when differentiated gives n copies of the original diagram, in each of which one dashed line is replaced by a dotted line with the factor

$$\left.\frac{d}{d\Lambda}\right|_{\Lambda=0} \overline{V(r)V(r')} = -|r-r'|^2 v^2 . \qquad (2.3)$$

For example the diagram in figure 2a when differentiated gives the diagrams in figures 2b and 2c.

One can show (Appendix 2.2) that in the same sense as before

$$\left.\frac{dG}{d\Lambda}\right|_{\Lambda=0} = \int P(U) \iint \left.\overline{\frac{dV(r)V(r')}{d\Lambda}}\right|_{\Lambda=0} \times$$

$$\times\ G^0(r,r_1;z-U)\ G^0(r_1,r_2;z-U)\ G^0(r_2,r';z-U)\ d^2r_1\ d^2r_2\ dU\ . \qquad (2.4)$$

We denote this by the diagram in figure 3. For the two-particle Green function

$$K(r_1,r_1';z_1;r_2,r_2';z_2) = \overline{\Delta(r_1,r_1';z_1)\ \Delta(r_2,r_2';z_2)}\ , \qquad (2.5)$$

the same arguments apply. The diagrammatic expansion for K is shown in figure 4.

2.3 Calculation of the Density of States

In order to calculate the density of states for the system at any order in Λ we employ the relation 5.7 of chapter one. At order Λ^0 this gives

$$\left.\overline{\rho(E)}\right|_{\Lambda=0} = (2\pi i)^{-1} \int_{-\infty}^{\infty} P(V) \lim_{\varepsilon\to 0} \left[G^0(r,r;z-V)\right]_{E+i\varepsilon}^{z=E-i\varepsilon} dV\ , \qquad (3.1)$$

where $$\left[x \right]_b^a = a-b \quad .$$

This yields (see Appendix 2.3)

$$\overline{\rho(E)}=(2\pi)^{-1} \sum_n P(E-E_n) \quad . \tag{3.2}$$

Thus, as expected, we have a sequence of Gaussian bands centred on the unperturbed Landau level energies.

The $O(\Lambda)$ correction to this is

$$\Lambda\Delta\rho(E) = \Lambda \left.\frac{d\bar{\rho}}{d\Lambda}\right|_{\Lambda=0} = \frac{\Lambda}{2\pi i} \lim_{\varepsilon\to 0} \left[\left.\frac{dG(r,r;z)}{d\Lambda}\right|_{\Lambda=0} \right]_{E+i\varepsilon}^{z=E-i\varepsilon} . \tag{3.3}$$

The expression can be evaluated (Appendix 2.4) to obtain

$$\begin{aligned}\Delta\rho(E) = \frac{v^2}{\pi} \sum_n \Bigg\{ & (2n+1)P(E-E_n)\left[1+\frac{1}{2v^2}\left[1-\frac{(E-E_n)^2}{v^2}\right]\right] \\ & + n\left[1+\frac{(E-E_n)}{v^2}\right] P(E-E_{n-1}) \\ & - (n+1)\left[1-\frac{(E-E_{n+1})}{v^2}\right] P(E-E_{n+1}) \Bigg\} \quad . \end{aligned} \tag{3.4}$$

In figures 5 and 6, ρ and $\Delta\rho$ are shown for $v=0.2$

The effect of this correction is to make the bands taller and narrower: the states are concentrated towards the centre of the band. In addition this narrowing is more pronounced for higher Landau levels. We can explain this by considering an eigenfunction composed wholly of basis states from a given Landau level. The energy of this eigenstate relative to the unperturbed Landau level energy is the average of the random potential over the region occupied by the wave-packet, weighted by the wave function for the state. Thus large fluctuations in the random potential will be smoothed out, and states far from the band centre will become less likely as the correlation length for the potential decreases. Since the area of the most localised wave-packet belonging wholly to the nth Landau level is proportional to n; this effect will be greater for higher Landau levels.

2.4 Transport Properties

A particular four-point Green function of especial interest is the diffusion propagator in the time domain

$$\Pi(r,r';t) = \frac{1}{4\pi^2}\int_{-\infty+i0}^{\infty+i0} dz \int_{-\infty-i0}^{\infty-i0} dz'\, e^{-i(z-z')t}\, \overline{\Delta(r,r';z)\Delta(r',r;z')} \quad (4.1)$$

Employing the zeroth order (in Λ) diagram for this, we find (Appendix 2.8) that

$$\Pi(r,r';t)\Big|_{\Lambda=0} = |\Gamma^0(r,r';t)|^2 \quad . \quad (4.2)$$

This is easily understood by considering the $\Lambda\to 0$ limit to give a system with a constant potential. The addition of such a constant potential $V(\mathbf{r})=U\ \forall \mathbf{r}$ merely shifts the zero of the energy scale and therefore just multiplies Γ^0 by a phase factor, e^{iUt}, which is invisible after taking the modulus.

The first order correction to the diffusion propagator gives, neglecting Landau level mixing, (see Appendix 2.9)

$$\Lambda \frac{d}{d\Lambda}\Big|_{\Lambda=0} \Pi(r,r';t) = -v^2t^2\Lambda\,\theta(t)\sum_n F_n(r,r') \ , \quad (4.3)$$

and where $F_n(\mathbf{r},\mathbf{r}')$ is a time independent function of positions. Thus the effective expansion parameter in the time domain is Λv^2t^2, so the expansion will only be useful for short times (or high frequencies), precluding its application to a calculation of the D.C. conductivity tensor.

The time dependence of the expansion parameter can be understood by considering the picture of the two-dimensional electron gas in a strong magnetic field and a slowly varying random potential due to Luryi and Kazarinov which was briefly described in section 1.2. Each electron moves on an equipotential contour subject to Bohr-Sommerfeld quantisation. We can, for very slowly varying disorder, expand the potential as

$$V(r) \approx V(r_0) + (r-r_0)\cdot\nabla V(r_0) \quad . \quad (4.4)$$

The first term is an irrelevant shift in the zero of the energy but the second is equivalent to applying an electric field of strength $\mathbf{E}=\nabla V$ to the electron. From section 1.1 we know that the mean velocity

of the electron is $u_\mu=\varepsilon_{\mu\nu}E_\nu=\varepsilon_{\mu\nu}\partial_\nu V(r)$ (the classical result). Hence the typical speed of the electron is proportional to $\overline{|\nabla V(r)|}$. Assuming that the disorder is isotropic

$$\overline{|\nabla V(r)|} = 2^{1/2}\left[\overline{\left(\frac{\partial V(x,y)}{\partial x}\right)^2}\right]^{1/2} . \tag{4.5}$$

Now

$$\overline{\left[\frac{\partial V(x,y)}{\partial x}\right]^2} = \lim_{\delta\to 0} \frac{\overline{[V(x+\delta,y)]^2} + \overline{[V(x,y)]^2} - 2\overline{V(x+\delta,y)V(x,y)}}{\delta^2} \tag{4.6}$$

$$= \lim_{\delta\to 0} \frac{2v^2-2v^2e^{-\Lambda\delta^2}}{\delta^2} = 2v^2\Lambda .$$

Hence the typical speed of an electron is proportional to vl_c/L_d.

There are two fundamental time scales for the electronic motion in this sytem. Firstly there is the time scale over which the motion of a wavepacket is effectively ballistic, t_B. Typically t_B is the time for the wavepacket to traver se a distance equal to its own width which will be proportional to l_c. Using the above estimate for the typical speed of an electron we find that

$$t_B \sim l_c \times \frac{L_d}{v\, l_c} = \left[l_c\Lambda^{1/2}\right]^{-1} . \tag{4.7}$$

This clearly diverges as $\Lambda\to 0$ so that in the small Λ regime a wavepacket only moves very slowly and ballistically. The other timescale is the time, t_1, for an electron to traverse a distance of the order of the length of a closed contour which is proportional to L_d. It is on this timescale that localisation effects will become visible. Using the estimate for the speed of the electron gives

$$t_1 \sim L_d \frac{L_d}{vl_c} = l_c \left[v\Lambda \right]^{-1} \tag{4.8}$$

clearly this timescale is much longer than t_B and consequently no localisation effects will be visible in the $\Lambda\to 0$ limit.

2.5 Conclusions

It has been shown that the standard perturbation series for the disorder averaged Green functions of the problem can be partially resummed to obtain a new perturbation series in powers of the inverse correlation area, Λ, of the random potential. The expansion has been employed in the evaluation of the single-particle density of states. At $\Lambda=0$ this has the form of a regular sequence of Gaussian bands centred on the Landau levels (3.1). The first order correction, for finite Λ, mixes adjacent bands and concentrates the states toward the centre of each band, the concentration being greater for higher Landau levels (3.2). It has been shown that this technique is not useful for the calculation of low frequency transport coefficients

Appendix 2.1: Resummation of the Edwards series in the limit $\Lambda=0$.

We can write the standard Edwards series in the form

$$G(r,r';z) = \sum_{n=0}^{\infty} \sum_{\eta} \int..\int \prod_{i=0}^{2n} G^0_{i,i+1} \prod_{<i,j>_\eta} \overline{V_i V_j} \prod_{1=0}^{2n} d^2 r_1 \quad (A1.1)$$

where the second sum is over all distinct 2n-vertex diagrams η, of which there are $(2n-1)!!$,

$$G^0_{i,j} = G^0(r_i,r_j;z) \text{ with } \quad r_0 = r \ , \ r_{2n+1} = r'$$

and $<j,k>_\eta$ is an ordered (j>k) pair of vertices which are connected by dotted lines in the diagram η. The product

$$\prod_{<i,j>_\eta}$$

is over all such connected pairs in the diagram η.In the limit $\Lambda \to 0$ $\overline{V_i V_j} = v^2$ for all pairs $<i,j>_\eta$ and all diagrams so that

$$G(r,r';z)\Big|_{\Lambda=0} = \sum_{n=0}^{\infty} v^{2(2n-1)!!} \int..\int \prod_{i=0}^{2n} G^0_{i,i+1} \prod_{j=1}^{2n} d^2 r_j \ . \quad (A1.2)$$

Now $$G^0_{i,j} = \sum_{\alpha} f_\alpha \Gamma_\alpha(r_i,r_j) \ ,$$

where $f_\alpha = (z-E_\alpha)^{-1}$ and $\Gamma_\alpha(r_i,r_j) = <r_i|\alpha><\alpha|r_j>$;

with $|\alpha> = |n,k>$ and $E_\alpha = E_n$. All the space integrations in equation (A1.2) are now trivial using

$$\int |r><r| \, d^2 r \quad = \quad 1 \ .$$

Use of the orthogonality relation, $<\alpha|\alpha'> = \delta_{\alpha,\alpha'}$, gives finally

$$G(r,r';z)\Big|_{\Lambda=0} = \sum_{\alpha} \Gamma_\alpha(r,r') \sum_{n=0}^{\infty} f_\alpha^{2n+1} \ (2n-1)!! \ v^{2n} \ .$$

This expression for the left-hand side of equation (2.1) is to be compared with

$$J^0(r,r';z) = \int_{-\infty}^{\infty} P(V) \ G^0(r,r';z-V) \ dV$$

$$= \sum_{\alpha} \Gamma_{\alpha}(r,r') \int_{-\infty}^{\infty} P(V)\ (z-V-E_{\alpha})^{-1}\ dV\ .$$

Expanding the resolvent in a Taylor series in V gives

$$(z-V-E_{\alpha})^{-1} = (z-E_{\alpha})^{-1} + V\ (z-E_{\alpha})^{-1} + \ldots\ldots\ldots$$

$$= \sum_{n=0}^{\infty} f_{\alpha}^{n+1}\ V^{n}\ .$$

Term by term integration of this gives

$$J^{0}(r,r';z) = \sum_{\alpha} \Gamma_{\alpha}(r,r') \sum_{n=0}^{\infty} f_{\alpha}^{n+1} \int P(V) V^{n}\ dV\ .$$

Now P(V) is an even function so the integration over V vanishes for odd values of n; while, for even values of n,

$$\int V^{2n} P(V)\ dV = (2n-1)!!\ v^{2n}\ .$$

It follows, therefore, that

$$J^{0}(r,r';z) = \sum_{\alpha} \Gamma_{\alpha}(r,r') \sum_{n=0}^{\infty} v^{2n}\ (2n-1)!!\ f_{\alpha}^{2n+1}$$

$$= G(r,r';z)\Big|_{\Lambda=0}\ , \qquad \text{as required.}$$

Appendix 2.2: Resummation of the series expansion for the derivative of the Green function in the $\Lambda \to 0$ limit

Differentiating A1.1 with respect to Λ gives

$$\left.\frac{dG}{d\Lambda}\right|_{\Lambda=0} = \sum_{n=1}^{\infty} \sum_{\eta} \int\!\ldots\!\int \prod_{i=0}^{2n} G^{0}_{i,i+1}\ \left.\frac{d}{d\Lambda}\right|_{\Lambda=0} \left[\prod_{<j,k>_{\eta}} \overline{V_j V_k} \right] \prod_{l=1}^{2n} d^{2}r_{l}\ ,$$

employing the product rule for derivatives yields

$$\left.\frac{dG}{d\Lambda}\right|_{\Lambda=0} = \sum_{n=1}^{\infty}(-v^{2n}) \sum_{\eta} \sum_{<\mu,\nu>_\eta} \iint |r_\mu - r_\nu|^2 \quad X$$

$$X \left\{ \int..\int \prod_{\kappa=0}^{\nu-1} G^0_{\kappa,\kappa+1} \prod_{\xi=1}^{\nu-1} d^2r_\xi \quad X \right.$$

$$X \int..\int \prod_{\kappa=\nu}^{\mu-1} G^0_{\kappa,\kappa+1} \prod_{\xi=\nu+1}^{\mu-1} d^2r_\xi \quad X$$

$$\left. X \int..\int \prod_{\kappa=\mu}^{2n} G^0_{\kappa,\kappa+1} \prod_{\xi=\mu+1}^{2n} d^2r_\xi \right\} \quad d^2r_\mu \, d^2r_\nu \, .$$

The space integrations inside the curly brackets can be performed as before, leaving

$$\left.\frac{dG}{d\Lambda}\right|_{\Lambda=0} = \sum_{\alpha\beta\eta} \Phi_{\alpha\beta\gamma}(r,r') \sum_{n=1}^{\infty} \sum_{\eta} \sum_{<\mu,\nu>_\eta} (-v^{2n}) \, f_\alpha^{\ \nu} \, f_\beta^{\ \mu-\nu} \, f_\gamma^{\ 2n+1-\mu} \, ,$$

where $\Phi_{\alpha\beta\gamma}(r,r') = \iint |r_1 - r_2|^2 \, \Gamma_\alpha(r,r_1) \, \Gamma_\beta(r_1,r_2) \, \Gamma_\gamma(r_2,r') \, d^2r_1 d^2r_2$

Each 2n-vertex diagram, in which vertices μ,ν are connected contributes with the same weight and there are (2n-3)!! of these, so

$$\left.\frac{dG}{d\Lambda}\right|_{\Lambda=0} = \sum_{n=1}^{\infty} (2n-3)!! v^{2n} \sum_{\mu=2}^{2n} \sum_{\nu=1}^{\mu-1} \sum_{\alpha} \Phi_{\alpha\beta\gamma}(r,r') \, f_\alpha^{\ \nu} \, f_\beta^{\mu-\nu} \, f_\gamma^{2n+1-\mu} \, .$$

Define

$$J^1(r,r';z) = \int_{-\infty}^{\infty} P(V) \iint \left.\frac{d}{d\Lambda}\right|_{\Lambda=0} \left[\overline{V(r_1)V(r_2)}\right] G^0(r,r_1;z-V) \, G^0(r_1,r_2;z-V) \, X$$

$$X \quad G^0(r_2,r';z-V) \, d^2r_1 \, d^2r_2 \, dV \, .$$

On expanding the propagator in terms of Landau states, this gives

$$J^1 = -v^2 \sum_{\alpha\beta\gamma} \Phi_{\alpha\beta\gamma}(r,r') \int_{-\infty}^{\infty} P(V) \, \frac{1}{z-E_\alpha-V} \, \frac{1}{z-E_\beta-V} \, \frac{1}{z-E_\gamma-V} \, dV \, .$$

Again expanding the resolvent in V gives

$$J^1 = -v^2 \sum_{\alpha\beta\gamma} \Phi_{\alpha\beta\gamma}(r,r') \sum_{i,j,k=0}^{\infty} f_\alpha^{i+1} f_\beta^{j+1} f_\gamma^{k+1} \int_{-\infty}^{\infty} V^{i+j+k} P(V)\, dV \quad .$$

We now make the convenient change of variables

$$\begin{array}{lll} \nu = i+1 & \mu-\nu = j+1 & 2n+1-\mu = k+1 \\ \nu \geq 1 & \mu \geq \nu+1 & \mu \leq 2n \quad n \geq 1 \end{array}$$

giving

$$J^1 = -v^2 \sum_{\alpha\beta\gamma} \Phi_{\alpha\beta\gamma}(r,r') \sum_{n=1}^{\infty} \sum_{\mu=2}^{2n} \sum_{\nu=1}^{\mu-1} \sigma^{2n-2} (2n-3)!!\, f_\alpha^\nu f_\beta^{\mu-\nu} f_\gamma^{2n+1-\mu} \quad ,$$

where we have again used the relation

$$\int V^{2n} P(V)\, dV = v^{2n}(2n-1)!! \quad .$$

So

$$\left.\frac{dG(r,r';z)}{d\Lambda}\right|_{\Lambda=0} = J^1(r,r';z)$$

as required.

Appendix 2.3: Zeroth Order Calculation of the Density of States

Substituting the bare propagator into the expression 3.1 for the density of states in terms of the one particle Green function gives

$$\rho^0(E) = \frac{1}{2\pi i} \operatorname*{Lim}_{\varepsilon\to 0} \sum_n \int P(V) \left[\frac{1}{z-E_n-V} \right]_{E+i\varepsilon}^{z=E-i\varepsilon} dV\, C_n(r,r)$$

taking the difference indicated by the square brackets and shifting the variable of integration gives

$$\rho^0(E) = \frac{1}{2\pi} \operatorname*{Lim}_{\varepsilon\to 0} \sum_n \int P(E-E_n-V) \frac{\varepsilon/\pi}{V^2+\varepsilon^2} dV$$

$$= \frac{1}{2\pi} \sum_n f_n^1$$

where f_n^i is defined and evaluated in appendix 2.7. Hence

$$\rho^0(E) = \frac{1}{2\pi} \sum_n P(E-E_n)$$

Appendix 2.4: The First Order Correction to the Density of States

Substituting the expression for the first order correction to the Green function (2.4) into 3.4 gives

$$\Delta\rho = \frac{-v^2}{2\pi i} \operatorname*{Lim}_{\varepsilon\to 0} \int d^2r_1 d^2r_2 \; |r_1-r_2|^2 \times$$

$$\int P(V) \left[G^0(r,r_1;z-V)G^0(r_1,r_2;z-V)\, G^0(r_2,r;z-V) \right]_{E+i\varepsilon}^{z=E-i\varepsilon} dV \; .$$

We now expand the propagators and multiply and divide by the area of the system, Ω, to give

$$\Delta\rho = \frac{-v^2}{2\pi i\Omega} \sum_{n,m,1} \operatorname*{Lim}_{\varepsilon\to 0} \left\{ \int d^2r d^2r_1 d^2r_2 \; |r_1-r_2|\; C_n(r,r_1)C_m(r_1,r_2)C_1(r_2,r) \times \right.$$

$$\left. \left[\int \frac{P(V)}{[z-V-E_n]\,[z-V-E_m]\,[z-V-E_1]}\, dV \right]_{E+i\varepsilon}^{E-i\varepsilon} \right\} .$$

The integration over r can be performed using equation 5.9b of chapter 1 to give

$$\Delta\rho = \sum_{n,m} T_{m,n}\, F_{n,m}(E)$$

where

$$T_{n,m} = \frac{1}{\Omega} \int d^2r_1 d^2r_2 |r_1-r_2|^2 C_n(r_1,r_2)C_m(r_1,r_2)$$

and $$F_{n,m}(E) = \frac{-v^2}{2\pi i} \operatorname*{Lim}_{\varepsilon\to 0} \int P(V) \left[\frac{1}{[z-V-E_n]^2\,[z-V-E_m]} \right]_{E+i\varepsilon}^{z=E-i\varepsilon} dV \; .$$

From appendix 2.5

$$T_{n,m} = \frac{1}{4\pi} \{(2n+1)\delta_{n,m} - (n+1)\delta_{n+1,m} - n\delta_{n-1,m}\}$$

so that

$$\Delta\rho = \frac{1}{4\pi} \sum_{n} \left[(2n+1)F_{n,n} - nF_{n,n-1} - (n+1)F_{n,n+1} \right] .$$

$F_{n,m}$ is calculated in appendix 2.6 giving

$$\Delta\rho = \frac{v^2}{4\pi}\sum_n \left[(2n+1)\frac{P(E-E_n)}{2v^2}\left\{1-\frac{(E-E_n)^2}{v^2}\right\}\right.$$

$$-(n+1)\left\{\frac{1}{\hbar\omega_c}\left\{\frac{1}{\hbar\omega_c}-\frac{(E-E_{n+1})}{v^2}\right\}P(E-E_{n+1})-\frac{1}{[\hbar\omega_c]^2}P(E-E_n)\right\}$$

$$\left.+n\left\{\frac{1}{\hbar\omega_c}\left\{\frac{1}{\hbar\omega_c}+\frac{(E-E_{n-1})}{v^2}\right\}P(E-E_{n-1})+\frac{1}{[\hbar\omega_c]^2}P(E-E_n)\right\}\right]$$

which, on regrouping terms and setting $\omega_c=1$, gives equation 3.5.

Appendix 2.5: Calculation of $T_{n,m}$

The definition of T is

$$T_{n,m} = \frac{1}{\Omega}\int d^2r_1 d^2r_2 \; |r_1-r_2|^2 \; C_n(r_1,r_2)C_n(r_1,r_2) \quad .$$

Substituting equation 5.7 of chapter 1 gives

$$T_{n,m} = \frac{1}{4\pi^2\Omega}\int d^2r d^2r' |r-r'|^2 \; e^{-\frac{1}{2}|r-r'|^2} L_n(\tfrac{1}{2}|r-\tfrac{2}{r}'|\;)L_m(\tfrac{1}{2}|r-\tfrac{2}{r}'|\;) \quad .$$

Let $\rho=r-r'$ and $R=\frac{1}{2}(r+r')$. The free integration over R cancels the area Ω.

$$T_{n,m} = \frac{1}{4\pi^2}\int d^2\rho \; |\rho|^2 e^{-\frac{1}{2}|\rho|^2} L_n(\tfrac{1}{2}|\rho|^2)\; L_m(\tfrac{1}{2}|\rho|^2)$$

Performinging the angular integration gives

$$T_{n,m} = \frac{1}{\pi}\int u e^{-u} L_n(u)L_m(u)du \quad .$$

This integral can be performed using a recurrence relation for Laguerre polynomials (Abramowitz and Stegun (1965)),

$$xL_n(x) = (2n+1)L_n(x) - (n+1)L_{n+1}(x) - nL_{n-1}(x),$$

and their orthogonality relation to give

$$T_{n,m} = \frac{1}{\pi}\left\{(2n+1)\delta_{n,m} - n\delta_{n-1,m} - (n+1)\delta_{n+1,m}\right\} \quad .$$

Appendix 2.6: Calculation of $F_{n,m}$

We must consider separately the two cases n=m and n≠m.

I. n=m

$$F_{n,n} = \frac{-v^2}{2\pi i}\lim_{\varepsilon\to 0}\int P(V)\left[\frac{1}{[z-V-E_n]^3}\right]dV = -v^2 f_n^3$$

where f^i_n is defined and calculated in appendix 2.7.

II. $n \neq m$

$$F_{n,m}(E) = \frac{-v^2}{2\pi i} \operatorname*{Lim}_{\varepsilon \to 0} \int P(V) \left[\frac{1}{[z-V-E_n]^2 [z-V-E_m]} \right]^{z=E-i\varepsilon}_{E+i\varepsilon} dV .$$

Now $$\frac{1}{(x-p)^2(x-q)} = \frac{1}{(p-q)(x-p)^2} - \frac{1}{(p-q)^2(x-p)} + \frac{1}{(p-q)^2(x-q)}$$

so

$$F_{n,m} = -v^2 \left\{ \frac{1}{(E_n-E_m)} f^2_n - \frac{1}{(E_n-E_m)^2} f^1_n + \frac{1}{(E_n-E_m)^2} f^1_m \right\} .$$

Appendix 2.7: Calculation of f^i_n

We define the integral as follows

$$f^i_n = \frac{1}{2\pi i} \operatorname*{Lim}_{\varepsilon \to 0} \int P(V) \left[\frac{1}{[z-V-E_n]^i} \right]^{z=E-i\varepsilon}_{z=E+i\varepsilon} .$$

For i=1 it is straightforward to find the difference within the square bracket to give

$$f^1_n = \operatorname*{Lim}_{\varepsilon \to 0} \int P(E-E_n-V) \frac{\varepsilon/\pi}{V^2+\varepsilon^2} dV$$

Taking the limit transforms the Lorentzian into a delta function giving

$$f^1_n = P(E-E_n)$$

For i=2 we arrive, on taking the difference, at the expression

$$f^2_n = \frac{1}{2\pi i} \operatorname*{Lim}_{\varepsilon \to 0} \int P(V) \frac{2V\ \varepsilon/\pi}{\left[(E-E_n-V)^2+\varepsilon^2 \right]^2} dV .$$

By inspection the second term is minus the derivative of a normalised Lorentzian so integrating by parts and taking the limit gives

$$f^2_n = \int \delta(E-E_n-V) \left[\frac{d}{dV} P(V) \right] dV = - \frac{(E-E_n)}{v^2} P(E-E_n) .$$

For i=3, on taking the difference, we find

$$f^3_n = \operatorname*{Lim}_{\varepsilon \to 0} \int P(V) \frac{\varepsilon/\pi(3V^2-\varepsilon^2)}{\left[(E\ E_n-V)^2+\varepsilon^2 \right]} dV .$$

The second term is half the second derivative of a normalised Lorentzian so integrating by parts twice and taking the limit gives

$$f_n^3 = \frac{1}{2}\int \delta(E-E_n-V)\,\frac{d^2}{dV^2}\,P(V)\,dV = \left[\,1 - \frac{(E-E_n)^2}{v^2}\,\right]\frac{P(E-E_n)}{2v^2}\,.$$

Appendix 2.8: The Zeroth Order Diffusion Propagator

At zeroth order in Λ the two-particle Green function has the form

$$\overline{\Delta(r,r';z)\Delta(r',r;z')} = \int P(V)\; G^0(r,r';z-V)\; G^0(r',r;z'-V)$$

so that, on expanding the propagator, we find

$$\Pi(r,r';t)\Big|_{\Lambda=0} = \frac{1}{4\pi^2}\sum_{n,m} C_n(r,r')C_m(r',r)\;\times$$

$$\int P(V)\left\{\int_{-\infty+i0}^{+\infty+i0} dz\;\frac{e^{-izt}}{z-V-E_n}\right\}\left\{\int_{-\infty-i0}^{+\infty-i0} dz'\;\frac{e^{iz't}}{z'-V-E_n}\right\}dV\,.$$

Employing the formula derived in appendix 1.6 gives

$$\Pi(r,r';t) = \theta(t)\left|\sum_n C_n(r,r')\;e^{-iE_nt}\right|^2 = |\Gamma^0(r,r';t)|^2\,.$$

Appendix 2.9: The First Order Correction to the Diffusion Propagator

At order Λ there are three contributions to the two-particle Green function derived from the three diagrams shown in Figures 4b, c and d. The first two are complex conjugates of one another, Π^1 and Π^{1*}, while the other is distinct Π^2. So

$$\left.\frac{d\Pi}{d\Lambda}\right|_{\Lambda=0} = \left[\Pi^1+\Pi^{1*}+\Pi^2\right]\,.$$

From the first diagram, after expanding the propagators and neglecting terms that mix different Landau levels, we find

$$\Pi^1 = \frac{-v^2}{4\pi^2}\sum_n \int d^2r_1 d^2r_2\;|r_1-r_2|^2 C_n(r,r_1)C_n(r_1,r_2)C_n(r_2,r')\;C_n(r',r)\;\times$$

$$\int P(V)\int_{-\infty-i0}^{+\infty+i0} dz\;\frac{e^{-izt}}{\left[\,z-V-E_n\right]^3}\int_{-\infty-i0}^{+\infty-i0} dz'\;\frac{e^{iz't}}{\left[z'-V-E_n\right]}$$

writing the integral over r_1 and r_2 as $X_n(r,r')$ and using the results of appendix 1.6 to do the intgrals over z and z′ gives

$$\Pi^1 = \frac{v^2t^2}{2}\,\theta(t)\sum_n X_n(r,r')C_n(r',r) \quad .$$

The complex conjugate of this is derived by simply interchanging r and r'. The contribution of the third diagram is

$$\Pi^3 = \frac{-v^2}{4\pi^2}\sum_n \int d^2r_1 d^2r_2\, |r_1-r_2|^2 C_n(r,r_1)C_n(r_1,r')C_n(r',r_2)C_n(r_2,r) \times$$

$$\int P(V) \int_{-\infty+i0}^{+\infty+i0} dz\, \frac{e^{-izt}}{[z-V-E_n]^2} \int_{-\infty-i0}^{+\infty-i0} dz'\, \frac{e^{iz't}}{[z'-V-E_n]^2} \quad .$$

Writing the double integral over r_1 and r_2 as $Y_n(r,r')$ and using the results of appendix 1.6 gives

$$\Pi^2 = -v^2t^2\theta(t)\sum_n Y_n(r,r') \quad .$$

Hence

$$\left.\frac{d\Pi(r,r';t)}{d\Lambda}\right|_{\Lambda=\theta} = \frac{1}{2}\,v^2t^2\theta(t)\sum_n \Big\{X_n(r,r')\,C_n(r',r) + C_n(r,r')X_n(r',r)$$

$$- 2\,Y_n(r,r')\Big\} = \frac{1}{2}\,v^2t^2\theta(t)\sum_n F_n(r,r') \quad .$$

Figure 1
The zeroth order (in Λ) diagram for the single-particle Green function

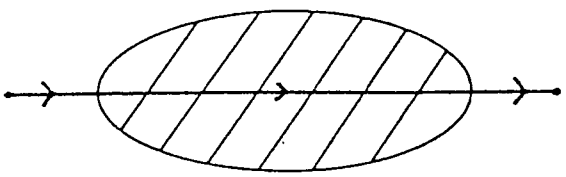

Figure 2
The generation of new diagrams by differentiation with respect to Λ
(a) An $O(\sigma^4)$ diagram: f and (b) and (c) the two diagrams obtained by differentiating with respect to Λ.

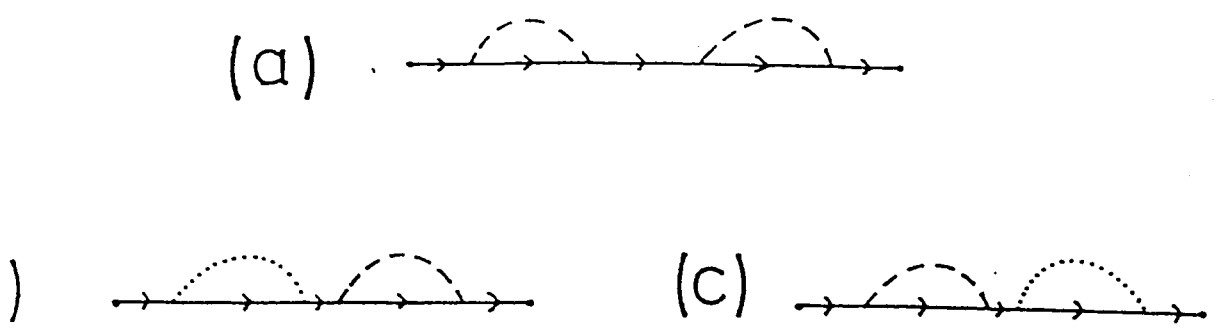

Figure 3
The first order (in Λ) correction to the single-particle Green function

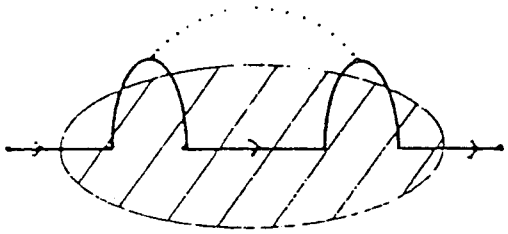

Figure 4
The first order (in Λ) diagrams for the two-particle Green function

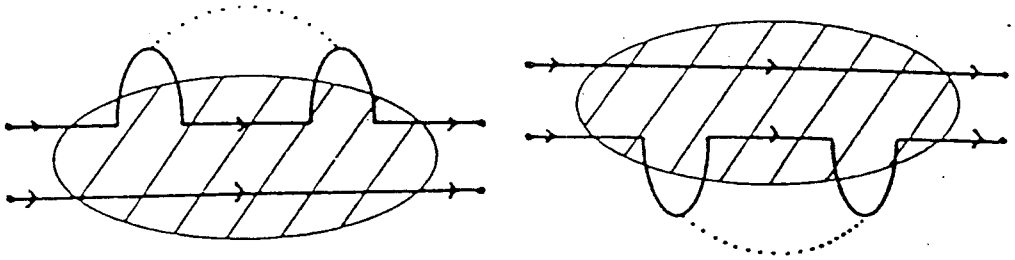

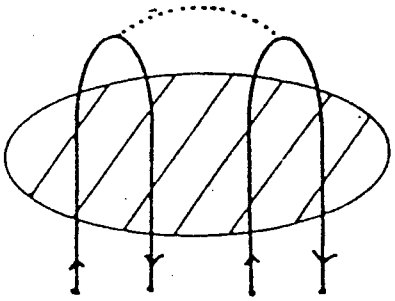

Figure 5
The zeroth order (in Λ) density of states per unit area, per unit energy, at a disorder of v=0.2

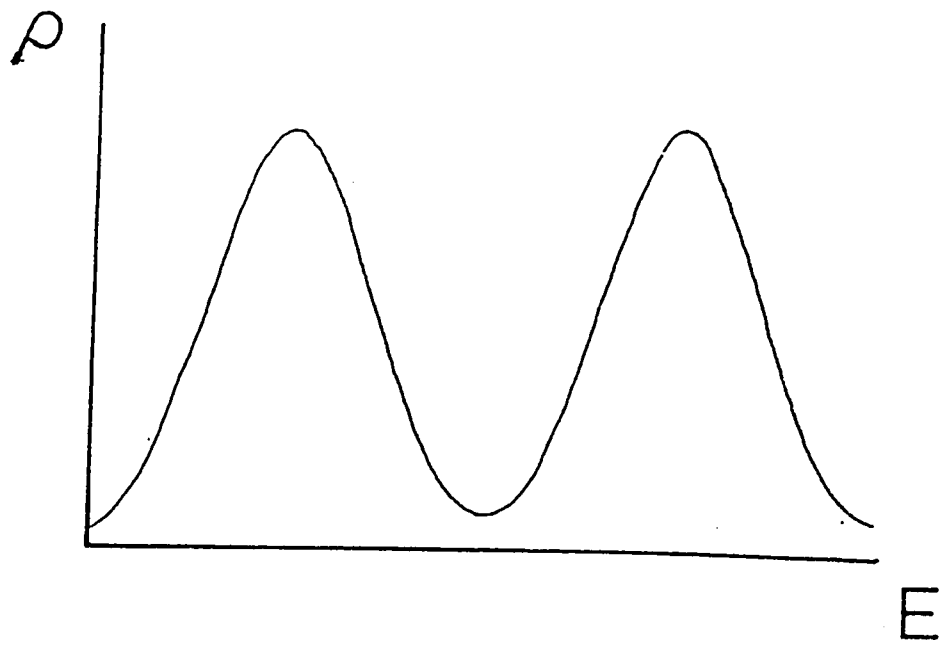

Figure 6
The first order correction to the density of states, also at v=0.2

Chapter 3

The Disordered Electron Gas in High Landau Levels

In this chapter another exactly solvable régime for the disordered two-dimensional electron gas in a strong magnetic field is found: the high Landau level limit. Results for the density of states, diffusion constant and conductivity tensor are presented. This limit is found to be the weak localisation régime for the model. A brief review of the systematic expansion in powers of 1/n for these quantities is also given.

The work in this chapter, except for that described in section 7, was performed by the author in collaboration with Dr. J.T. Chalker and has been published as Benedict and Chalker (1986). The work described in section 7 is included for completeness although it was carried out by Dr. J.T. Chalker and Dr. P. Carra with minor contributions from the author; this work will be described in detail in a forthcoming preprint (Carra, Chalker and Benedict (1986)). The whole of the work described is reviewed in Chalker, Carra and Benedict (1986).

3.1. Introduction

The aim of the present chapter is to examine the two-dimensional electron gas in a strong magnetic field (such that $\hbar\omega_c \gg v$ allowing us to neglect Landau level mixing) in a particular simplifying limit in which a generalised single-site approximation (for the case of Gaussian white-noise this is the generalised Born approximation of Ando (1974)) becomes exact and the model can be solved. The approximations made are similar to the coherent Potential approximation (CPA) in common use for disordered systems in the absence of magnetic fields. We consider the states in the n^{th} Landau level and take the limit $n\to\infty$. This is, in some respects, similar to the n-orbital model of Wegner (1979b) which has been applied to a tight binding model of the two-dimensional electron gas in a strong magnetic field by Streit (1984). In this limit the quantum interference between scattered wavepackets is suppressed, in the sense

that repeated, coherent scattering between pairs of impurities becomes unimportant. A detailed discussion of this will be given in section 2. The following is a physical interpretation of this result.

In order to discuss the simplifications induced by the high Landau level limit it is helpful to choose a set of basis states defined as follows. First, construct the most localised wavepacket possible from states in the n^{th} Landau level. The probability density for this state, $|\psi|^2$, is exponentially small except on a disc of radius $l_c(n+\frac{1}{2})^{1/2}$. Then place these wavepackets on the vertices of a square lattice. The lattice spacing should be chosen to be $(2\pi)^{1/2}l_c$ in order that there be the same number of states per unit area as would be given by a complete set. This basis set is superficially similar to the Wannier functions used in tight binding models of metals; however true Wannier functions cannot be formed within one Landau level (Thouless 1984) and the set of states constructed here is complete but is not orthonormal. Define the region of spatial overlap of two such states $|i\rangle$ and $|j\rangle$ to be the region in which neither $|\psi_i|^2$ nor $|\psi_j|^2$ are exponentially small. It is then clear that each state has spatial overlap with ~n others. Now suppose that an electron is initially in one of these basis states, say $|i\rangle$, and consider the time evolution of the wavepacket. The random potential may scatter the electron into any of the n states that overlap with $|i\rangle$. From the second state the electron may be scattered into any one of a possible n third states. The probability that it is actually scattered back into the initial state, $|i\rangle$, clearly falls to zero as $n\to\infty$. Thus when all scatterings are considered, processes in which the electron is repeatedly scattered between a given pair of basis states contribute with vanishing weight in the large n limit. Within this picure we can consider the motion of the electron to be a random walk between these pseudo-Wannier states. The suppression of multiple reflections, which would tend to trap the electron, implies that it will always move diffusively and not be localised in the large n limit.

The statistical properties of the disorder in the physical realisations of two-dimensional electron gases are not well known, so we have chosen to examine three types of random potential: Gaussian white-noise; a uniform spatial distribution of zero-ranged scattering

centres of fixed strength; and a uniform spatial distribution of zero-ranged scattering centres with a Lorentzian distribution of strengths.

In outline, the proceedure that we use for the calculation of the Green functions is the following. Firstly, the Green function is expanded as a formal power series in the random potential (as in section 1.5); this series is then averaged, term by term, over the disorder; the large n limit is taken, causing most diagrams to vanish (in the case of Gaussian white-noise, those not included in the self-consistent Born approximation); finally the remaining terms are resummed.

The rest of this chapter is arranged as follows: section 2 defines the statistical properties of the types of random potentials that we have investigated. Section 3 considers the effect of the large n limit on the diagrammatic perturbation theory and the calculation of the Green functions. Section 4 describes the calculation and properties of the density of states of the system. Section 5 examines the existence of diffusion in the system. Section 6 contains the calculation and behaviour of the conductivity tensor. Section 7 contains a brief review of the expansion of physical quantities about the large n limit in terms of the small parameter 1/n. The final section contains a short summary.

3.2. The Random Potential

We have examined three choices for the statistics of the random potential which are specified below.

(a) Gaussian white-noise

In this case the value of the potential at each distinct point in the plane is an independent Gaussian random variable. The only non-vanishing cumulant is

$$\Xi_2(\mathbf{r},\mathbf{r}') = \overline{V(\mathbf{r})V(\mathbf{r}')} = v^2\,\delta^2(\mathbf{r}-\mathbf{r}') \;; \qquad (2.1)$$

(b) Fixed strength delta function scatterers

In this case a fixed number, $\rho\Omega$, of zero-range scattering centres of fixed strength v are randomly and independently placed with uniform probability over a region of the plane with area Ω so that

$$V(\mathbf{r}) = v \sum_{i=1}^{\rho\,\Omega} \delta^2(\mathbf{r}-\mathbf{R}_i) \qquad (2.2)$$

and the probability density that a given scattering centre is at a point $\mathbf{R}_i$ is the inverse area of the system, Ω^{-1}.

(c) Delta function scatterers with a Lorentzian Distribution of Strengths

This is an extension of (b) in which the strength of each scatterer is an independent random variable with probability density function

$$P(v) = \frac{1}{\pi} \frac{\Gamma}{\Gamma^2 + v^2} \quad ; \qquad (2.3)$$

where Γ is a parameter describing the strength of the on-site disorder.

3.3 The Calculation of the Green Functions

In this section we show how the limit $n\to\infty$ allows resummation of the standard perturbation expansion detailed in section 1.5. First we will consider some consequences of the neglect of Landau level mixing. If the disorder strength v is much smaller than the Landau level spacing, $(n+\frac{1}{2})\hbar\omega_c$, we can project the full Hamiltonian onto the n^{th} Landau level

$$H^{(n)} = P_n H P_n \qquad (3.1)$$

where the projection operator is defined by

$$P_n = \sum_k |n,k\rangle \langle n,k| \quad , \qquad (3.2)$$

the normalised kets $\{|n,k\rangle\}$ being the eigenstates of H_0 that span the n^{th} Landau level (in this chapter we work entirely in the Landau gauge). In order to calculate conductivities it is actually necessary to allow weak level mixing since the only non-zero matrix elements of the velocity operators connect states from adjacent levels. Therefore in section 6 we begin with the Hamiltonian $H^{(n-1)}+H^{(n)}+H^{(n+1)}$ (supposing the Fermi energy to lie in the n^{th} Landau level) but retain

only those terms in the conductivity that remain finite in the limit $\hbar\omega\to\infty$. From equation 5.10 of chapter 1 we can see that, in the absence of Landau level mixing ($\hbar\omega_c\to\infty$), the Green function will have the form

$$G(r,r';z) = g_n(z)C_n(r',r) \tag{3.3}$$

In addition, since all high Landau levels are equivalent, we expect that

$$g_n(z) = g(z-(n+\tfrac{1}{2})\hbar\omega_c) \tag{3.4}$$

This is indeed found to be the case. The $n\to\infty$ limit is simplifying because it suppresses quantum interference; this manifests itself in the diagrammatic perturbation theory as the vanishing of all but a subclass of diagrams. We can see qualitatively why some diagrams will vanish in the large n limit and others not in the following manner. Consider the second order diagrams for a Gaussian white-noise potential shown in Figure 1. The first diagram corresponds, neglecting Landau level mixing, to the expression

$$v^4[g_n(z)]^5 \int d^2r d^2r' C_n(R,r)C_n(r,r)C_n(r,r')C_n(r',r')C_n(r',R') . \tag{3.5}$$

Use of the properties of C_n given in section 1.1 (equations 5.9) reduces this to

$$\frac{v^4 g^5}{4\pi^2 l_c^4} C_n(R,R') . \tag{3.6}$$

Similarly the second diagram corresponds to the expression

$$\frac{v^4 g^5}{2\pi l_c^2} C_n(R,R') \int d^2r \, |C_n(r',0)|^2 , \tag{3.7}$$

while the third is

$$v^4 g^5 \int d^2r d^2r' \, C_n(R,r) \, |C_n(r,r')|^2 C_n(r,r') \, C_n(r',R') . \tag{3.8}$$

The first diagram has no integrations left to do while the second contains one integration over a positive definite function: $|C_n|^2$. The third diagram, however, has an integral over a product of functions including $C_n(r,r')$ which is complex and oscillates many times in the range of integration in the large n limit. This leads to significant cancellations in the integral and, consequently, this diagram is much smaller than the other two for large n.

We shall now attempt to estimate the n dependence of a general diagram. We will commence by considering those diagrams comprising only four-point vertices(those relevant to Gaussian white-noise) for which purpose it is convenient to use as a basis set the simultaneous eigenfunctions of H_0 and P_y, $\psi_{n,k}(r)$, that span the n^{th} Landau level. In this basis the propagator has the form

$$G^0(k,k':z) = g_n^0(z)\ \delta(k-k') \tag{3.9}$$

represented diagrammatically by a solid line. The potential has off-diagonal elements in this basis, given by

$$V_{k,k'} = \int d^2r\ \ \psi^*_{n,k}(r)\ \ V(r)\ \ \psi_{n,k'}(r)\ . \tag{3.10}$$

Hence the four-point vertex in this basis is (figure 2)

$$v^2\int d^2r\ \psi^*_{n,k_1}(r)\ \psi_{n,k_2}(r)\ \psi^*_{n,k_3}(r)\ \psi_{n,k_4}(r)$$

$$= \frac{v^2}{4\pi^2}\ \delta(k_1-k_2+k_3-k_4)\ M_n(k_1-k_3,k_1-k_2)$$

where M_n can be shown (appendix 1) to have the form

$$M_n(k,q) = \int d\lambda\ e^{-ik\lambda}\ m_n(\lambda^2+q^2) \tag{3.11}$$

with $$m_n(x) = e^{-x/2}\ \left[\ L_n(x/2)\ \right]^2\ .$$

It is useful to note that $M_n(k,q)$ satisfies the following relations

$$M_n(k,q) = M_n(q,k) \tag{3.12a}$$

$$M_n(k,-q) = M_n(k,q) \tag{3.12b}$$

$$|M_n(0,q)| \geq |M_n(k,q)|\ . \tag{3.12c}$$

If a diagram has N vertices then the total contribution of the diagram will contain the factor

$$D = \int \prod_{i=1}^{N} M_n(q_i,k_i) \prod_{i=1}^{N} dq_i \tag{3.13}$$

where the q_i's are the momenta transferred through the vertex and the k_i's are the momentum differences across the vertices. Clearly, the k_i's are linear combinations of the q_i's of the form $k_i=S_{ij}q_j$ (summation over j implied). The anti-symmetric matrix which has elements $S_{ij}\in\{\pm1,0\}$ describes the topology of the diagram. For example, the diagram in figure 3a has the two vertex parts shown in figure 3b, so that $k_1=q_2$ while $k_2=-q_1$. If a diagram is such that $k_i=0$

Vi then each factor in the integrand depends only on one q_i and no q_i appears in more than one factor, so that all the integrations decouple to give (see appendix 2).

$$D = \left[\int dq\ M_n(0,q) \right]^N = (2\pi)^N \qquad (3.14)$$

Hence the contribution of the diagram is independent of n. If a diagram has V vertices for which k_i does not vanish then the terms and integrations involving k=0 vertices still factorise as N-V constants leaving

$$D = \text{const.} \int d^V q \prod_{i=1}^{V} M_n(q_i,k_i) \ . \qquad (3.15)$$

We can place an upper bound on the integral by replacing each factor with its modulus. Thus

$$D \leqslant \int d^V q \prod_{i=1}^{V} \left| M_n(q_i,k_i) \right| \ . \qquad (3.16)$$

Since each factor in the integral is positive definite, if we can find an upper bound on any factor, then replacing that factor by the bound can only increase the value of the integral as a whole. Using equation 3.12c to provide an upper bound on the last V-2 factors gives

$$D \leqslant \int d^V q \ \left| M_n(q_1,k_1) \right| \left| M_n(q_2,k_2) \right| \prod_{i=3}^{V} \left| M_n(q_i,0) \right| \ . \qquad (3.17)$$

We can always choose the ordering of the q's to be such that the matrix element $S_{12}=+1=-S_{21}$, and then write $k_1=a+q_2$, $k_2=b-q_1$, where a and b are functions of all the remaining q's. Also, since we have removed the k dependence of the last V-2 factors, none of them depend on q_1 or q_2, so we have

$$D \leqslant \int d^{V-2}q \prod_{i=3}^{V} \left| M_n(q_i,0) \right| \iint dq_1 dq_2 \left| M_n(q_1,a+q_2) \right| \left| M_n(q_2,b-q_2) \right| . \qquad (3.18)$$

An upper bound on the inner integral is derived from the Schwartz inequality

$$J = \iint dq_1 dq_2 \left| M_n(q_1,a+q_2) \right| \left| M_n(q_2,b-q_2) \right| \leqslant$$

$$\left[\iint dq_1 dq_2 \left| M_n(q_1,a+q_2) \right|^2 \times \iint dq_1 dq_2 \left| M_n(q_2,b-q_1) \right|^2 \right]^{\frac{1}{2}} . \qquad (3.19)$$

Hence

$$J \leq \iint dq_1 dq_2 \left| M_n(q_1,q_2) \right|^2 . \qquad (3.20)$$

Substituting equation 3.20 into 3.18 gives

$$D \leq \int d^{V-2}q \prod_{i=3}^{V} \left| M_n(q_i,0) \right| \iint dq_1 dq_2 \left| M_n(q_1,q_2) \right|^2 . \qquad (3.21)$$

The V-2 outer integrations are now fully decoupled and just give a harmless n-independent factor; the non-trivial double integral can be performed asymptotically (see appendix 3) to find the upper bound on D.

$$D \leq \frac{4 \log n}{n} \qquad (3.22)$$

As a consequence, a diagram composed of four-point vertices that contains any vertices for which not all the k's are zero vanishes in the large n limit.

To conclude, for the potential distribution (a) which gives rise to diagrams with four-point vertices only, the one-particle diagrams in which all k's vanish (those for which at each vertex the momenta are pairwise equal) are generated by the Dyson equation of figure 4. Similarly, the two-particle diagrams that survive in the limit $n\to\infty$ are generated by the Bethe-Salpeter equation of figure 5 (note that in this diagram and in figure 7 the solid lines represent complete one-particle propagators). These are the defining equations for the self-consistent Born approximation (Ando 1974).

Before discussing the solutions to these equations, we describe the selection of diagrams containing general 2p-point vertices in the large n limit. Representation of these vertices in the Landau basis is rather cumbersome for large p so the analysis is presented in direct space. We begin by recalling a property of the function $C_n(r,r')$ given in equation 5.9b of chapter 1 which allows us to perform trivially all integrations over two-point vertices. Further since $C_n(r,r)=(2\pi l^2)^{-1}$, a propagator that starts and ends on the same vertex makes no contribution to the n-dependence: for the present purpose such a propagator can be removed and the vertex replaced by another, smaller in p by one. Suppose, after these two types of reduction, that a

diagram for the s-particle function contains a number a_p of 2p-particle vertices (p=2,3,..). The number of propagators in the diagram is

$$A = s + \sum_{p=2}^{\infty} pa_p \quad , \tag{3.23}$$

while the number of (two-dimensional) internal integrations remaining is

$$B = \sum_{p=2}^{\infty} a_p \quad . \tag{3.24}$$

Since the propagator, $C_n(r,r')$, is of order $n^{-1/2}$ for $r-r'$ within a distance of order $n^{1/2}$ of the origin, and exponentially small outside this region, the n-dependence of this diagram is estimated to be of order $n^{B-A/2}$. Hence, after reduction, only diagrams composed entirely of four-point vertices survive in the limit $n\to\infty$. Within this class, the estimates described previously can be applied.

In summary, we obtain the Dyson equation of figure 6 and the Bethe-Salpeter equation of figure 7 in the limit $n\to\infty$ for the potential distributions (b) and (c). We now discuss the solution of the self-consistent equations for each potential distribution.

Use of the relation 5.9b of chapter 1 reduces the Dyson equation of figure 4 to the quadratic equation

$$g_n(z) = g_n^0(z) + \frac{v^2}{2\pi l_c^2} \; g_n^0(z) \left[g_n(z) \right]^2 , \tag{3.25}$$

which has the solution

$$g(\zeta) = \frac{1}{2\lambda} \left[\zeta \pm \left(\zeta^2 - 4\lambda \right)^{1/2} \right] , \tag{3.26}$$

where $\lambda = v^2/2\pi l_c^2$, $\zeta = (z-E_n)$ and $E_n = (n+\frac{1}{2})\hbar\omega_c$. The sign of the square root is chosen so that of $\mathrm{Sgn}(\mathrm{Im}[g]) = \mathrm{sgn}(\mathrm{Im}[z])$ in order that $g(z)\sim 1/z$ as $|z|\to\infty$.

As a solution to the Bethe-Salpeter equation (figure 5) we will require only the function,

$$\tilde{Q}(r-r';z) = K(r,r';z\,;r',r;z^*) \; , \tag{3.27}$$

in which the arguments are identified pairwise. This function is dependent on only the relative separation of its arguments so it is convenient to introduce the Fourier representation introduced in section 1.6

$$Q(\mathbf{q}) = \int \exp\{i\mathbf{q}.\mathbf{r}\}\ Q(\mathbf{r})\ d^2\mathbf{r} \qquad (3.28)$$

The (disconnected) first term in the Bethe-Salpeter equation is also a function of the relative separation, $\mathbf{r}-\mathbf{r}'$, only and can be written as

$$G(\mathbf{r},\mathbf{r}';z_1)\ G(\mathbf{r}',\mathbf{r};z_2) = g(z_1)\ g(z_2)\ f(\mathbf{r}-\mathbf{r}') \quad , \qquad (3.29)$$

where

$$f(\mathbf{r}-\mathbf{r}') = |\ C_n(\mathbf{r},\mathbf{r}')\ |^2 \ ; \qquad (3.30)$$

which has the Fourier transform

$$F(\mathbf{q}) = \int \exp\{i\mathbf{q}.\mathbf{r}\}\ f(\mathbf{r})\ d^2\mathbf{r} \qquad (3.31)$$

$$= (2\pi l_c^2)^{-1} \exp\left\{ -\tfrac{1}{2} l_c^2 q^2 \right\} \left[L_n\left(\tfrac{1}{2} l_c^2 q^2 \right) \right]^2 .$$

$$= (2\pi l_c^2)^{-1} m_n(l_c^2 q^2/2) \qquad (3.32)$$

In terms of these functions the solution of the Bethe-Salpeter equation is

$$Q(\mathbf{q};z) = \frac{g(z)g(z^*)F(\mathbf{q})}{1 - \left[v^2 g(z)g(z^*)F(\mathbf{q}) \right]} \ . \qquad (3.33)$$

Similarly the coupled Dyson equations of figure 6 can be reduced to the form

$$g_n(z) = g_n^0(z) + \rho\ g_n^0(z)\ \Sigma_n'(z)\ g_n(z) \qquad (3.34)$$

$$\Sigma_n'(z) = v + \frac{v}{2\pi l_c^2}\ \Sigma_n'(z)\ g_n(z) \ . \qquad (3.35)$$

We introduce new parameters $\nu = 2\pi l_c^2 \rho$, $\lambda = v/2\pi l_c^2$, $\Sigma_n(z) = \Sigma'_n(z)/2\pi l_c^2$ and $\zeta = z - E_n$ as before. After re-arrangement this yields a quadratic equation

$$\lambda\ \zeta\ g^2(\zeta) + g(\zeta)\ [\ \lambda\ (\nu-1) - \zeta\ ] + 1 = 0 \ ; \qquad (3.36)$$

which has the solution

$$g(\zeta) = \frac{1}{2\lambda\zeta} \left[\zeta - \lambda[\nu-1] \pm \left([\zeta - \lambda(\nu - 1)]^2 - 4\lambda\zeta \right)^{\frac{1}{2}} \right] \qquad (3.37)$$

where again the sign of Im[g] is chosen to coincide with the sign of Im[z].

The two-particle Green function for the case of fixed strength scattering centres is, in the notation of equations 3.28-3.32

$$Q(\mathbf{q};z) = \frac{g(z)\, g(z^*)\, F(\mathbf{q})}{1 - \left[\rho\Gamma(z,z^*)g(z)g(z^*)F(\mathbf{q}) \right]} \tag{3.38}$$

where the proper vertex part Γ is the product of the one particle self energy parts,

$$\Gamma(z_1,z_2) = \Sigma'(z_1)\, \Sigma'(z_2) \,. \tag{3.39}$$

It remains to discuss the averaging over the strengths of scattering centres for the potential distribution (c). The Green functions in this case are obtained from those of case (b) by averaging the strength of each separate scatterer with a Lorentzian distribution. Since the self energy part and the proper vertex part contain all the dressings of the bare interaction with the scatterer which do not lead to diagrams that vanish in the limit $n\to\infty$, we merely have to average these two quantities. Now $\Sigma(z,\lambda)$ is an analytic function in one half of the complex λ plane, which vanishes sufficiently fast on the semicircle at infinity, so that when evaluating the integral along the real λ axis of $P(\lambda)\Sigma(z,\lambda)$, the contour may be closed. Evaluating the residue at the pole merely replaces λ by $\pm i\gamma$, the sign again chosen to coincide with that of Im[-z]. Thus

$$g(\zeta) = \pm \frac{[\zeta \pm i\gamma(\nu-1)]}{2i\gamma\zeta} \left[1 - \left(1 \mp \frac{4i\gamma\zeta}{[\zeta \mp i\gamma(\nu-1)]^2} \right)^{\frac{1}{2}} \right] \,. \tag{3.40}$$

The proper vertex part has poles on both sides of the real λ axis, so that, when the integral of $P(\lambda)\Gamma(z,z';\lambda)$ along the real λ axis is evaluated by closing the contour, residues are obtained from one of these and from the pole enclosed at $\pm i\gamma$.

3.4. The Density of States

The density of states per unit energy range per unit area is once again obtained from the single-particle Green function using equation 5.7 of chapter 1. The density of states for the nth Landau level is obtained from the Green function for that level and the total density of states is then recovered by the summation

$$\rho_{total}(E) = \sum_n \rho_n(E). \qquad (4.1)$$

From equation 3.4 it is clear that

$$\rho_n(E) = \rho(E-E_n) \qquad (4.2)$$

where $\rho(E)$ is a function which is independent of n as $n\to\infty$.

We now describe the density of states for each choice of random potential.

(a) Gaussian white-noise

Substituting the expression 3.26 for g(z) into the general expression for the Green function yields

$$\rho(\eta) = \frac{1}{4\pi^2 l_c^2 \lambda} \left[4\lambda - \eta^2 \right]^{\frac{1}{2}} \theta(4\lambda-\eta^2). \qquad (4.3)$$

Thus the introduction of the Gaussian white-noise potential has smeared out the Landau level into an elliptical band centred on the Landau level energy E_n, as shown in figure 8.

(b) Fixed Strength Delta Function Scatterers

We use the expression 3.37 for the Green function. In this case there are two distinct régimes according to whether ν, the dimensionless density of scattering centres, is smaller or larger than one. The density of states has the form

$$\rho(\eta) = (2\pi l_c^2)^{-1}(1-\nu)\theta(1-\nu)\delta(\eta) + \rho_{band}(\eta)\,\theta(\eta-\eta_0)\,\theta(\eta_1-\eta) \qquad (4.4)$$

where

$$\rho_{band}(\eta) = \frac{1}{4\pi^2 l^2 \lambda\eta} \left[4\lambda\eta - \left(\eta - \lambda[\nu-1] \right)^2 \right]^{\frac{1}{2}}, \qquad (4.5)$$

$$\eta_0 = (1-\nu^{\frac{1}{2}})^2\lambda \quad \text{and} \quad \eta_1 = (1+\nu^{\frac{1}{2}})^2\lambda.$$

Thus when $\nu<1$ there is a discrete level at the Landau energy E_n, which is a remnant of the Landau level from which a fraction ν of the states have been removed into the impurity band (see figure 9a). As ν is increased, more states are transferred into the band which grows both in height and width. If $\nu>1$ then all the states have been removed from the Landau level into the band (see figure 9b). The case $\nu=1$ connects the two régimes, there being only a band which has a weak (square root) divergence at the Landau level energy.

This is analogous to the behaviour noted by Ando (1974) and Brézin et al (1984) and can be explained as follows. If $\nu<1$, there are fewer scatterers than there are states in the Landau level; it is therefore possible to find a set of basis states within the Landau level which is such that a fraction $(1-\nu)$ of the states have zero amplitude at the positions of all the scattering centres. These states cannot be affected by the random potential and so their energies remain at the unperturbed value: they remain in the Landau level. The other states have non-zero amplitude at the scattering centres and so may be mixed by the disorder and will be shifted in energy into the band centred on the potential energy of the scattering centres. If $\nu>1$ then there are more scatterers than there are states in the Landau level and so it is no longer possible to construct any states with an energy independent of the disorder.

(c) Delta Function Scatterers with a Lorentzian Distribution of Strengths

We omit the complete analytic expression for the density of states in this case as it is rather unwieldy. The result is shown graphically (figure 10) for the parameter value $\nu=2.5$. Two limiting régimes are rather simpler.

First, the density of states in the tails of the broadened Landau level is Lorentzian for all values of ν and γ.

$$\rho(\eta) \sim \frac{1}{2\pi^2 l^2} \quad \frac{\gamma\,\nu}{\eta^2 + \gamma^2\nu^2} \qquad |\eta| \to \infty \qquad (4.6)$$

Thus the sharp band edges found for potential distributions (a) and (b), which are presumably special to the high Landau level limit, are replaced by band tails in the presence of the much broader potential distribution (c).

Second, if we take the limit of Lorentzian white-noise ($\nu\to\infty$, $\gamma\to 0$ with $\nu\gamma=\rho\Gamma$=constant: a continuum version of the Lloyd model (Lloyd 1969)) the density of states is Lorentzian at all energies.

3.5. Diffusion

To demonstrate that the eigenfunctions for the model are extended we shall examine the behaviour of the two-particle Green function, $Q(\mathbf{q},E+i\omega)$, in the hydrodynamic régime. As we have seen in section 1.6, the behaviour of this function for small ω and small q^2 is expected to have the form

$$Q(q,E+i\varepsilon) \sim \frac{\pi\rho(E)}{\omega + \tfrac{1}{2}\hbar D(E)q^2} \quad : \quad q^2,\omega\to 0 \tag{5.1}$$

where $D(E)$ is the energy dependent diffusion constant which is expected to go to zero at the mobility edge. From equation (3.33) we see that for the case of Gaussian white-noise

$$Q(q;z) = \frac{g(z)g^{*}(z)\ F(q)}{1 - 2\pi l_c^2\lambda\left[\ g(z)g^{*}(z)F(q)\ \right]} \tag{5.2}$$

where $F(q)=(2\pi l_c^{\,2})^{-1}m_n(l_c^{\,2}q^2/2)$. From equation 3.26 we can evaluate $|g(E+i\omega)|^2$ for small ω. This gives

$$|g(E+i\omega)|^2 = \frac{1}{\lambda}\left[\ 1 - \frac{\omega}{2\pi^2 l_c^2\lambda\rho(E)} + O(\omega^2)\ \right] \tag{5.3}$$

where $\rho(E)$ is given by equation (4.3). Similarly to lowest order in q^2 we can expand $F(\mathbf{q})$ as

$$F(\mathbf{q}) = (2\pi l_c^2)^{-1}\left[\ 1 - (n+\tfrac{1}{2})l_c^2q^2 + O(q^4l_c^4)\right] . \tag{5.4}$$

Thus we arrive at

$$Q(q,E+i\varepsilon) = \frac{\pi\rho(E) + O(q^2,\omega)}{\omega + 4\pi^2 l_c^4\lambda\rho(E)(n+\tfrac{1}{2})\ \tfrac{1}{2}q^2 + O(q^4,\omega^2)} \tag{5.5}$$

and consequently we find the diffusion constant

$$D(E) = 4\pi^2 l_c^4\lambda\rho(E)(n+1/2)/\hbar \tag{5.6}$$

In a similar manner the the two particle function for the case of fixed strength delta function scatterers can be shown to have the form

$$Q(q,E+i\varepsilon) = \frac{\pi\rho_{band}(E)}{\omega + 2\lambda\pi^2 l_c^4 (n+\tfrac{1}{2}) E\rho_{band}(E)\tfrac{1}{2}q^2} \qquad (5.7)$$

and therefore the diffusion constant is

$$D(E) = E\rho_{band}(E)\lambda 2\pi^2 l_c^4 (n+\tfrac{1}{2})/\hbar \qquad (5.8)$$

where $\rho_{band}(E)$ is given in equation (4.5).

The suppression of quantum interference effects in the high Landau level limit thus results in all eigenstates being extended. The decrease in the diffusion constant as the band edges are approached may be a remnant of the strong localisation expected near the band edges at finite n.

3.6. The Conductivity

In this section we will describe the results of the calculation of the components of the conductivity tensor using the linear response formalism described in chapter one. The conductivities σ_{xx} and σ_{xy}^I are derived from the diagram shown in figure 11a in which the open circles represent components of the velocity operator: v_x or v_y. The only vertex corrections which are finite in the large n limit are the ladder insertions (12b) which have been shown (Bastin et al 1971) to give zero contribution to the conductivities .

The matrix elements of the operators v_x and v_y are only non-zero between states in adjacent Landau levels (see appendix 1 to chapter one). Also, they are proportional to $\hbar\omega_c$, whilst the bare propagator within a Landau level adjacent to the one containing the Fermi energy decreases as $(\hbar\omega_c)^{-1}$ for $\hbar\omega_c$ large. Hence, in order to calculate the conductivities we consider weak mixing between Landau levels, expanding the full Green functions to $O(1/\hbar\omega_c)$. Higher terms make vanishing contribution to the conductivity in the limit $\hbar\omega_c \to \infty$.

For each choice of potential distribution we find, using Streda's formulae 7.9-11 of chapter 1 (page 31), that

$$\sigma_{xx} = e^2 D\ \rho(E_f) \qquad (6.5)$$

(to illustrate the general method this is explicitly calculated for the case of Gaussian white-noise in appendix 4) and

$$\sigma_{xy}^I = \frac{\hbar e^2}{m}\ (n+\tfrac{1}{2})\ \rho(E_f). \qquad (6.6)$$

It is interesting to note in passing that σ^{I}_{xy} is associated by Streda with the classical result of the Drudé-Zener theory, while $\sigma_{xy}{}^{II}$ is considered to be a quantum correction. As might be expected in the presence of a quantising magnetic field, in the present calculation when the derivative with respect to the field is expanded to obtain $\sigma_{xy}{}^{II}$ there is always a term of the form $-\sigma_{xy}{}^{I}$ which exactly cancels the "classical" result. This can be seen from the following. The expression 7.11 of chapter 1 for $\sigma_{xy}{}^{II}$ gives

$$\sigma^{II}_{xy}(E_f) = e \frac{d}{dB} \int_{-\infty}^{\Delta E_f} \rho(\eta)\, d\eta \,, \tag{6.7}$$

where $\Delta E_f=(E_f-(n+\tfrac{1}{2})\hbar\omega_c)$. We can separate the derivative into two terms, one involving the derivative of ρ, the other involving the derivative of the upper limit of integration,

$$\sigma^{II}_{xy}(E_f) = e \int_{-\infty}^{\Delta E_f} \frac{d\rho(\eta)}{dB}\, d\eta \;-\; \rho_n(E_f)\, \frac{dE_n}{dB} \,. \tag{6.8}$$

From the definition of E_n we find that $dE_n/dB = (n+\tfrac{1}{2})\hbar e/m$ and obtain finally

$$\sigma_{xy} = e \int_{-\infty}^{\Delta E_f} \frac{d\rho(\eta)}{dB}\, d\eta \,. \tag{6.9}$$

The results of the calculation of the Hall conductivity are as given below.

(a) Gaussian White-Noise

The Hall conductivity can be written as

$$\sigma_{xy} = \frac{e}{B} N(E_F) - \frac{e}{2B}(E_F-E_n)\, \rho_n(E_F). \tag{6.10}$$

The variation of σ_{xy} with the electron density, N, is shown in figure 12.

(b) Fixed Strength Delta Function Scatterers

The Hall conductivity as a function of the Fermi Energy is

$$\sigma_{xy}(E_f) = \frac{e^2}{h} \left\{ \theta(1-\nu)\ \theta(E_f-E_n) + \tilde{\sigma}\ ((E_f-E_n)/\lambda) \right\} \tag{6.11}$$

where

$$\tilde{\sigma}(\Delta) = \left[\frac{\pi}{2} - \mathrm{Sin}^{-1}[f_1(\Delta)] \right] + \mathrm{sgn}(\nu-1) \left[\frac{\pi}{2} + \mathrm{Sin}^{-1}\ [f_2(\Delta)] \right]$$

with

$$f_1(\Delta) = \frac{\nu+1-\Delta}{2\ \nu^{\frac{1}{2}}}\ , \qquad f_2(\Delta) = \frac{(\nu+1)^2\Delta - (\nu-1)}{2\ \Delta\ \nu^{\frac{1}{2}}}$$

$$\text{and}\quad \mathrm{sgn}(x) = \frac{x}{|x|}\ .$$

We give graphs of Hall conductivity against electron density in figures 13 a and b, for the values ν=.4 and ν=3.

(c) Delta Function Scatterers with a Lorentzian Distribution of Strengths

For the two limiting cases of Lorentzian white-noise ($\nu\to\infty$, $q\to0$, ν_Y=constant) and of a Fermi energy in the band tails, the Hall conductivity has the same variation with electron density as in the free electron gas. More generally, the Hall conductivity increases most rapidly with the electron density at the band centre and more slowly in the band tails, as illustrated in figure 14.

To summarise, we have calculated exactly the longitudinal and Hall conductivities for the three choices of random potential in the large n limit. σ_{xx} obeys the Einstein relation $\sigma_{xx}=e^2\rho D$, where ρ is the density of states within the impurity band, in all cases. We note that in case (b), in the low density régime (ν<1), electrons in the Landau level remnant are not scattered by the potential and therefore cannot take part in any dissipative process; thus σ_{xx} is zero for these states. On very general grounds we expect that when the Fermi energy lies in a band gap the Hall conductivity will take on its quantised value (Laughlin 1981, Thouless 1981). This is indeed found in the present work, notably in the case of a low density of fixed strength delta function scatterers: when the Fermi energy lies between the Landau level remnant and the impurity band the Hall conductivity

is that of the filled level. Finally we note that in cases (a) and (b) in which the impurity band has hard edges ($\rho \sim (\eta - \eta_0)^{1/2}$ as $\eta \to \eta_0$) the current per state ($\partial\sigma_{xy}/\partial N$) is infinite at the band edges, whereas in case (c), where the density of states has Lifshitz tails, $\partial\sigma_{xy}/\partial N$ is finite everywhere.

3.7: A Review of the 1/n Expansion

In this section the systematic expansion for physical quantities about the large n limit in powers of the small parameter 1/n is reviewed.

As has been said in section 1.5, the two-dimensional electron gas in a strong magnetic field, owing to its rather singular spectrum in the absence of disorder, has no weak scattering limit; the disorder strength is the only relevant energy scale in the problem. Studies of Anderson localisation in the absence of any magnetic field are based largely on the fact that the weak scattering limit, which exists because there are two relevant energy scales: the disorder and the Fermi energy, corresponds to the weak localisation régime. This arises because, when the disorder is small on the scale of the Fermi energy, there is a wide disparity between the phase coherence length and the localisation length and, therefore, on any length scale between these two the motion of an electron is diffusive.

In studying the quantum Hall effect one would like to be able to identify a régime in which the effects of localisation could be turned on in a controlled manner. In the absence of a field the controlling parameter is the ratio v/E_f; one would like to identify such a parameter in the strong field case. We have seen, in the first part of this chapter, that in the large n limit the quantum inteference effects which give rise to localisation are suppressed and that the localisation length diverges for all energies. We are thus drawn to the conclusion that the large n limit is a weak localisation régime. It is then apparent that 1/n is an appropriate small parameter in which to set up a systematic expansion for physical quantities in order to introduce the effects of Anderson localisation in a controlled manner.

The principal result of the calculation of the 1/n corrections to the two particle Green function involves a generalisation of the energy dependent diffusion constant D(E) defined in section 1.6. This was defined as

$$\lim_{q^2\to 0}\ \lim_{\omega\to 0} Q(q,E+i\varepsilon) = \frac{\pi\rho(E)}{\omega + \tfrac{1}{2}D(E)q^2} \quad . \tag{7.1}$$

We need to define a generalised diffusion constant $D(q;E,\varepsilon)$ in the following manner

$$Q(q,E+i\omega) \sim \frac{\pi\rho(E)m_n(q^2)}{\omega + \tfrac{1}{2}D(q,E,\varepsilon)q^2} \quad \omega\to 0 \quad . \tag{7.2}$$

As was to be expected the corrections to Q at higher orders in 1/n are divergent as $\omega\to 0$. We can understand this by recalling the identification of ω with the inelastic scattering rate in the system and thence with the effective system size via the inelastic scattering length L_{in} (see section 1.5). The most important result of the systematic expansion in 1/n is that the corrections to this generalised diffusion constant at non-zero wave vector act to decrease its value at all energies except at the band centre ($E=(n+\tfrac{1}{2})\hbar\omega_c$). However the corrections at zero wavevector, ie the corrections to the diffusion constant defined in section 1.6, vanish identically throughout the band. The correction to the modified diffusion constant is greatest for $q_0\sim(n^{1/2}l_c)^{-1}$, the inverse size of a typical wavepacket composed of states in the n^{th} Landau level. This behaviour implies the existence of an instability because at $q=q_0$ the diffusion constant $D(q_0,E,\omega)$ will fall to zero as ω is decreased (ie the system size is increased) at some energy inside the band, leading to an unphysical negative value at energies further from the centre of the band. The energy at which this occurs will move in towards the band centre as the system size diverges (ie the infra red regulator $\omega\to 0$). This behaviour can be taken as an indication that all states, except those at the Landau level energy, $(n+\tfrac{1}{2})\hbar\omega_c$, become localised for finite values of n in the limit of an infinite system.

The corrections to the components of the conductivity tensor have also been calculated. At O(1/n) the corrections to both components vanish while at $O(1/n^2)$ only the dissipative conductivity is changed.

3.8 Conclusions

By considering the limit of a very high Landau level we have an exactly solvable model of the disordered two-dimensional electron gas in a strong magnetic field. The model is solvable because in this limit quantum interference is suppressed. This suppression precludes the existence of localised states; consequently the plateaus which are the most distinctive feature of the experimental observations of the integer quantum Hall effect do not appear. The model does, however, show marked variations in the electron mobility across the impurity band. The solution of this model has been given for three choices of random potential: Gaussian white-noise, the simplest form of random potential to treat theoretically; randomly placed fixed strength delta function scatterers, which provide a quite different type of potential; and finally delta function scatterers with a Lorentzian distribution of strengths, which provides an example of an impurity band with Lifshitz tails.

Appendix 1: Evaluation of the Four Point Vertex in The Landau Basis

The four point vertex is given by equation 3.11 as

$$v^2 \int d^2r \, \langle n,k_1|r\rangle\langle r|n,k_2\rangle\langle n,k_3|r\rangle\langle r|n,k_4\rangle$$

$$= \frac{v^2}{4\pi^2} \int dxdy \, \exp\left\{iy(k_1-k_2+k_3-k_4)\right\} \chi_n(x+k_1)\chi_n(x+k_2)\chi_n(x+k_3)\chi_n(x+k_4) \, .$$

Performing the y integration leaves

$$\frac{v^2}{2\pi} \delta(k_1-k_2+k_3-k_4) \, Z(k_1,k_2,k_3,k_4)$$

where $Z(k_1,k_2,k_3,k_4) = \frac{1}{2\pi} \int dx \, \chi_n(x+k_1)\chi_n(x+k_2)\chi_n(x+k_3)\chi_n(x+k_4)$.

We can define $k_1=K+q$, $k_2=K$, $k_3=K+k$, $k_4=K+k+q$ so that the delta function is automatically satisfied to give

$$\tilde{Z}(K,k,q) = \frac{1}{2\pi} \int dx \, \chi_n(x+K)\chi_n(x+K+q)\chi_n(x+K+k)\chi_n(x+K+k+q)$$

$$= \frac{1}{2\pi} \int dx \, \chi_n(x)\chi_n(x+q) \, \chi_n(x+k)\chi_n(x+k+q) = \Xi_n(k,q) \qquad (A1.1)$$

We now employ the result of appendix 7 of chapter 1

$$I_n(u,v) = \int dw e^{iwv} \chi_n(w)\chi_n(w+u) = e^{-iuv/2} \, e^{-\frac{1}{4}(u^2+v^2)} \, L_n\left[\tfrac{1}{2}(u^2+v^2)\right] .$$

Fourier transforming with respect to v gives

$$\frac{1}{2\pi} \int dv \, e^{-iwv} I(u,v) = \chi_n(w)\chi_n(w+u) \, .$$

Substituting this into A1.1 yields

$$\Xi_n(k,q) = \frac{1}{8\pi^3} \int dxdpd\lambda \, e^{-ipx} \, I_n(q,p) \, e^{-i\lambda(x+k)} \, I_n(q,\lambda) \, .$$

The integration over x results in a delta function $\delta(p+\lambda)$ so the subsequent integration over p is trivial leaving

$$\Xi_n(k,q) = \frac{1}{4\pi^2} \int e^{-i\lambda k} \, e^{iq\lambda/2} \, e^{-\frac{1}{4}(q^2+\lambda^2)} \, L_n\left[\tfrac{1}{2}(q^2+\lambda^2)\right] \times$$

$$e^{-iq\lambda} \, e^{-\frac{1}{4}(q^2+\lambda^2)} \, L_n\left[\tfrac{1}{2}(q^2+\lambda^2)\right]$$

$$= \frac{1}{4\pi^2} \int e^{-ik\lambda} m_n(q^2+\lambda^2) \, d\lambda \text{ where } m_n(x)=e^{-x/2}L_n(x)$$

and therefore the vertex part is as given in equation 3.11.

Appendix 2: Evaluation of the Integral 3.14

The required integral is

$$A = \int dq\ M_n(0,q) = \int d\lambda dq\ m_n(q^2+\lambda^2) .$$

Let $q=u^{1/2}\cos\theta$ and $\lambda=u^{1/2}\sin\theta$ then

$$A = 2\pi\int_0^\infty m_n(2u)\ du = 2\pi\int_0^\infty e^{-u}[L_n(u)]^2 du = 2\pi$$

where the last step follows by the orthonormality of the Laguerre polynomials.

Appendix 3: Asymptotic Evaluation of the Integral in Equation 3.21

The integral to be estimated is

$$I = \int dkdq\ |M_n(k,q)|^2$$

Using the integral representation of M_n gives

$$I = \int dkdqd\lambda d\mu\ e^{ik(\lambda-\mu)}\ m_n(\lambda^2+q^2)\ m_n(\mu^2+q^2)$$

$$= 2\pi \int dqd\lambda\ [m_n(\lambda^2+q^2)\ ]^2 .$$

Changing to polar coordinates gives

$$I = 4\pi^2 \int e^{-2u}\ [\ L_n(u)\ ]^4\ du .$$

Now $(L_n)^2$ can be written as a series in Laguerre polynomials (Gradsteyn and Ryzhik (1979) formula 8.976.3) such that

$$[L_n(x)]^2 = \sum_{k=0}^{n} S_k\ L_{2k}(2x)$$

$$S_k = \frac{(2k)!\ (2n-2k)!}{2^{2n}\ [\ k!\ (n-k)!\ ]^2} .$$

Thus

$$I = 4\pi^2 \sum_{k,p=0}^{n} S_k S_p \int e^{-2u}\ L_{2k}(2u)L_{2p}(2u)\ du$$

The orthonormality of the Laguerre polynomials allows the evaluation of the integral leaving

$$I = 2\pi^2 \sum_{k=0}^{n} (S_k)^2 .$$

For large n this sum is dominated by the majority of terms for which $0 \ll k \ll n$ so that Stirlings formula can be applied to the factorials to give

$$I \sim 2 \sum_{k=\alpha}^{n-\alpha} \frac{1}{k(n-k)} \quad . \qquad n \to \infty$$

Converting the sum into an integral then gives $I \sim 4\log(n)/n$.

Appendix 4: Calculation of the Longitudinal Conductivity for the Case of Gaussian white-noise

The Kubo-Streda formula for the longitudinal conductivity is given in equation 7.9 of chapter 1. In the large-n limit the only contribution to the conductivity comes from the diagram in Figure 11b. in which $K(\mathbf{r},\mathbf{r}';z;\mathbf{r}',\mathbf{r};z^{*}) = |G(\mathbf{r},\mathbf{r}';z)|^2 = |g_n(z)|^2 |C_n(\mathbf{r},\mathbf{r}')|^2$. In order to calculate this diagram we note first that in the large n limit the one particle Green function in the Landau basis is $G_{n,k;n',k'} = \delta(k-k')\delta_{n,n'} g_n(z)$. Secondly the matrix elements of v have the form $\langle n,k|v_\mu|m,q\rangle = \delta(k-q)\upsilon_{n,m}$. Hence

$$\sigma_{xx} = \frac{\pi\hbar e^2}{(2\pi i)^2 \Omega} \sum_{\substack{m,m' \\ k}} \langle m,k|v_x|m',k\rangle\langle m',k|v_x|m,k\rangle \, \tilde{g}_{m'}(E_f)\, \tilde{g}_m(E_f) \quad .$$

The free summation over k counts the total number of states in a Landau level, ie $\Omega/2\pi l_c^2$. Using the explicit forms for the matrix elements of v contained in the first appendix of chapter 1 we find

$$\sigma_{xx} = \frac{\pi\hbar e^2}{(2\pi i)^2 2\pi l_c^2} (l_c^2\omega_c^2) \sum_{m,m'} \left\{ \frac{n+1}{2} \delta_{m',m+1} + \frac{n}{2} \delta_{m',m-1} \right\} \tilde{g}_{m'} \tilde{g}_m \quad .$$

We wish to weakly couple the n^{th} Landau level with the $(n+1)^{th}$ and the $(n-1)^{th}$. So we assume that only for these values of m is g_m relevant. The sum therefore reduces to $(n+\tfrac{1}{2})\tilde{g}_n(\tilde{g}_{n+1} + \tilde{g}_{n-1})$. It is shown in appendix five that to lowest order in $(\hbar\omega_c)$ $\tilde{g}_{n\mp1} = \lambda\tilde{g}_n/(\hbar\omega_c)^2$ so that

$$\sigma_{xx} = \frac{\pi\hbar e^2 l_c^2 \omega_c^2}{(2\pi i)^2 2\pi l_c^2} \, 2(n+\tfrac{1}{2}) \, \frac{\lambda}{(\hbar\omega_c)^2} \left[\tilde{g}_n(E_f) \right]^2$$

Now $\tilde{g}_n$ is simply related to the density of states by

$$\tilde{g}_n(E) = 2\pi l_c^2 \, 2\pi i \rho(E)$$

So that

$$\sigma_{xx} = \frac{4\pi e^2 l_c^4 \lambda(n+\frac{1}{2})}{\hbar} \left[\rho(E_f) \right]^2 = e^2 D\rho(E_f) \quad .$$

Appendix 5: Relation Between Green Functions in different Landau Levels

We wish to evaluate, to lowest order in $(\hbar\omega_c)^{-1}$, the value of a Green function in the $n\pm1^{th}$ Landau level. To include mixing between adjacent Landau levels we must add some terms to the Dyson equation (3.25). We must allow the middle propagator in the last diagram of Figure 4 to be the sum of Green functions for the $n-1^{th}$, n^{th} and the $n+1^{th}$ levels.

This gives the following form for the Dyson equation

$$g_n = g_n^0 + \lambda g_n^0 \Sigma_n g_n \quad \text{where } \Sigma_n = g_{n-1} + g_n + g_{n+1} \ .$$

$$g_{n\pm1} = g_{n\pm1}^0 + \lambda g_{n\pm1}^0 \Sigma_{n\pm1} g_{n\pm1} \quad \text{where } \Sigma_{n\pm1} = g_{n\pm1} + g_n$$

In the $n\pm1^{th}$ level we can write therefore

$$g_{n\pm1}(z) = \frac{1}{z \mp \hbar\omega_c - \lambda\Sigma_{n\pm1}} = \frac{\mp1}{\hbar\omega_c}\left[1 \pm \frac{z-\lambda\Sigma_{n\pm1}}{\hbar\omega_c} \right]$$

$$= \frac{\mp1}{\hbar\omega_c} + \frac{\lambda g_n - z}{(\hbar\omega_c)^2} + O\left[(\hbar\omega_c)^{-3} \right] \ .$$

Consequently the difference between $g_{n\pm1}$ and its complex conjugate is, to lowest order in $(\hbar\omega_c)^{-1}$

$$\tilde{g}_{n\pm1}(E) = \frac{\lambda \tilde{g}_n(E)}{(\hbar\omega_c)^2} \quad .$$

Figure 1
The three diagrams contributing to $G(r,r';z)$ at second order in v^2

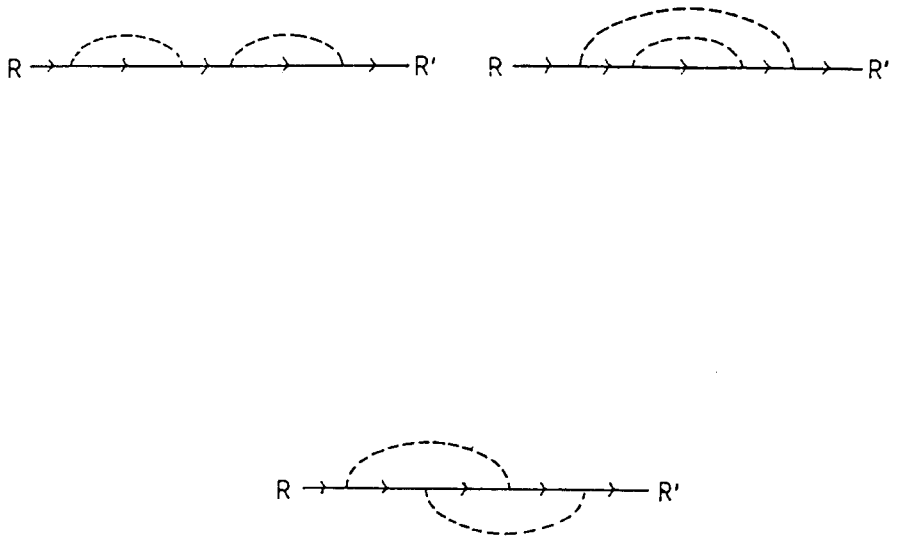

Figure 2
The diagram representing the interaction part $M_n(q,k)$.

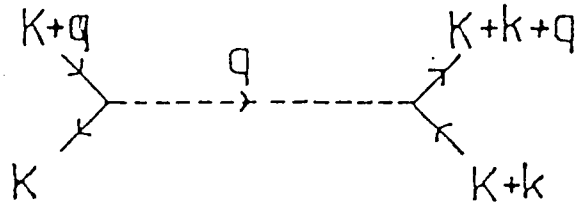

Figure 3
a) A second order diagram

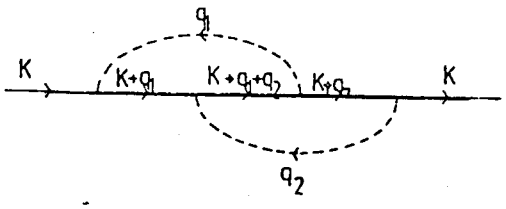

b) The amputated interaction parts of 3a: $M_n(q_1,-q_2)$ and $M_n(q_2,q_1)$

Fig. 3b

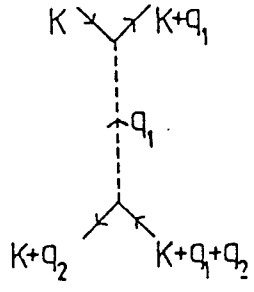

Fig. 3c

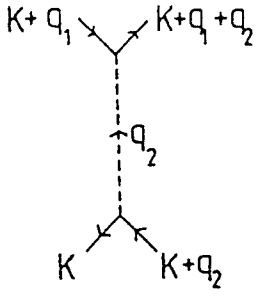

Figure 4
The Dyson equation for the Gaussian white-noise potential.

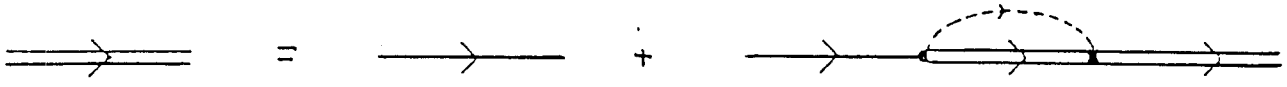

Figure 5
The Bethe-Salpeter equation for the Gaussian white-noise potential (solid lines represent complete propagators).

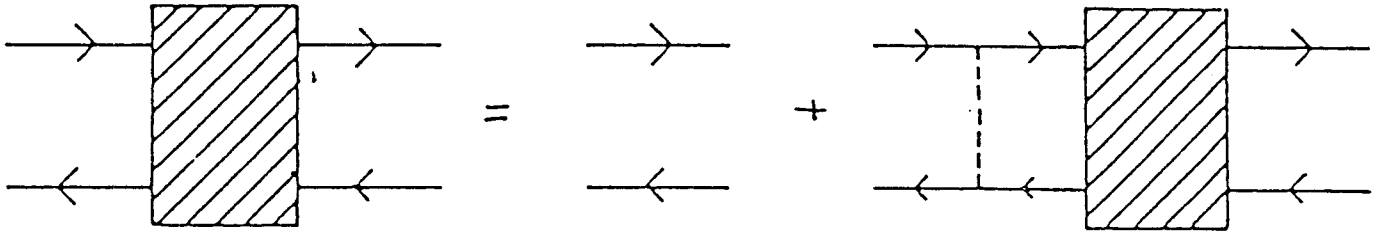

Figure 6
The self-consistent Dyson equations for the delta function potentials.

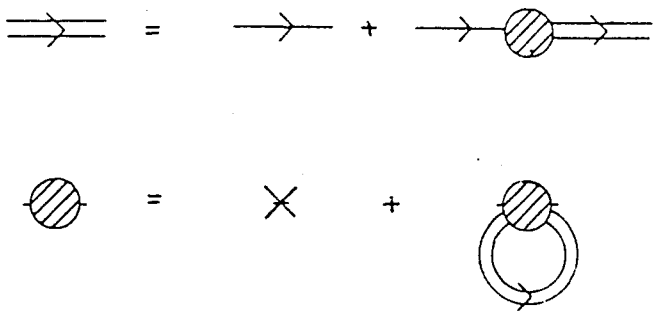

Figure 7
The Bethe-Salpeter equation for the delta function potentials (solid lines represent complete propagators) cross hatched circle is the irreducible two-particle vertex $\Gamma(z_1,z_2)$.

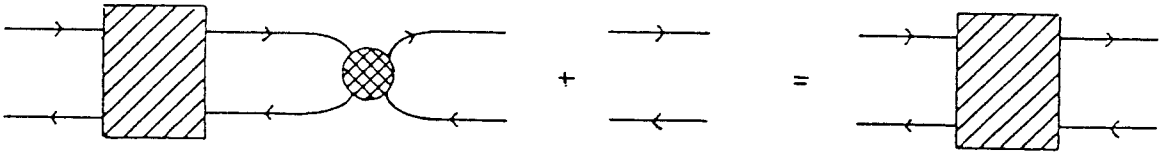

Figure 8
The density of states for the Gaussian white-noise potential.

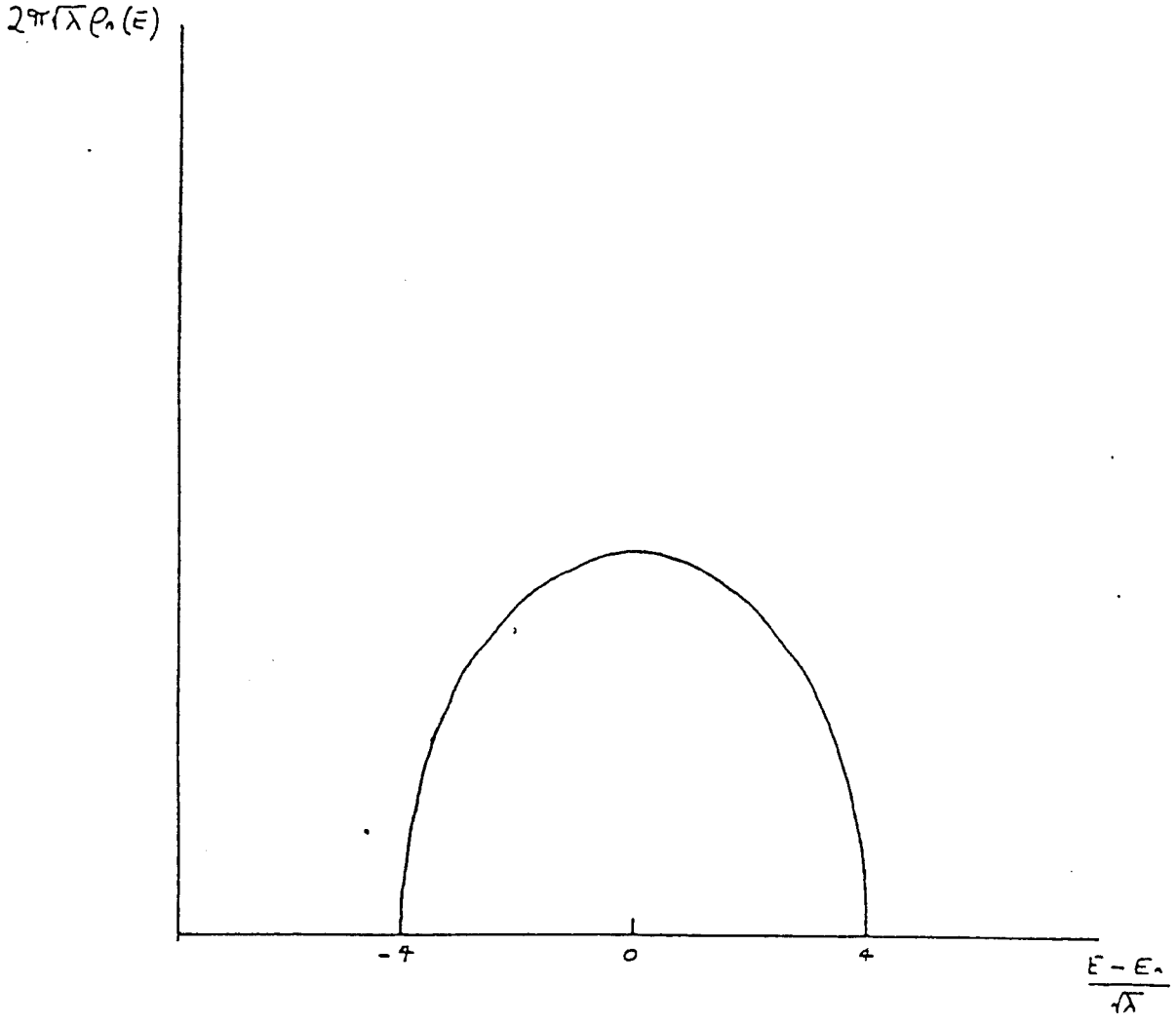

Figure 9
a) The density of states for the fixed strength delta function scatterers with $\nu=0.4$.

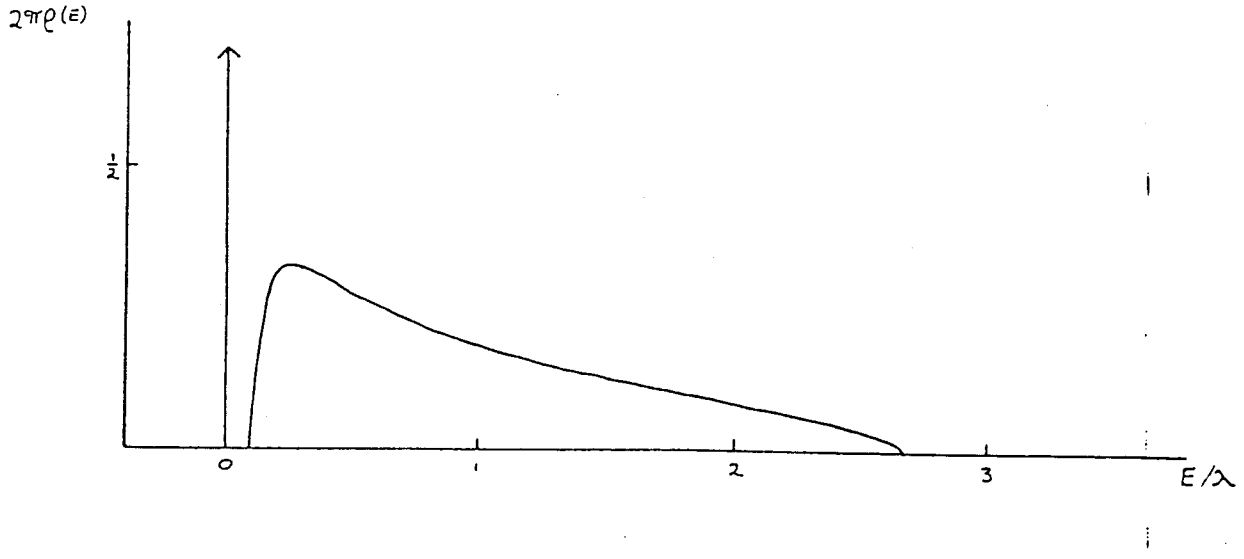

b) The density of states for the fixed strength delta function scatterers with $\nu=3$.

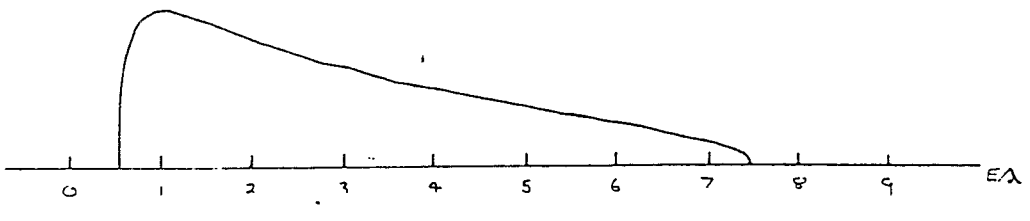

Figure 10
The density of states for the delta function scatterers with a Lorentzian distribution of strengths with ν=2.5.

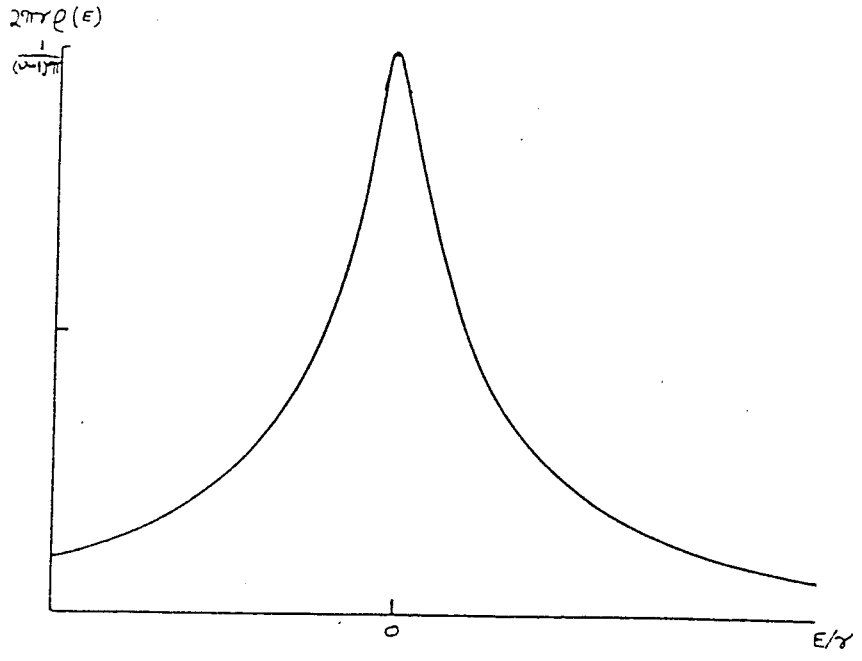

Figure 11
a) The disconnected conductivity diagram.
b) A conductivity diagram with ladder insertions.

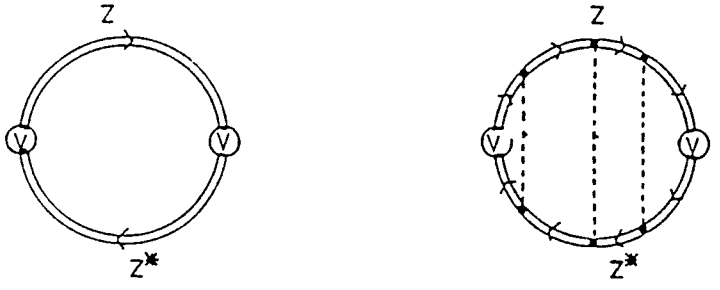

Figure 12
A graph of the Hall conductivity versus electron number density for the Gaussian white-noise potential.

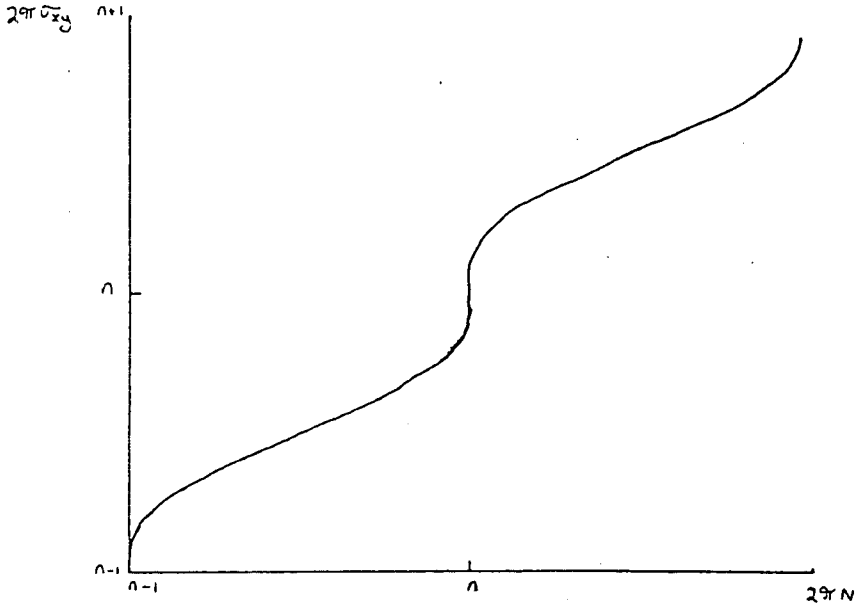

Figure 13
a) A graph of the Hall conductivity versus electron number density for the fixed strength delta function scatterers with ν=0.4.

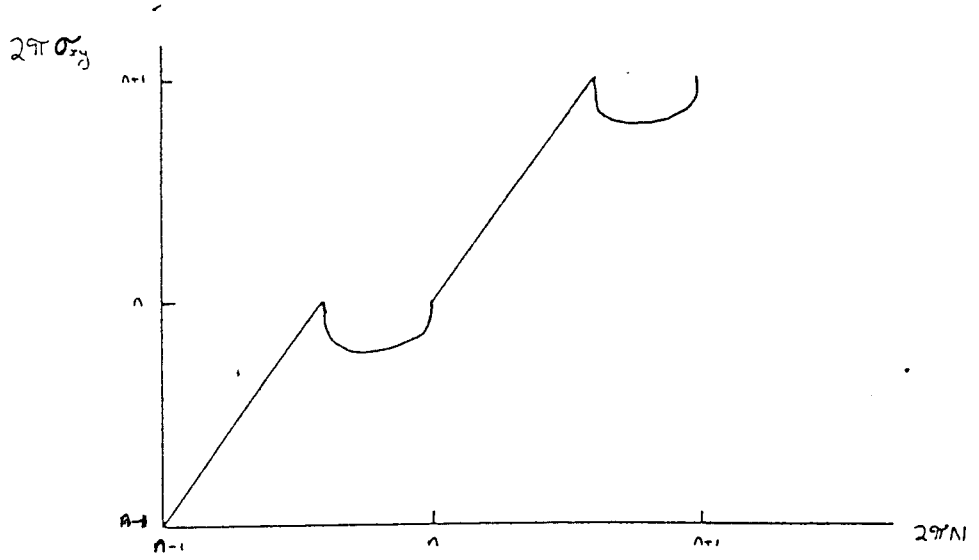

Figure 13
b) A graph of the Hall conductivity versus electron number density for the fixed strength delta function scatterers with ν=3.

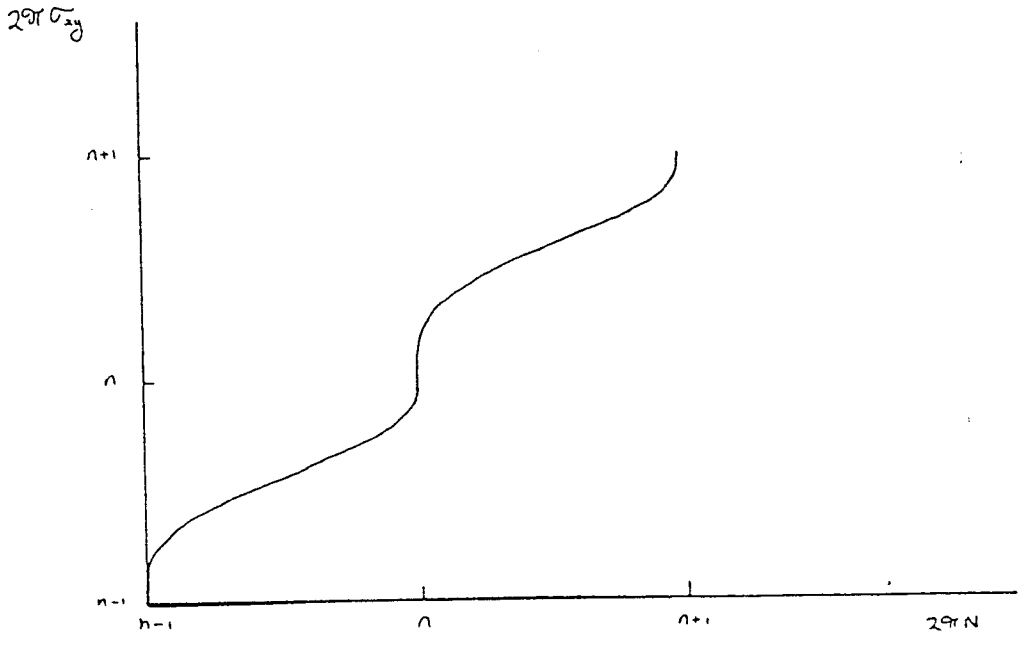

Figure 14
A graph of the Hall conductivity versus electron number density for the delta function scatterers with a Lorentzian distribution of strengths with ν=1.25.

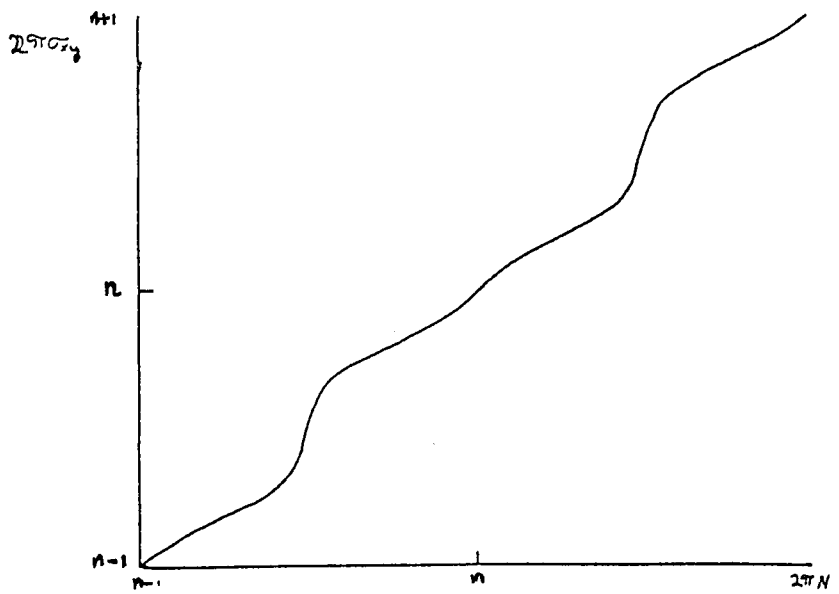

Chapter 4

The Fate of the Lifshitz Tails of High Landau Levels

In this chapter we will describe a calculation of the density of states in the tails of a disorder broadened, high, Landau level using a field theoretic technique.

The work described in this chapter was carried out by the author at the suggestion of Dr. J.T. Chalker and is to appear as Benedict 1986.

4.1: Lifshitz Tails and the Large-n Limit

In chapter 1 Lifshitz's work on the density of states of disordered systems (Lifshitz (1964)) was referred to, particularly the fact that for many types of random potential there will be an exponentially small density arbitrarily far from the level of the ordered system. The states in these Lifshitz tails are supported by regions of exceptionally high or low potential.

Lifshitz argument for electronic systems in the absence of a magnetic field is essentially the following. Consider a free electron gas in a system of area Ω. The density of states for this system varies as $E^{1/2}$. The addition of a fixed number N of short ranged, purely repulsive scattering centres placed at random will shift most of the electronic states to higher energy. The density of states for an energy E, close to zero, will be proportional to the probability that there is a region of sufficiently large area which is free from any scattering centres. A state with energy E will have a wave function which is a nodeless plane wave over the impurity free region and is exponentially small elsewhere. The area must be sufficiently large that there is little kinetic energy cost. We assume that the wavefunction vanishes at the edge of the region and is zero outside it so that the only contribution to the energy is from the kinetic term in the Hamiltonian. This assumption only induces a small error for a sufficiently large region. If we consider the region to be a square of side $\Lambda^{1/2}$, then the energy of the state is $E_0=4\pi^2\hbar^2/2m\Lambda$. The density

of states at energy E is therefore proportional to the probability that a region of area $4\pi^2\hbar^2/2mE_0$ is free of impurities. The probability that an area Λ contains a given impurity is Λ/Ω, hence the probability that it contains no impurities is $(1-\Lambda/\Omega)^N$. In the limit $\Omega\to\infty$, $N\to\infty$, $N/\Omega=\rho$ this is $e^{-\rho\Lambda}$, hence the density of states is proportional to $\exp(-C\rho E^{-1})$. Strictly the region should have been chosen to be circular, but this only modifies C. Contributions from excited modes (ie plane wave states with nodes) over the region are subdominant to this term. Lifshitz and subsequent workers (Friedberg and Luttinger 1975) have calculated the pre-exponential factor and this kind of argument has been extended to show the existence of Lifshitz tails to the bands of a variety of disordered systems (see Thouless 1974 for example).

We shall now consider the situation in a two-dimensional electron gas in a strong magnetic field. We have seen in the previous chapter that, unless the probability distribution for the disorder is made to be extremely broad (for example Lorentzian), the impurity band in the large-n limit has hard edges, that is $\rho(E)\sim|E-E_0|^{1/2}$ as $E\to E_0$, where E_0 is the band edge. The existence of these hard band edges lead to pathological features in the large-n conductivity tensor and to the breakdown of the 1/n expansion at the band edge. Clearly the Lifshitz tails of the n^{th} Landau level are suppressed in the large-n limit and it is the aim of this chapter to show how this occurs.

One of the most successful techniques for the theoretical examination of the density of states in the Lifshitz tails is to map the problem of finding the density of states onto the problem of finding the imaginary part of the two-point function of a field theory. The ratio of disorder strength to the energy plays the role of the coupling constant in this field theory and so the band tails correspond to the weak coupling régime. A normal Feynmann graph perturbation expansion for this theory, expanding around the trivial field configurations (vacuum), reproduces the conventional scattering expansion of Edwards (1958). Each term in the expansion of the two-point function is entirely real: imaginary parts only arising when terms are taken to all orders in the coupling constant. The large n calculation of the previous chapter, for example, sums an infinite subset of terms in the formal expansions of Green functions at all

orders in v to give the Green functions imaginary parts for energies inside the band. The leading contribution to the imaginary part of the two-point function for energies outside the band comes from expanding around the non-trivial or instanton (Langer (1967), Callan and Coleman (1977) and Friedberg and Luttinger (1978)) solutions to the field equations of the theory which are known to control the high order behaviour of the perturbation expansion (see Brézin and Parisi (1980) for example). This method was employed specifically for the two-dimensional electron gas in a strong magnetic field in the lowest Landau level by Affleck (1984); his results coincided, in their region of validity, with the exact expression for the density of states in this level found by Wegner (1983).

The rest of this chapter relates the application of the instanton method to the n^{th} Landau level for large n and is arranged as follows. Section 2 illustrates some of the ideas used in the calculation by describing a zero dimensional toy problem as discussed by Affleck (1984). Section 3 reviews the way the problem of finding the density of states is turned into a field theoretic problem. Section 3 deals with finding the instantons and selecting the one with the lowest action to yield the controlling energy dependence of the density of states. This section also contains a more physical interpretation of the significance of the instanton. Section 4 looks at the treatment of the fluctuations around the saddle-point in the Gaussian approximation and section 5 contains a summary of the results.

4.2: Affleck's Zero Dimensional Toy Model

In order to clarify the method to be used in subsequent sections, whichare based on a Euclidian field theory in two-dimensions, we will present here an analagous zero dimensional calculation due to Affleck 1984. We will attempt to calculate

$$\rho(E) = \frac{1}{\pi} \underset{\varepsilon\to 0}{\text{Lim}}\ \text{Im}\ (2\pi\lambda)^{-1/2}\int dV\ e^{-V^2/2\lambda}\ \frac{1}{E-i\varepsilon-V} = \frac{1}{\pi} \underset{\varepsilon\to 0}{\text{Lim}}\ \text{Im}\ \overline{\left[\ \frac{1}{E-i\varepsilon-V}\ \right]}. \tag{2.1}$$

Clearly since the limit of the imaginary part of $\pi^{-1}(E-i\varepsilon-V)^{-1}$ is a delta function it is trivial to show that

$$\rho(E) = (2\pi\lambda)^{-1/2}\ e^{-V^2/2\lambda}\ . \tag{2.2}$$

We will however attempt to use a more roundabout method of achieving this result which can be generalised to higher dimensions. From the properties of Grassmann numbers (appendix 1) it is easy to verify that

$$(E-i\varepsilon-V)^{-1} = i\int du^{*}\, du\, d\psi^{\dagger} d\psi\; e^{-S(V)}\; \psi\psi^{\dagger} \qquad (2.3)$$

where $$S(V)=u^{*}(E-i\varepsilon-V)u + \psi^{\dagger}(E-i\varepsilon-V)\psi$$

(see appendix 4) where u and ψ are complex and Grassmann variables respectively. We can now easily average this expression over the Gaussian distribution of Vs to give

$$G(E) = (E-i\varepsilon-V)^{\overline{-1}} = i\int du^{*}\, du\, d\psi^{\dagger} d\psi\; e^{-iS(0)}\; \psi\psi^{\dagger} \times$$

$$(2\pi\lambda)^{-1/2} \int dV\; e^{-V^2/2\lambda}\; e^{-iV(u^{*}u+\psi^{\dagger}\psi)} \qquad (2.4)$$

The integral over V can be easily performed by completing the square in the exponent to give

$$G(E) = i\int du^{*}\, du\, d\psi^{\dagger} d\psi\; e^{-iu^{*}(E-i\varepsilon)u\, -i\psi^{\dagger}(E-i\varepsilon)\psi\, -\frac{1}{2}\lambda(u^{*}u+\psi^{\dagger}\psi)^2}\; \psi\psi^{\dagger} \qquad (2.5)$$

We can now integrate out the Grassmann fields as follows.

$$G(E) = i\int du^{*}\, du\; e^{-iu^{*}(E-i\varepsilon)u-\frac{1}{2}\lambda(u^{*}u)^2} \int d\psi^{\dagger} d\psi\; e^{-i\psi^{\dagger}(E-i\varepsilon-\lambda u^{*}u)\psi}\; \psi\psi^{\dagger}$$

$$= \frac{i}{\pi}\int du^{*}\, du\; e^{-iu^{*}Eu-\frac{1}{2}\lambda(u^{*}u)^2} \qquad (2.6)$$

The term in the action that is quartic in the Grassmann numbers vanishes by vitrue of their antisymmetry. This feature of the model calculation does not carry forward to higher dimensions but we will not gain anything by not using it. We have taken the $\varepsilon\to 0$ limit because its role in regulating the integral for large $|u|$ is now redundant because of the presence of the quartic term. This integral can be done exactly (appendix 5) but again the method will not generalise to functional integrals so we will proceed by attempting its evaluation by the method of steepest descents. First, however it is convenient to change from using the complex variable u to a two-component real variable $\underline{\phi}=(\phi_1,\phi_2)^{T}$ defined by $u=\phi_1+i\phi_2$. We then get

$$G(E) = \frac{i}{\pi}\int d\underline{\phi}\; e^{-S(\underline{\phi})}$$

where $$S(\underline{\phi}) = -i\underline{\phi}^{T}E\underline{\phi} - \tfrac{1}{2}\lambda(\underline{\phi}^{T}\underline{\phi})^2 \; . \qquad (2.7)$$

For small values of λ the integral will be dominated by the saddle points of the integrand. The saddle point condition is

$$\frac{\partial S(\phi)}{\partial \phi_i} = \left[-iE - \lambda(\underline{\phi}^T \underline{\phi}) \right] \phi_i = 0 \qquad (2.8)$$

which has a trivial solution $\phi_i=0$ $i=1,2$ and a one-parameter family of non-trivial solutions

$$\underline{\phi}^0(\theta) = (-iE/\lambda)^{1/2} \begin{bmatrix} \cos\theta \\ \sin\theta \end{bmatrix} . \qquad (2.9)$$

If we now allow both components of $\underline{\phi}$ to be complex we find that the stationary phase contours are given by $(x^2-y^2+u^2-v^2)\{E+2\lambda(xy+uv)\}=C$ where $\phi_1=x+iy$, $\phi_2=u+iv$ and C is a constant. The steepest descents path is given by the stationary phase contours passing through the saddle points (Bender and Orszag 1978) which are those with $C=0$. These contours are shown in the ϕ_1 plane in Figure 2 for $E>0$ (for $E<0$ take $y\to -y$, $v\to -v$); c_1 is the line pair $x^2=y^2$ and c_2 is the hyperbola $y=-(E-2\lambda uv)/2\lambda x$. The steepest descents paths inevitably intersect at the saddle points (see Bender and Orszag). The orientation of the saddles is as indicated and consequently the integration contour is the full line in the figure.

The values of the action at the saddles are: $S(0)=0$, $S(\underline{\phi}^0)=E^2/2\lambda$. It is therefore natural to initially only consider the trivial saddle-point since the value of the integrand is exponentially smaller at the others. Expanding to quadratic order about $\underline{\phi}=\underline{0}$ gives

$$S \simeq 0 + iE(\phi_1^2+\phi_2^2) . \qquad (2.10)$$

The contour c_1 is parameterised by $\phi_i = e^{-i\pi\sigma/4}x$, where $\sigma=\text{sign}(E)$, so the leading contribution to G is given by integrating across the saddle for $x\in[-\varepsilon,\varepsilon]$ but, as usual in the method of steepest descents, we only make a small (subdominant) error by extending the integral to $x\in[-\infty,+\infty]$. Hence

$$G(E) \sim \frac{1}{\pi} \int_{-\infty}^{+\infty} dxdy\ e^{-|E|(x^2+y^2)} . \qquad (2.11)$$

However this integral is real and had we kept higher terms in the expansion of the action to generate a series for G(E) in powers of $\lambda/|E|$ each term would have been real. Thus we see that although the

trivial saddle point controls the real part of G, the leading contribution to the imaginary part must come from somewhere else: the set of non-trivial saddlepoints.

Expanding around a particular saddlepoint, $\phi^0{}_1=(-iE/\lambda)^{1/2}$, $\phi^0{}_2=0$ (ie the parameter $\theta=0$) gives

$$S(\phi) \simeq \frac{E^2}{2\lambda} - 2iE(\phi_1-\phi_1^0)^2. \qquad (2.12)$$

Notice that this is independent of ϕ_2. An infinitesimal increase in ϕ_2 is equivalent to an infinitesimal increase in θ, ie a transformation from one saddlepoint to another, since all the non trivial saddles have the same action then the lowest order expansion of S is independent of ϕ_2. This is an important point which will recurr in the two-dimensional field theory. If we were to use this as an approximation to the integrand naively then the free integration over ϕ_2 would diverge we must find some way around this. The spirit of the steepest descents method is to make a parabolic approximation to the function in the exponent of an integrand. Since the function $S(\phi)$ is invariant under a small increase of ϕ_2 the parabolic approximation is clearly bad. The technique employed is to replace the free integration over ϕ_2 by an integration over the compact collective coordinate θ. This transformation introduces a Jacobian

$$\Delta = \left[\frac{-iE}{\lambda}\right]^{1/2} = e^{-i\sigma\pi/4}\left[\frac{|E|}{\lambda}\right]^{1/2} \qquad (2.13)$$

(to leading order) and renders the integral finite. The saddlepoint is at the end of the contour so we integrate from the saddle along the descending contour. We make only a small error by taking the line $\phi=C+e^{i\pi\sigma/4}x$ as our contour instead of the hyperbola c_2. If $\phi^0{}_1=x_0+iy_0$, then $C=2y_0=-2\sigma x_0$ and x ranges from $x_0(=(|E|/2\lambda)^{1/2})$ up to ∞ (again we extend the contour to infinity with only subdominant error). The contour of integration, as shown in Figure 2, passes through two saddle points, one is our chosen saddlepoint with $\theta=0$, the other is the saddle with $\theta=\pi$, consequently by integrating the collective coordinate over the range 0 to 2π we need only perform one Gaussian integration. Thus

$$G(E) \sim \frac{i}{\pi} e^{-i\sigma\pi/4}\left(\frac{|E|}{\lambda}\right)^{1/2} \int_0^{2\pi} d\theta \times e^{i\sigma\pi/4} \frac{1}{2} \int_{-\infty}^{\infty} dx\, e^{-2|E|x^2}\, e^{-E^2/2\lambda}$$

$$= i\left(\frac{|E|}{\lambda}\right)^{1/2} \left(\frac{\pi}{2|E|}\right)^{1/2} e^{-E^2/2\lambda} \qquad (2.14)$$

and therefore $\rho(E)=(2\pi\lambda)^{-1/2}\exp\{E^2/2\lambda\}$. The important points to note in this calculation are the following.

(i) The introduction of collective coordinates to remove spurious divergences arising from inappropriate use of a parabolic approximation. This will appear in the field theory as the presence of zero-modes, fluctuations in the field, about a non-trivial solution of the field equations, which do not change the action. They will be handled in the same way by introducing collective coordinates which parameterise the saddlepoint manifold.

(ii) The factor of a half appearing outside the Gaussian integral which appears because the integration should actually only be over the range 0 to ∞. Because the functional integrals are always between $-\infty$ and $+\infty$ this factor will appear in the field theory version of this calculation.

(iii) The net factor of $\pi^{1/2}$ left in G(E). One factor of π came from the integration over the collective coordinates, so we must account for the presence of a factor of $\pi^{-1/2}$. This arises from an imbalance in the number of Grassmann and real Gaussian integrations. There were two Grassmann Gaussian integrals performed giving a net factor of $1/\pi$. Only one (ϕ_1) of the real integrals was Gaussian because the other was transformed to the θ integration so the real integrals only gave a factor of $\pi^{1/2}$. This feature will also carry forward to the field theory where each real collective coordinate will carry a factor of $\pi^{-1/2}$

(iv) If we had attempted to expand around the non-trivial saddle point along the contour which passes through $\phi_i=0$, which is a steepest ascent curve, the resulting intgral would have been

$$\frac{1}{\pi}\int dx\, e^{E^2/2\lambda+\frac{1}{2}\lambda x^2} \quad \text{where } x=e^{-i\sigma\pi/4}\,\phi_1$$

which is of course divergent. It was clear that the contour had to rotate through $\pi/2$, at the saddlepoint, back toward the real axis in order that the integral converge. It is this rotation through $\pi/2$

which gives an imaginary part to the integral in the form of a Jacobian factor of σi. Something like this will arise in the field theory where there will be a negative mode tending to make the functional integral diverge. The integration contour for this mode has to be rotated through $\pi/2$ to make the expression converge leading to an overall factor of i giving the Green function an imaginary part.

4.3: Field Theoretic Formulation

The basic model to be examined is that of a two-dimensional electron gas in a strong magnetic field and a quenched Gaussian white-noise potential, V(r). The symmetric gauge is chosen for the vector potential (see chapter one).

We can write the one particle Green function for a particular configuration of the random potential as a functional integral using the formulae presented in appendix 2:

$$\Delta(r,r';z) = \langle r|(z-H[V])^{-1}|r'\rangle$$

$$= i \frac{\int \mathcal{D}u^{*}\mathcal{D}u\ e^{-W[u,V]}\ u(r)u^{*}(r')}{\int \mathcal{D}u^{*}\mathcal{D}u\ e^{-W[u,V]}} \qquad (3.1)$$

where $$W[u,V] = i \int u^{*}(r)\ (z-H[V])\ u(r)\ d^{2}r$$

and u(r) is a complex scalar field. We can rewrite the denominator as a factor in the numerator using the properties of Grassmannian integrals (Appendices 1 and 2) giving

$$\Delta(r,r';z) = i \int \mathcal{D}u^{*}\mathcal{D}u\ \mathcal{D}\psi^{\dagger}\ \mathcal{D}\psi\ e^{-W'[u,\psi,V]}\ u(r)u^{*}(r') \qquad (3.2)$$

where $$W'[u,\psi,V] = i \int \Big[u^{*}(r)\ (z-H^{0})\ u(r) + \psi^{\dagger}(r)\ (z-H^{0})\ \psi(r)$$

$$+ i\ V(r)\ [\ u^{*}(r)u(r) + \psi^{\dagger}(r)\psi(r)\ ]\ \Big] d^{2}r$$

and $\psi(r)$ is a complex Grassmann number. We may now average $\Delta(r,r';z;[V(r)])$ over the disorder to find $G(r,r';z)$.

$$G(r,r';z) = \frac{i \int \mathcal{D}u^{*}\ \mathcal{D}u\ \mathcal{D}\psi^{\dagger}\ \mathcal{D}\psi\ e^{-S\ [u,\psi]}\ u(r)u^{*}(r') \int \mathcal{D}V\ e^{-W''[u,\psi,V]}}{\int \mathcal{D}V\ e^{-W''[0,0,V]}} \qquad (3.3)$$

with $$W''[u,\psi,V] = \int \left\{ \frac{1}{2\lambda} [\ V(r)\ ]^{2} + V(r)[\ u^{*}(r)u(r) + \psi^{\dagger}(r)\psi(r)\ ] \right\} d^{2}r$$

We can complete the square in W″ and shift the integration variable, V, by a constant in the numerator so that the two integrals over V cancel. This leaves the expression

$$G(\mathbf{r},\mathbf{r}';z) = i \int \mathcal{D}u^{*}\mathcal{D}u\, \mathcal{D}\psi^{\dagger}\mathcal{D}\psi\; e^{-S[u,\psi]}\psi(\mathbf{r})\psi^{\dagger}(\mathbf{r}') \qquad (3.4)$$

where the "action", S, is given by

$$S[u,\psi] = \int \Big\{ i\, u^{*}(\mathbf{r})\,(z-H^{0})\,u(\mathbf{r}) + i\,\psi^{\dagger}(\mathbf{r})\,(z-H^{0})\,\psi(\mathbf{r}) ,$$

$$- \tfrac{1}{2}\lambda \left[u^{*}(\mathbf{r})u(\mathbf{r}) + \psi^{\dagger}(\mathbf{r})\psi(\mathbf{r}) \right]^{2} \Big\} d^{2}\mathbf{r} .$$

The Grassmannian fields are performing the same role as the ghost fields in the Faddeev-Popov procedure in common use in quantum gauge theories, ie moving a determinant in the denominator into a functional integral in the numerator.

By considering energies close to the Landau level centre, that is $|E-(n+\tfrac{1}{2})| \ll \hbar\omega_c$, we can restrict the domain of functional integration to field configurations wholly within the n^{th} Landau level, ie

$$u(\mathbf{r}) = \sum_{m=-n}^{\infty} B_m\, \xi_m(\mathbf{r}) \qquad \text{and} \qquad \psi(\mathbf{r}) = \sum_{m=-n}^{\infty} \beta_m\, \xi_m(\mathbf{r}) \qquad (3.5)$$

where $\xi_m(\mathbf{r}) = e^{im\theta}R_{n,m}(r) = \langle r,\theta|n,m\rangle$: the eigenstates of H^0 and L_z, the angular momentum in the plane, as defined in chapter one. B_m and β_m are complex and Grassmann parameters respectively. Hence $H^0u(\mathbf{r}) = (n+\tfrac{1}{2})u(\mathbf{r})$ and $H^0\psi(\mathbf{r}) = (n+\tfrac{1}{2})\psi(\mathbf{r})$.

Consider now the value of the Green function for energies in the tails of the Landau level, that is $\hbar\omega_c \gg |E-(n+\tfrac{1}{2})| \gg \lambda^{1/2}$. This corresponds to the weak coupling régime of the field theory and the functional integral (2.1) will be dominated by the saddle point configurations of the integrand. It is convenient to split the complex scalar field into two real fields by defining $u(\mathbf{r}) = \phi_1(\mathbf{r})+i\phi_2(\mathbf{r})$ and considering the two component object $\underline{\phi}=(\phi_1,\phi_2)^{T}$. Clearly $u^{*}u = \underline{\phi}^{T}\underline{\phi} = \|\underline{\phi}\|^{2}$, while

$$u^{*}(\mathbf{r})\,(z-H^{0})\,u(\mathbf{r}) = \phi_i(\mathbf{r})\,(z-H^{0}_{ij})\,\phi_j(\mathbf{r}) \qquad (3.6)$$

where $$H^{0}_{ij} = -\tfrac{1}{2}\delta_{ij}(\nabla^{2}-A^{2}) - \varepsilon_{ij}\mathbf{A}\cdot\nabla .$$

The restriction of $\underline{\phi}$ to the n^{th} Landau level implies that it can be written in the form

$$\underline{\phi}(r) = \sum_{m=-n}^{\infty} \sum_{a=1}^{2} b_m^a \, \underline{\zeta}_m^a(r) \qquad (3.7)$$

where $\underline{\zeta}_m^a(r) = \underline{T}_m^a(\theta) \, R_{n,m}(r)$;

$\underline{T}_m^1(\theta) = \begin{bmatrix} \cos m\theta \\ \sin m\theta \end{bmatrix}$ and $\underline{T}_m^2(\theta) = \begin{bmatrix} -\sin m\theta \\ \cos m\theta \end{bmatrix}$; while $R_{n,m}(r)$ is defined as above. It follows then that $H^0_{ij}\phi_j(r) = (n+\tfrac{1}{2})\phi_i(r)$. The steepest descents path, for the integration over the $\underline{\phi}$ field, passing through the trivial saddle point, $\phi_i(r)=0$, is along the ray $\exp(-i \, \mathrm{sgn}(\varepsilon)\pi/4)$. It is, therefore, natural to re-define all the fields, ϕ_i, ψ and $\psi^\dagger$, to be multiplied by this phase factor. The functional integral representation of the diagonal part of the Green function then reads

$$G(r,r;z) = \mathrm{sgn}(\varepsilon) \int D\underline{\phi} \, D\psi^\dagger D\psi \; e^{-S[\underline{\phi},\psi]} \; \psi(r) \; \psi^\dagger(r) \qquad (3.8)$$

$$S[\underline{\phi},\psi] = \int \left[\, |\varepsilon| \, \|\underline{\phi}\|^2 + |\varepsilon| \, \psi^\dagger\psi - \tfrac{1}{2}\lambda\|\underline{\phi}\|^4 - \lambda\|\underline{\phi}\|^2(\psi^\dagger\psi) \, \right] d^2r \, .$$

If one attempts to evaluate this by expanding around the trivial saddle point each term in the expansion will be real: imaginary parts will only arise when all orders are considered and, as we have seen, even a partial resummation to all orders will not give an imaginary part outside the band. Expansion around a higher action, non-trivial saddle point (instanton) will, however, lead to imaginary quantities, so computing the lowest action non-trivial saddle point and treating fluctuations about it in the Gaussian approximation will yield the leading order behaviour of the imaginary part of G and hence of the density of states.

4.4: The Field Equations and Instantons

Differentiating the action, 3.8, gives the field equations

$$\mathrm{sgn}(\varepsilon) \, (H^0_{ij} - E) \, \phi_j - \lambda(\phi_j\phi_j + \psi^\dagger\psi) \, \phi_i = 0 \qquad (4.1a)$$

$$\mathrm{sgn}(\varepsilon) \, (H^0 - E) \, \psi - \lambda(\phi_j\phi_j) \, \psi = 0 \, . \qquad (4.1b)$$

A convenient simplification is made by looking for solutions for which Ψ vanishes but $\underline{\phi}$ is non-trivial. Clearly if $\lambda=0$ and $\varepsilon=0$ the solutions of equation 4.1a are the basis functions, $\underline{\zeta}^a{}_m$. Affleck's ansatz for an approximate solution for non-zero λ and ε, which is based on the solution to a linearised version of the field equations, is

$$\underline{\phi}_{cl}(r) = \Gamma_m(\varepsilon)\ \underline{\zeta}^a_m(r), \quad \text{where } \Gamma_m(\varepsilon)\to 0 \text{ as } \varepsilon\to 0. \tag{4.2}$$

This is exact in the absence of Landau level mixing. The action of this solution is clearly $S_{cl}=|\varepsilon|\Gamma_m{}^2(\varepsilon) - \lambda\Gamma_m{}^4(\varepsilon)f_m/2$ where

$$f_m = \int \left\| \underline{\zeta}^1_m(r) \right\|^4 \ d^2r \tag{4.3}$$

The value of Γ can then be determined by extremising this action with respect to variations in Γ for fixed ε: this gives

$$\Gamma_m^2(\varepsilon) = \frac{|\varepsilon|}{\lambda f_m} \quad \text{and} \quad S_{cl} = \frac{\varepsilon^2}{2\lambda f_m}\ . \tag{4.4}$$

The behaviour of f_m is shown in figure 1 for n=8. Asymptotic analysis of the integraldefining f_m in the large n régime indicates that, for $m\gg n$, f_m falls off as $n^{-3/2}$, the local maximum at m=0 has $f_m \sim \ln(n)/n$, while the global maximum is at m=-n and has

$$f_{-n} \sim \frac{1}{4\pi(n\pi)^{1/2}} \qquad n\to\infty \tag{4.5}$$

Hence the least action instanton comes from taking m=-n and its action is,

$$S_{cl} \sim \frac{2\pi\varepsilon^2(n\pi)^{1/2}}{\lambda} \qquad n\to\infty \tag{4.6}$$

The instanton is

$$\underline{\phi}^{cl}(r) = \Gamma_{-n}(\varepsilon)\ \underline{\zeta}^1_{-n} = \Gamma_{-n}(\varepsilon) \begin{bmatrix} \cos n\theta \\ -\sin n\theta \end{bmatrix} r^n\ e^{-r^2/4} \tag{4.7}$$

and the controlling factor in $\rho(\varepsilon)$ is therefore $\exp(-S_{cl})$.

Clearly there is a whole family of instantons, with the same action, derived from this one by translations and rotations, including $\underline{\zeta}^2{}_{-n}$; this multiplicity of solutions, related by the symmetries of the Hamiltonian, will give rise to zero-modes in the calculation of the fluctuations about the instanton.

This form of the controlling factor can be understood as follows. If an electron is in a state described by the wavefunction, $\Psi(r)$, in the pure system and the random potential is then switched on then the first order (in λ) shift in the energy of the state is given by

$$\varepsilon = \int \Psi^{*}(r)\, V(r)\, \Psi(r)\, d^2r. \tag{4.8}$$

Since V has a Gaussian white-noise distribution ε will clearly be a Gaussian random variable with mean zero and variance

$$\sigma^2 = \int\int |\Psi(r)|^2\, |\Psi(r')|^2\, \overline{V(r)V(r')}\, d^2r\, d^2r' \tag{4.9}$$

$$= \lambda \int |\Psi(r)|^4\, d^2r .$$

Thus the probability that the energy of the state is shifted by ε is

$$P(\varepsilon) \propto \exp\left\{ - \frac{\varepsilon^2}{2\sigma^2[\Psi]} \right\} . \tag{4.10}$$

The density of states at energy ε for a macroscopic sytem will be proportional to the probability that a state will be shifted in energy to ε. For large values of $|\varepsilon|$ only the state with the largest σ^2 will contribute. For the basis states considered here $\sigma^2[\xi_m] = f_m$, so for large $|\varepsilon|$ only the state with m=-n (the instanton) will contribute (physically this state is dominant because it has its probability density concentrated on the smallest area) and its probability of having energy ε is proportional to $\exp\{-S_{cl}\}$. This argument is clearly quite crude and makes no attempt to include any mechanism wherebye the wavefunction accomodates itself to the configuration of the disorder by concentrating its probability density in regions of low potential

4.5: Treatment of Fluctuations in the Gaussian Approximation

If the ϕ field is expanded around the classical solution $\underline{\phi}^{cl}$, the Green function can be written,

$$G(r,r';z) \sim e^{-S_{cl}} \int \mathcal{D}\underline{\rho}\, \mathcal{D}\psi^{\dagger}\mathcal{D}\psi\, e^{-\mathcal{F}^b[\rho,\underline{\phi}^{cl}]-\mathcal{F}^f[\psi,\underline{\phi}^{cl}]}\psi(r)\, \psi^{\dagger}(r') \tag{5.1}$$

where $\underline{\rho}(r) = \underline{\phi}(r) - \underline{\phi}^{cl}(r)$,

$\mathcal{F}^b[\underline{\rho},\underline{\phi}^{cl}] = \tfrac{1}{2}\int \rho_i(r)\, \hat{O}^b_{ij}\, \rho_j(r)\, d^2r$ and $\mathcal{F}^f = \int \psi^{+}(r)\, \hat{O}^f \psi(r)\, d^2r$

with

$$\hat{O}^f = \mathrm{sgn}(\varepsilon) \left[H^0 - E \right] - \lambda \left\| \underline{\phi}^{cl}(r) \right\|^2 ,$$

$$\hat{O}^b_{ij} = \mathrm{sgn}(\varepsilon)\left[H^0_{ij} - E \right] - \lambda\, Q_{ij}$$

and $$\left[Q_{ij} \right] = \begin{bmatrix} 3(\phi_1^{cl})^2 + (\phi_2^{cl})^2 & 2\phi_1^{cl}\phi_2^{cl} \\ 2\phi_1^{cl}\phi_2^{cl} & (\phi_1^{cl})^2 + 3(\phi_2^{cl})^2 \end{bmatrix}.$$

The Gaussian functional integral 5.1 can be evaluated by analogy with the zero dimensional integral of section 2 to give

$$\rho(\varepsilon) = -\frac{1}{\pi}\,\mathrm{Im}\left\{ \frac{1}{2}\; e^{-S^{cl}}\; \frac{\Delta_0}{\pi^{1/2}}\; \frac{\Delta_T^2}{\pi}\; \frac{\mathrm{Det}'\hat{O}^f}{\left[\mathrm{Det}'\hat{O}^b_{ij}\right]^{1/2}}\; \times 2\pi \right\}, \qquad (5.2)$$

where the primes on the determinants indicate the omission of zero-modes and the Jacobians, Δ_0 and Δ_T, are for the transformation from integrations over zero-modes to integrations over collective co-ordinates. In the Gaussian approximation the factor $\psi(r)\psi^\dagger(r)$ is replaced by the squared modulus of the normalised zero-mode of O^f, translated by the collective coordinate r^0 and phase shifted by $e^{i\chi}$ (in fact the product of fields is expanded in the eigenmodes of O^f, but only this one term survives the integration over the zero-mode). Since the action is, by definition, indpendent of r^0 and χ the integration over the the collective coordinates is

$$\int_0^{2\pi} d\chi \int d^2 r^0 \left| \xi_{-n}(r-r^0) \right|^2 = 2\pi \qquad (5.3)$$

The factor of 1/2 in 5.2 arises as usual because the integration over the negative mode is only over half of a Gaussian (the contour rotates at the saddle point through $\pi/2$ which gives rise to the factor of i making the integral pure imaginary as happened in the toy model described in section two for the ϕ_1 integration). The factor of $\pi^{-3/2}$ associated with the Jacobians arises because there is one factor of $\pi^{1/2}$ from each Gaussian bosonic integral and one factor of $\pi^{-1/2}$ from each Gaussian fermionic integration. These no longer cancel because three of the bosonic Gaussian integrations have been replaced by integrations over collective coordinates.

The eigenfunctions of O^b and O^f are, in the absence of Landau level mixing, the basis functions $\underline{\zeta}^{(a)}{}_m$ and ξ_m respectively. The eigenvalues of the operators can be calculated exactly in the absence of Landau level mixing, this yields the following expressions for the determinants.

$$\mathrm{Det}'\hat{O}^f = \prod_{i=1}^{\infty} |\varepsilon| \left\{ 1 - \frac{U_{i-n}}{2\pi f_{-n}} \right\} \tag{5.4a}$$

$$\mathrm{Det}'\hat{O}^b_{ij} = -2|\varepsilon| \prod_{i=2}^{\infty} |\varepsilon|^2 \left\{ 1 - \frac{U_{i-n}}{\pi f_{-n}} \right\}^2. \tag{5.4b}$$

where

$$U_m = \int_0^{\infty} \left[R_{n,m}(r) \right]^2 \left[R_{n,-n}(r) \right]^2 r dr \tag{5.5}$$

There is a negative eigenvalue, $-2|\varepsilon|$, coming from the mode $\underline{\zeta}^2{}_{-n}(r)$ which will provide the factor of i in the averaged Green function.

The zero modes arise when the instanton solution has lower symmetry than the original action. Given a solution, $\underline{\phi}$, one can form the following distinct solutions with equal action

$$e^{i\varepsilon_{\mu\nu} r_\mu r^0_\nu} R(\chi)\, \underline{\phi}(r+r^0) \quad 0 \leqslant \chi \leqslant 2\pi, \tag{5.6}$$

where $R(\chi)$ is a 2×2 rotation matrix corresponding to the internal O(2) symmetry of the Lagrangian, and r^0 is an arbitrary translation. The zero modes of O^b are $\underline{\zeta}^a{}_{1-n}$, a=1,2 for the translations and $\underline{\zeta}^1{}_{-n}$ for the O(2) transformation. The position dependent phase factor appears in 5.6 because the symmetry operation under which the Hamiltonian H^0 is invariant is not simply translation but a combined translation and gauge transformation. The action is also invariant under real space rotations, but the structure of the instantons is such that the solution generated by a real space rotation can also be produced by applying an internal O(2) transformation; there are, consequently, only three independent zero-modes. O^f also has a zero mode corresponding to the supersymmetry in the model, generated by the graded (ie mixing normal and Grassmann quantities) transformation

$$\begin{bmatrix} u(r) \\ \psi(r) \end{bmatrix} \rightarrow \begin{bmatrix} 1 & -\Upsilon \\ \Upsilon & 1 \end{bmatrix} \begin{bmatrix} u(r) \\ \psi(r) \end{bmatrix} \tag{5.7}$$

where Υ is an infinitesimal Grassmann number. The Jacobian factors are

$$\Delta_0^2 = \int \|\phi^{cl}(r)\|^2 \, d^2r = \Gamma_{-n}^2(\varepsilon) \tag{5.8}$$

for the O(2) zero mode and

$$\Delta_T^2 = \int \phi_i^{cl}(r) \, H_{ij}^0 \, \phi_j^{cl}(r) \, d^2r = (n+\tfrac{1}{2}) \, \Gamma_{-n}(\varepsilon) \tag{5.9}$$

for the translational zero modes.

Hence the complete Jacobian factor is assymptotically

$$8\pi^{15/8} \left[\frac{|\varepsilon|}{\lambda} \right]^{3/2} n^{7/4} \qquad n\to\infty \tag{5.10}$$

The integral U (defined in equation 5.5) involved in calculating the eigenvalues has not been done in general. However the ratio of the determinants can be written in the form

$$\frac{\text{Det}\,\hat{O}^f}{[\text{Det}'\hat{O}^b]^{1/2}} = \frac{1}{2} |\varepsilon| \left[-2|\varepsilon| \right]^{-1/2} J \tag{5.11}$$

$$= \frac{i \, |\varepsilon|^{1/2}}{2^{3/2}} \, J$$

where J is the infinite product

$$J = \prod_{i=2}^{\infty} \frac{(1-\tfrac{1}{2}a_i)}{(1-a_i)} \qquad \text{with} \qquad a_i = \frac{U_{i-n}}{\pi f_{-n}} \, . \tag{5.12}$$

Now this can be written in the form $J=e^K$ where

$$K = \sum_{i=2}^{\infty} \log \left[\frac{1-\tfrac{1}{2}a_i}{1-a_i} \right] . \tag{5.13}$$

Since $a_i \to 0$ as $i\to\infty$ a cut-off, Λ, can be defined such that $a_i \ll 1$ for $i>\Lambda$ giving

$$K = \sum_{i=2}^{\Lambda-1} \log \left[\frac{(1-\tfrac{1}{2}a_i)}{(1-a_i)} \right] + \sum_{i=\Lambda}^{\infty} \frac{1}{2} a_i + O\left[\sum_{i=\Lambda}^{\infty} a_i^2 \right] \tag{5.14}$$

The completeness of the wavefunctions $R_{n,m}$ implies that

$$\sum_{i=0}^{\infty} a_i = \frac{1}{\pi f_{-n}} \tag{5.15}$$

while the a_i s fall to zero sufficiently fast, for large i, that the terms of order a_i^2 will only produce corrections of order ln(n) or weaker, hence

$$K \approx K_\Lambda + \frac{1}{2\pi f_{-n}} - \sum_{i=0}^{\Lambda} \frac{1}{2} a_i \qquad (5.16)$$

and therefore

$$J = \exp\left\{ \frac{1}{2\pi f_{-n}} \right\} \prod_{i=2}^{\Lambda} \left\{ \frac{(1-\frac{1}{2}a_i)}{(1-a_i)} \exp - \frac{1}{2} a_i \right\} e^{-3/2} \qquad (5.17)$$

The regulated product will have some power law dependence on n, but the first term will give a factor $\exp\{2(n\pi)^{1/2}\}$ which is the controlling n-dependence of the prefactor. The energy dependence of the prefactor is known completely, a factor of $|\varepsilon|^{3/2}$ coming from the zero mode Jacobians and a factor of $|\varepsilon|^{1/2}$ from the ratio of determinants giving a factor of ε^2.

The complete expression for the density of states is, therefore:

$$\rho(\varepsilon) = C\ \lambda^{-1}\ n^{\nu}\ \varepsilon^2 \exp\left\{ - \frac{2\pi(n\pi)^{1/2}(\varepsilon^2-\varepsilon_0^2)}{\lambda} \right\};\quad \varepsilon_0^2 = \frac{\lambda}{\pi}\ . \qquad (5.18)$$

Where C and ν are undetermined constants (independent of n or ε).

4.6: Conclusions

The density of states in the Lifshitz tails of the disorder broadened n^{th} Landau level has been calculated to leading order, for large n, using instanton techniques and has the form (5.18). The tails are found to be suppressed by the factor $n^{1/2}$ in the exponent. This exponential suppression explains the hard band edges found in the $n\to\infty$ limit of the previous chapter and means that the Lifshitz tails will not be seen at any order in a 1/n expansion.

Appendix 1: Grassmann Variables

Grassmann numbers are classical (ie not operator) anticommuting quantities. An n-dimensional Grassmann algebra is a set of n-objects $\{\psi_i : i=1,n\}$ satisfying the relations $\{\psi_i,\psi_j\}=0$ for all i,j in particular they are nilpotent $[(\psi_i)^2=0]$. Any function of the Grassmann numbers has a finite Taylor's series representation

$$f(\{\psi_i\}) = f^0 + \sum_{i=1}^{n} f_i^1 \psi_s + \sum_{i<j} f_{ij}^2 \psi_i\psi_j + \ldots\ldots + f^n \psi_1\psi_2\psi_3\ldots\psi_n .$$

We can define differentiation for the Grassmann functions as follows; we define the derivation operator $\partial/\partial\psi_i$ by

$$\left\{ \frac{\partial}{\partial\psi_i} , \psi_j \right\} = \delta_{ij} \quad \text{and} \quad \left\{ \frac{\partial}{\partial\psi_i} , \frac{\partial}{\partial\psi_j} \right\} = 0 .$$

So, for example, if $f(\psi)=\alpha+\psi\beta$ then $\dfrac{\partial}{\partial\psi} f(\psi) = \beta$.

We can also define formally the integral over a Grassmann variable in such a way that it corresponds with some of our intuitive ideas about definite integrals over an infinite interval. We require principally that the integral be invariant under the addition of a constant to the dependent variable, ie that

$$\int d\psi(\psi+\alpha) = \int d\psi\ \psi .$$

We therefore define the Grassmann integral as follows

$$\int d\psi\ 1 = 0$$

and

$$\int d\psi\ \psi = \pi^{-1/2}$$

The latter integral could have been chosen to take any constant value but the above choice is useful when one is interested in Gaussian type integrals.

For the purposes of generalisation to functional integrals it is useful to consider the Gaussian integral over a pair of conjugate Grassmann variables

$$\int d\psi^\dagger d\psi\ e^{-a\psi^\dagger\psi} = \int d\psi^\dagger d\psi \left[1 - a\psi^\dagger\psi \right]$$

$$= 0 + a \int d\psi^\dagger \left[\int d\psi\ \psi \right] \psi^\dagger = \frac{a}{\pi}$$

Compare this with the corresponding expression for normal variables

$$\int d\phi^* d\phi \; e^{-a\phi^*\phi} = \frac{\pi}{a} \quad .$$

Hence the Grassmannian integral is the reciprocal of the normal one. This result generalises to Gaussian integrals over N variables when a is a matrix and to integrals over fields when a is an Hermitian operator as given in the next appendix.

The use of Grassmann numbers in condensed matter physics is quite widespread now, useful references include M^{c}Kane (1981), Efetov (1983), and Sourlas (1985).

Appendix 2: Functional Integral Formulae

The following is a short list of useful formulae for functional integrals.

1. Complex scalar field u(r).

$$\int \mathcal{D}u\mathcal{D}u^* \exp\left\{-\int u^*(r)\hat{O}u(r)d^2r\right\} = \left[\text{ Det } \hat{O} \right]^{-1}$$

$$\int \mathcal{D}u\mathcal{D}u^* \; u(r)u^*(r')\exp\left\{-\int u^*(r)\hat{O}u(r)d^2r\right\} = \left[\text{ Det } \hat{O} \right]^{-1} \langle r|\hat{O}^{-1}|r'\rangle$$

where $\hat{O}$ is a Hermitian operator.

2. Real two-component field $\underline{\phi}(r)=(\phi_1,\phi_2)^T$

$$\int \mathcal{D}f \exp\left\{ -\int \phi_i(r)\, \hat{O}_{ij}\phi_j(r)\, d\,\underline{r}^2 \right\} = \left[\text{Det } \hat{O}_{ij} \right]^{-1/2}$$

$$\int \mathcal{D}f \; \phi_i(r)\phi_j(r) \exp\left\{ -\int \phi_i(r)\, \hat{O}_{ij}\phi_j(r)\, d\,\underline{r}^2 \right\} = \left[\text{Det } \hat{O}_{ij}\right]^{-1/2} \langle r|\hat{O}_{ij}^{-1}|r'\rangle$$

where $\hat{O}$ is a real symmetric matrix operator.

3. Complex Grassmannian Fields

$$\int \mathcal{D}\psi^\dagger\mathcal{D}\psi \exp\left\{ \int \psi^\dagger(r)\, \hat{O}\, \psi(r)\, d\, r^\dagger \right\} = \text{Det } \hat{O}$$

$$\int \mathcal{D}\psi^\dagger\mathcal{D}\psi \; \psi(r)\psi^\dagger(r') \exp\left\{ \int \psi^\dagger(r)\, \hat{O}\, \psi(r)\, d\, r^\dagger \right\} = \text{Det } \hat{O}\, \langle r|\hat{O}^{-1}|r'\rangle$$

where $\hat{O}$ is a Hermitian operator.

Appendix 3: Asymptotic Analysis of the Integral f_m as $n\to\infty$

The integral f_m is defined to be

$$f_m = (2\pi)^{-2} \left|C_{n,m}\right|^4 \int_0^{2\pi} d\theta \int_0^{\infty} r^{4|m|} e^{-r^2} \left[L_{\nu_m}^{|m|}(r^2/2) \right]^4 r dr$$

$$= \pi^{-1} \left|C_{n,m}\right|^4 \int_0^{\infty} u^{2|m|} e^{-u} \left[L_{\nu_m}^{|m|}(u/2) \right]^4 du$$

The case m=-n can be solved straightforwardly.

$$f_{-n} = (4\pi)^{-1} (2^n n!)^{-2} \int_0^{\infty} x^{2n} e^{-x} dx = \frac{1}{2^{2n+2}\pi} \frac{(2n)!}{(n!)^2} .$$

In the asymptotic large n limit we can use Stirling's formula for the factorials to give

$$f_{-n} \sim (4\pi)^{-1} (n\pi)^{-1/2} \qquad n\to\infty .$$

In the general case we can express f_m as a the some of a series as follows. The square of an associated Laguerre polynomial can be expressed in the following form (Gradsteyn and Ryzhik (1979) formula 8.976.3)

$$\left[L_{\nu}^{|m|}(u/2) \right]^2 = \sum_{k=0}^{\nu} S_k L_{2k}^{2|m|}(u)$$

where

$$S_k = \frac{(\nu+|m|)!}{\nu!\, 2^{2\nu}} \frac{(2k)!}{k!} \frac{(2\nu-2k)!}{(k+|m|)!\, [(\nu-k)!]^2} .$$

Hence we can write

$$f_m = (4\pi)^{-1} |C_{n,m}|^4 \sum \sum S_k S_p \int_0^{\infty} u^{2|m|} e^{-u} L_{2k}^{2|m|}(u) L_{2p}^{2|m|}(u)\, du .$$

The integral is that which appears in the orthonormality relation for the associated Laguerre polynomials and gives

$$f_m = (4\pi)^{-1} |C_{n,m}|^4 \sum_{k=0}^{\nu_m} (S_k)^2 \frac{(2k+2|m|)!}{(2k)!} \qquad (A3.1)$$

This can be analysed in two regions using Stirlings formula for the factorials

(i) $$f_m \sim \text{Const.}(nm)^{-1/2}\log(n) \qquad m \gg n \quad n\to\infty$$

and (ii) $$f_m \sim \text{Const.}\ n^{-1}\log(n) \qquad m \approx 0 \quad n\to\infty \ .$$

So in both these régimes f_m for $m\neq -n$ vanishes much faster than f_{-n} in the large n limit. The general behaviour of f_m is shown in figure 1 for n=8. This was calculated by explicit summation of the series A1.1.

Appendix 4: Verification of Equation 2.3

Consider the expression

$$X = i\int du^* du\ e^{-iCu^*u} \int d\psi^\dagger d\psi\ e^{-iC\psi^\dagger\psi}\ \psi\psi^\dagger \ .$$

We can simplify the complex integral by letting $u=re^{i\theta}$ and the Grassmann integral by expanding the exponential as a Taylor series which, because of the anticommutativity property, truncates at the second term. Thus

$$X = i\int_0^{2\pi} d\theta \int_0^{\infty} e^{-iCr^2} r dr \int d\psi^\dagger d\psi\ \left[1-iC\psi^\dagger\psi\right]\psi\psi^\dagger$$

The second term in the expansion of the Grassmann integral vanishes because it contains the squares of both Grassmann variables while the real integrals are trivial. Thus

$$X = 2\pi i\ \frac{1}{2iC} \int d\psi^\dagger d\psi\ \psi\psi^\dagger = \frac{1}{C} \ .$$

Substituting C=(E-iε-V) gives equation 2.3.

Appendix 5: Exact Evaluation of The Integral Expression for G(E)

Equation 2.6 gives an expresses G(E) as an integral over the complex u-plane:

$$G(E) = \frac{i}{\pi}\int du^* du\ e^{-iEu^*u - \frac{1}{2}\lambda(u^*u)^2} \ .$$

This can be simplified by setting $u=x^{1/2}e^{i\theta}$ to give

$$G(E) = i\int_0^{\infty} e^{-iEx-\frac{1}{2}\lambda x^2} dx \ .$$

The integrand is analytic so we can distort the contour of integration from the real x-axis in the manner shown in figure 1. Along the first contour we set y=ixsgn(E) and in the second y=x-iE/λ. Thus we find

$$G(E) = \mathrm{sgn}(E)\int_0^{|E|/\lambda} e^{-|E|y+\frac{1}{2}\lambda y^2}dy + ie^{-E^2/2\lambda}\int_0^{\infty} e^{-\lambda y^2/2}dy$$

$$= \mathrm{sgn}(E)\int_0^{|E|/\lambda} e^{-|E|y+\frac{1}{2}\lambda y^2}dy + \frac{i}{2}\left[\frac{2\pi}{\lambda}\right]^{1/2} e^{-E^2/2\lambda}.$$

The remaining integral is entirely real so that

$$\rho(E) = \frac{1}{\pi}\,\mathrm{Im}G(E) = (2\pi\lambda)^{-1/2}e^{-E^2/2\lambda}.$$

Figure 1

The contour used for the exact evaluation of the integral G(E)

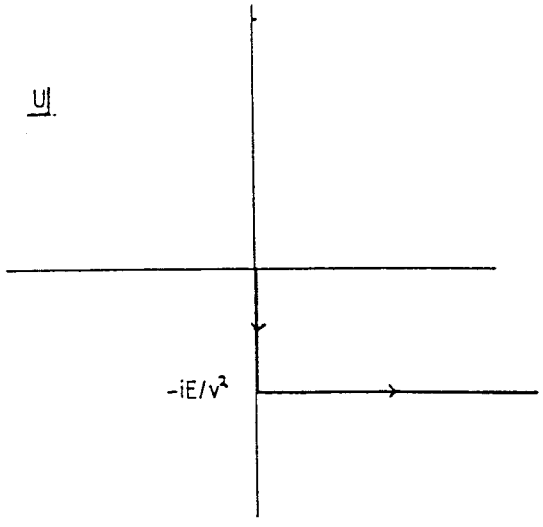

Figure 2

The Steepest descents contours in the complex ϕ_1 plane. $y_0=(E/2\lambda)^{1/2}$

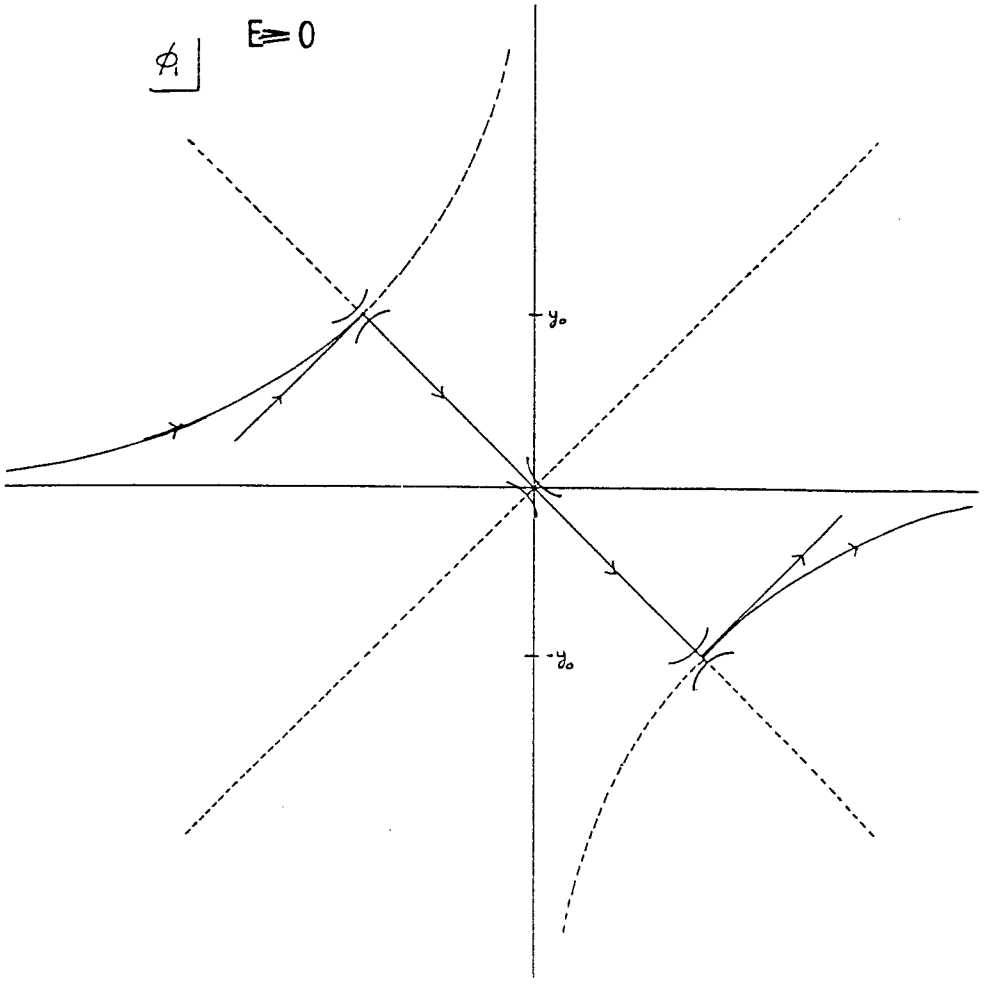

Figure 3
The varitaion of the Integral f_m with m for n=8

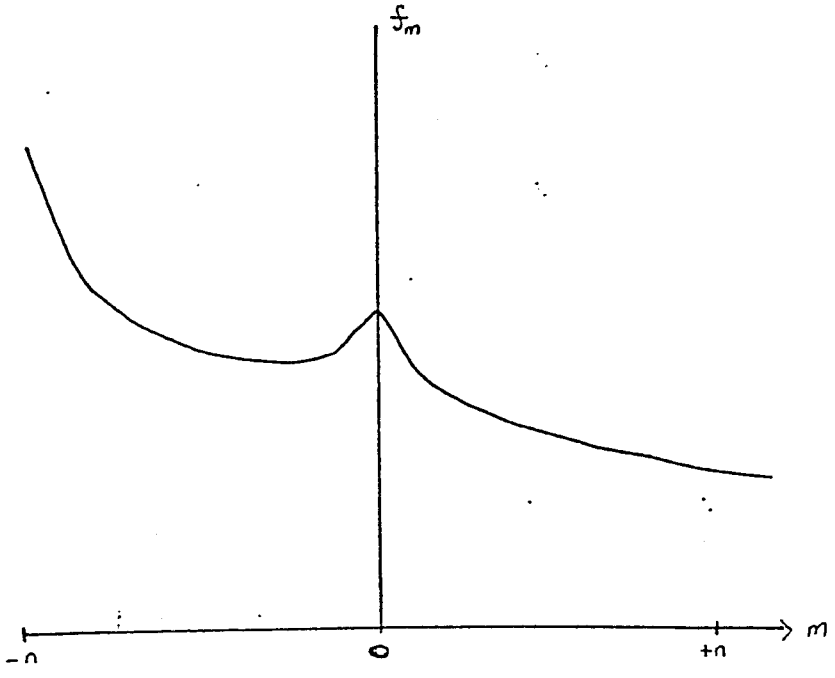

References

E. Abrahams, P.W. Anderson, D.C. Licciardello and T.V. Ramakrishnan (1979) Phys. Rev. Lett. **42**, 673

M. Abramowitz and I. Stegun (1965) "Handbook of Mathematical Functions" (New York:Dover)

A.A. Abrikosov, L.P. Gorkov and I.E. Dzyaloshinski (1963) "Methods of Quantum Field Theory in Statistical Physics" (New York: Dover)

P.W. Anderson (1958) Phys. Rev. **109** 1492

I. Affleck (1984) J. Phys. C: Solid State Physics **17**, 2323

T. Ando and Y. Uemura (1974) J. Phys. Soc. Japan **36**, 959

T. Ando (1974a) J. Phys. Soc. Japan **36**, 1521
(1974b) J. Phys. Soc. Japan **37**, 622
(1974c) J. Phys. Soc. Japan **37**, 1233

T. Ando, Y. Matsumoto and Y. Uemura (1975) J. Phys. Soc. Japan **39**, 279

T. Ando, Fowler and Stern (1982) Rev. Mod. Phys. **54**, 437

H. Aoki and T. Ando (1985) Phys. Rev. Lett. **54**, 831

S.M. Apenko and Y.E. Lozovik (1984) J. Phys. C: Solid State Physics **17**, 3585

J. Avron and R. Seiler Phys. Rev. Lett. (1985) **54**, 259

M. Ya Azbel (1986) Phys Rev B **33**, 8844

A. Bastin, C. Lewiner, O. Betbeder-Matibet and P.Nozieres (1971) J. Phys. Chem. Solids **32**, 1811

K.A. Benedict and J.T. Chalker (1985) J. Phys. C: Solid State Physics **18**, 3981

K.A. Benedict and J.T. Chalker (1986) J. Phys. C: Solid State Physics **19**, 3587

K.A. Benedict (1986) to appear in Nucl. Phys. B. [FS]

F.A. Berezin (1966) The Method of Second Quantisation (London: Academic Press)

E. Brézin, S. Hikami and J. Zinn-Justin (1980) Nucl. Phys. B **165**, 528

E. Brézin and G. Parisi (1980) J. Phys. C: Solid State Physics **13**, L307

E. Brézin, D.J. Gross and C.Itzykson (1984) Nucl. Phys. B **235 FS11**, 3585

M.E. Cage and S.M. Girvin (1983) Comments Solid State Physics **11**, 1 and 47

C.G. Callen and S. Coleman (1977) Phys. Rev. D **16**, 1762

P. Carra, J.T. Chalker and K.A. Benedict, in preparation

J.T. Chalker (1983) J. Phys. C: Solid State Physics **16**, 4297

J.T. Chalker, P. Carra and K.A. Benedict (1986) Southampton University Preprint

S. Doniach and E.H. Sondheimer (1974) "Green's Functions for Solid State Physicists" (Reading Massachusetts: Benjamin, Advanced Book Program)

E.N. Economou (1979) Green's Functions in Quantum Physics (Berlin: Springer)

S.F. Edwards (1958) Phil. Mag. **3**, 1020

K.B. Efetov (1982) Sov. Phys JETP **55**, 514
(1983) Advances in Physics **32**, 53

J.P Eisenstein, H.L. Stormer, V. Narayanamurti, A.Y. Cho, A.C. Gossard and C.W. Tu (1985) Phys. Rev. Lett. **55**, 875

R.J. Elliot, J.A. Krumhansl and P.L. Leath (1974) Rev. Mod. Phys **46**, 465

R.P. Feynman (1972) "Statistical Mechanics" chapter 11 (Reading Massachusetts: Benjamin, Advanced Book Program)
R. Friedberg and J.M. Luttinger (1975) Phys. Rev. B **12**, 4460
H. Fukuyama (1976) Solid State Commun. **19**, 551
(1979) Proceedings of the Kyoto Summer Institute "The Physics of Low Dimensional Systems" Kyoto University ed. Y. Nagaoka and S. Hikami
M.G. Gavrilov and I.V. Kukushkin (1986) JETP Lett. **25**, 103
R. Gerhardts (1975a) Z. Phys. B, **21**, 275
(1975b) Z. Phys. B, **21**, 285
S.M. Girvin, A.H. MacDonald and P.M. Platzman (1985) Phys. Rev. Lett. **54**, 581
(1986) Phys. Rev. B. **33**, 2481
E. Gornik, R. Lassnig, G. Strasser, H.L. Stormer, A.C. Gossard and W. Wiegmann (1985) Phys. Rev. Lett. **16**, 1820
Gradsteyn and Ryzhik (1979) "Tables of Integrals, Series and Products" (London: Academic Press). Note that formula 8.976.3 contains an error: the factor $\Gamma(k+\alpha-1)$ in the denominator on the rhs should read $\Gamma(k+\alpha+1)$
C.C. Grimes and G. Adams (1979) Phys. Rev. Lett. **12**, 795
F.D.M. Haldane (1983) Phys. Rev. Lett. **51**, 605
B. Halperin (1983) Helv. Phys. Acta **56**, 75
H. Keiter (1967) Z. Phys **198**, 215
S. Kivelson, C. Kallin, D.P. Arovas and J.R. Schrieffer (1986) Phys. Rev. Lett. **56**, 873
K. von Klitzing, G. Dorda and M. Pepper (1980) Phys. Rev. Lett. **45**, 494
J.M. Kosterlitz and D.J. Thouless (1974) J. Phys. C: Solid State Physics **6**, 1181
R. Kubo (1957) J. Phys. Soc. Jpn. **12**, 570
(1965) Solid State Physics **17**, 269
L.D. Landau and E.M.Lifshitz (1975) "The Classical Theory of Fields" (Oxford: Pergamon Press)
L.D. Landau and E.M. Lifshitz (1977) "Quantum Mechanics" (Oxford: Pergamon Press)
J. Langer (1967) Ann. of Physics **41**, 108
R.B. Laughlin (1981) Phys. Rev. B **23**, 5632
(1983) Phys. Rev. Lett. **50**, 1395
H. Levine, S. Libby and A.Pruisken (1983) Phys.Rev.Lett. **51**, 1915
(1984) Nucl.Phys.B. **240FS12**, 30
I.M. Lifshitz (1964) Advances in Physics **13**, 483
P. Lloyd (1969) J. Phys. C: Solid State Physics **2**, 1717
S.W. Lovesey (1980) "Condensed Matter Physics: Dynamic Correlations" (Reading Massachusetts: Benjamin, Advanced Book Program)
Yu.E. Lozovik and V.I. Yudson (1975) Sov Phys JETP Lett. **22**, 11
S. Luryi and R. Kazarinov (1982) Phys. Rev. B. **27**, 1386
A.J. M^{c}Kane (1980) Phys. Lett. **76A**, 22
A.J. M^{c}Kane and M. Stone Ann. of Phys. (1981) **131**, 36
N. Mott (1968) J. Non-Cryst. Solids **1**, 1
D.R. Nelson and B.I. Halperin (1979) Phys. Rev. B. **19** 2457
R.J. Nicholas, R.G. Clark, A. Usher, C.T. Foxon and J.J. Harris (1985) Oxford University Preprint
Q. Niu, D.J. Thouless and Y.S. Wu (1985) Phys. Rev. B. **31**, 3372
P.M. Platzman and H. Fukuyama (1974) Phys. Rev. B. **10**, 3150
L. Schweitzer, B. Kramer and A. MacKinnon (1984) J. Phys. C: Solid State Physics **17**, 4111
J. Sher and T. Holstein (1966) Phys. Rev. **148**, 598

V.B. Shikin (1970) Sov Phys JETP **31**, 936
(1971) Sov Phys JETP **33**, 387
(1979) "The Physics of Low Dimensional Systems" Proceedings of the Kyoto Summer Institute (ed. Y. Nagaoka and S. Hikami) (Kyoto University)
T.P. Smith, B.B. Goldberg, P.J. Stiles and M. Heilblum (1985) Phys. Rev. B. **32**, 2696
L. Smrcka and P. Streda (1977) J. Phys. C: Solid State Physics **10**, 2153
N. Sourlas (1985) Physica D **15**, 115
E. Stahl, D. Weiss, G. Weimann, K. von Klitzing and K. Ploog (1985) J. Phys. C: Solid State Physics **18**, L783
P. Streda (1982) J. Phys. C: Solid State Physics **15**, L717
T. Streit J. Phys. (Paris) (1984) **45**, L713
R. Tao and D.J. Thouless Phys. Rev. B. (1983) **28**, 1142
D.C. Tsui, H.L. Stormer and A.C. Gossard Phys. Rev. Lett. **48**, 1559
D.J. Thouless (1974) Phys. Repts. **13**, 93
(1981) J. Phys. C: Solid State Physics **14**, 3475
(1984) J. Phys. C: Solid State Physics **17**, L325
(1985) Phys. Rev. B. **31**, 8305
S.A. Trugman (1983) Phys. Rev. B. **27**, 7539
(1985) Phys. Rev. B. **31**, 5280
M. Tsukada (1977) J. Phys. Soc. Japan **42**, 391
B. Velicky (1969) Phys. Rev. **184**,614
F. J. Wegner(1979a) Z. Phys B **35**, 208
(1979b) Phys Rev B.
(1982) "Anderson Localisation" (ed. Y. Nagaoka and H. Fukuyama) (Berlin: Springer-Verlag)
(1983) Z. Phys B **51**, 279
E.P. Wigner (1934) Phys Rev **46**,1002
A.P. Young (1979) Phys. Rev. B. **19**, 1855
J.M. Ziman (1979) "Models of Disorder" (Cambridge: Cambridge University Press)